Nanomaterial Solutions for the Protection of Insulin Producing Beta Cells

A DISSERTATION
SUBMITTED TO THE FACULTY OF
UNIVERSITY OF MINNESOTA
BY

Nicole Ann Atchison

IN PARTIAL FULFILLMENT OF THE REQUIREMENTS
FOR THE DEGREE OF
DOCTOR OF PHILOSOPHY

Efrosini Kokkoli and Michael Tsapatsis, Advisors

November 2013

ACKNOWLEDGEMENTS

This work could not have been completed without the assistance of many people. First I would like to thank my advisors Efie Kokkoli and Michael Tsapatsis for their guidance and support throughout this project. I would also like to thank Professor Klearchos K. Papas for supplying his knowledge on islet isolation and transplantation, as well as giving me access to his lab and instrumentation. I also thank the members of my committee, Professors Chun Wang and Ben Hackel, for providing time and insight on this project.

A large portion of this work was completed at University Imaging Centers, the University of Minnesota Flow Core, and Schulze Diabetes Institute. I am indebted to the staff at these facilities for answering countless questions. Specifically I thank John Oja for his assistance on any issues I had with confocal microscopy. Kate Mueller and Jenna Kitzman of SDI were extremely generous with their time, providing and maintaining islets, as well as teaching me various experimental techniques. Graduate students in the Papas lab were excellent resources for information regarding islets and I thank each of them for their assistance.

For work in chapter 3 I acknowledge partial support through a 3M Science and Technology Fellowship. I acknowledge Dr. Wei Fan for the cryo-TEM image of the liposomes and the staff at the Schulze Diabetes Institute for their assistance in procuring and maintaining the islets as well as Dr. Hering for critiquing this work. I also thank Dr. Döne Demirgöz for contributions at the initiation of this project. I acknowledge the assistance of the Flow Cytometry Core Facility of the University of Minnesota Cancer Center, supported in part by P30CA77598. The cryo-TEM was carried out at the University of Minnesota Characterization Facility, which receives partial support from NSF through the NNIN program. The work was supported in part by the National Science Foundation (CBET-0553682), the Camille Dreyfus Teacher-Scholar Awards Program, and by the National Institute of Biomedical Imaging and Bioengineering (R03EB006125). The content is solely the responsibility of the authors and does not necessarily represent the official views of the

National Institute of Biomedical Imaging and Bioengineering or the National Institute of Health.

For the work in Chapter 4 I acknowledge our funding source, NSF CBET 0956601, NIH NIDDK R41DK075211 and NIH NIDDK R44DK070400, and the assistance of the Flow Cytometry Core Facility of the University of Minnesota Cancer Center.

The work in Chapter 5 was completed in collaboration with Dr. Wei Fan. Special thanks to Dr. Fan for work developing fluorophore containing nanoparticles. Funding was provided by the Center for Nanostructured Applications, the Amundson Chair Fund at University of Minnesota and the NSF (CBET 0956601). Computational support from the Minnesota Supercomputing Institute (MSI) is gratefully acknowledged.

I thank both current and former students of the Kokkoli and Tsapatsis labs, especially Maroof, Brett, Matt, Tim, Rachel, Garrett, Carolyn, and Kamlesh. They have all made the time more enjoyable and I am thankful for their camaraderie. I would like to thank Professor Wei Fan, Professor Mark Snyder, and Garrett Swindlehurst for collaborations on the silica nanoparticle work. I would like to thank Dr. Döne Demirgöz for her tutelage when I joined the lab.

Finally, I thank my family and friends for providing encouragement through this process. I thank my parents for their unwavering support throughout my life. I thank my brother for setting a great example of chasing your dreams. Lastly, I thank my husband Jordan for being a constant in the ups and downs of graduate school and supporting me along the way.

This work is dedicated to my family.

For inspiring, supporting, and encouraging me throughout it all.

ABSTRACT

Islet transplantation is a promising treatment for type 1 diabetes. However, even with the many successes, islet transplantation has yet to reach its full potential. Limited islet sources, loss of cell viability during isolation and culture, and post-transplant graft loss are a few of the issues preventing extensive use of islet transplantation. The application of biomaterial systems to alleviate some of the stresses affecting islet viability has led to improvements in isolation and transplantation outcomes, but problems persist. In this work we approach two distinct issues affecting islet viability; ischemic conditions and immunological attack post-transplant. Ischemic conditions have been linked to a loss of islet graft function and occur during organ preservation, islet isolation and culture, and after islets are transplanted. We show that liposomal delivery of adenosine triphosphate (ATP) to β cells can limit cell death and loss of function in ischemic conditions. We demonstrate that by functionalizing liposomes with the fibronectin-mimetic peptide PR_b, delivery of liposomes to porcine islets and rat β cells is increased compared to nontargeted controls. Additionally, liposomes are shown to protect by providing both ATP and lipids to the ischemic cells. The delivery of ATP was investigated here but application of PR_b functionalized liposomes could be extended to other interesting cargos as well. The second area of investigation involves encapsulation of islets with silica nanoparticles to create a permselective barrier. Silica nanoparticles are an interesting material for encapsulation given their ability to be fine-tuned and further functionalized. We demonstrate that size-tunable, fluorescent silica nanoparticles can be assembled layer-by-layer on the surface of cells and that silica nanoparticle encapsulated islets are able to secrete insulin in response to a glucose challenge.

TABLE OF CONTENTS

LIST OF TABLES

LIST OF FIGURES

CHAPTER 1

INTRODUCTION

Shapiro et al. published a seminal paper in 2000 indicating the application of islet transplantation to reestablish normal glycemic control in patients with type 1 diabetes (Shapiro et al., 2000). This paper offered a solution to the problems associated with insulin based therapies, namely hypoglycemia(Atkinson & Eisenbarth, 2001). However, over a decade later the promise of islet transplantation has yet to be fully realized due to the difficulties associated with this procedure (R Paul Robertson, 2010). Investigations into the areas affecting islet transplantation results will lead to better, more predictable clinical outcomes and greatly enhance the ability of this cell-based therapy to affect the lives of patients suffering from type 1 diabetes.

The 2000 paper spurred an increase in investigations into the transplantation of islets of Langerhans, clusters of nonendocrine and endocrine cells, including the insulin producing β cells, for the treatment of type 1 diabetes. Through these studies the promise of islet transplantation as a minimally invasive method of restoring normoglycemia was confirmed (Hering et al., 2005; Ryan et al., 2002, 2005; Shapiro et al., 2000, 2006). However multiple islet infusions, coming from different donor preparations, were typically necessary to gain insulin independence (Ryan et al., 2005; Shapiro et al., 2000, 2006). The necessity of multiple donors stresses the already limited supply of donor pancreata (Shapiro & Ricordi,

2004), limiting the application of this therapy. To broaden the clinical reality of this procedure, single donors or alternative islet sources must be used.

1.1 MOTIVATION

Though islet transplantation has shown promise as an alternative treatment for type 1 diabetes, many issues remain with this therapy. The limited supply of human donor pancreata necessitates the examination of other islet supplies such as stem cells, islet regeneration, and xenogeneic islets (Godfrey et al., 2012; Pileggi, Cobianchi, Inverardi, & Ricordi, 2006; Ricordi & Edlund, 2008). Porcine islets offer many advantages including the on-demand availability of young, healthy, living, pathogen-free donors (Bottino et al., 2007; Rood, Buhler, Bottino, Trucco, & Cooper, 2006) and have restored glycemic control in nonhuman primates (Cardona et al., 2006; Hering et al., 2006). However, porcine and human islets both suffer from stresses during the procurement, isolation, culture period, and after transplant that lead to cell death (Bennet et al., 2000; Emamaullee & Shapiro, 2006; Papas, Hering, et al., 2005; Paraskevas, Maysinger, Wang, Duguid, & Rosenberg, 2000; Rosenberg, Wang, Paraskevas, & Maysinger, 1999; R. Wang & Rosenberg, 1999). Furthermore, transplanted islets can be attacked by the host's immune system (Gray, 2001; Ricordi & Strom, 2004)causing additional damage. To ward off the immune attack, immunosuppression therapy must be administered which poses its own risks (Ricordi & Strom, 2004; Van Belle & von Herrath, 2008). Thus it is necessary to determine the benefit/risk ratio before proceeding with islet therapy. Technology which circumvents these issues could further promote the use of this cell based therapy for the treatment of type 1 diabetes.

The primary motivation behind this work is to develop and investigate techniques which improve islet transplantation outcomes, harnessing technologies developed in the Kokkoli and Tsapatsis groups. We aim to target specific stresses that the islets encounter during organ procurement, isolation, purification, and after transplantation. These stresses, including ischemia, matrix detachment, and immune system mediated toxicity, lead to a loss of viable islet yield per pancreas as well as a loss of graft function after transplantation (Pileggi et al., 2006). In this work we investigate two different approaches to modulating islet cell death:

1. *Targeted drug delivery system: nanoparticles that transport cytoprotective molecules to insulin producing β cells to protect from an ischemic insult.*
2. *Cell encapsulation: silica nanoparticle based semipermeable membrane to protect cells from recognition and destruction by immune system components.*

In the first approach, we hypothesize that utilizing a drug delivery system that has proven effective in prior work with cancer cells (Demirgöz, Garg, & Kokkoli, 2008; Garg & Kokkoli, 2011; Garg, Tisdale, Haidari, & Kokkoli, 2009; Shroff & Kokkoli, 2012), can increase the delivery of cytoprotective molecules to the islet cells. We investigate the effectiveness of liposomes which are functionalized with a fibronectin-mimetic peptide, PR_b, for internalizing into islet cells and delivering molecules of interest. Liposomes are a widely studied delivery vehicle and have been used for a variety of applications (Pangburn, Petersen, Waybrant, Adil, & Kokkoli, 2009; Pearce, Shroff, & Kokkoli, 2012). In this study we examine the efficacy of liposomal delivery of adenosine triphosphate (ATP) to β cells exposed to ischemia. Delivery of ATP has been shown to prevent cell death in other models of ischemia, including heart (Hartner, Verma, Levchenko, Bernstein, & Torchilin, 2009; Levchenko, Hartner, Verma, Bernstein, & Torchilin, 2010; Verma, Levchenko, Bernstein, &

Torchilin, 2005) and liver (Korb et al., 2008; Neveux, De Bandt, Chaumeil, & Cynober, 2002; Tep et al., 2009), and we hypothesize that ATP delivery could provide similar protection to ischemic islet cells and that functionalizing the liposomes with PR_b will increase the delivery of ATP. While we study the delivery of ATP to the β cells, this technology could be extended to the delivery of other interesting substances as well (genes, siRNA, antioxidants, etc.).

The second approach, islet encapsulation, has been an area of interest in the islet community since Lim and Sun published a study in 1980 showing that rat islets encapsulated in alginate performed better than control islets *in vivo* (Lim & Sun, 1980). The encapsulation material provides a permselective barrier around the islets that shields them from recognition by the host's immune system but allows the transport of molecules such as nutrients, glucose, insulin, and waste products. Many different materials have been investigated for islet encapsulation (reviewed in (Beck et al., 2007)) but limitations in the size of the capsule and molecular size cutoffs have restricted the application of these technologies on a broad scale. The Tsapatsis lab has developed a protocol for synthesizing small, monodispersed silica nanoparticles in an amino acid buffered aqueous environment (T. M. Davis, Snyder, Krohn, & Tsapatsis, 2006; Fan et al., 2008) which can form hexagonal packed monolayers with defined pore sizes (Fan et al., 2008; Snyder, Demirgöz, Kokkoli, & Tsapatsis, 2009). We hypothesize that the ability to fine-tune the particles to a range of sizes and the variety of surface modifications that can theoretically be employed provide many advantages to using silica nanoparticles as an encapsulation material. In this study we demonstrate the surface modification of these particles to create both positively and

negatively charged silica nanoparticles[1] which are assembled layer-by-layer on the surface of living cells using electrostatic interactions. Furthermore, we show that islets encapsulated with silica nanoparticles are still capable of sensing and responding to changes in glucose concentration.

While different, these two approaches both utilize nanomaterials for modulation of islet cell death during the process of islet transplantation. In this work we investigate proof of concept in these areas and demonstrate the feasibility of these designs. Additionally, both treatment strategies boast the ability to be extended by adding further functionalities or different payloads.

1.2 Thesis Overview

The increasing awareness of islet transplantation as a viable treatment option for patients with type 1 diabetes has motivated the field to develop methods to improve therapy outcomes (Beck et al., 2007; Emamaullee & Shapiro, 2006; R Paul Robertson, 2010; Van der Windt, Bottino, Casu, Campanile, & Cooper, 2007). However, despite improvements in isolation techniques, donor selection, and immunosuppression therapy, the limited number of donor pancreata, low islet yield per pancreas, and poor graft survival rates limit the therapeutic benefit of this therapy (Hering et al., 2005; R Paul Robertson, 2010; Shapiro & Ricordi, 2004). Improving islet recovery from donor pancreata and prolonging transplanted graft survival would increase the ability to use a single donor pancreas per patient, reducing the risk and cost of the islet transplantation (Hering et al., 2005). The two strategies investigated in this work aim to accomplish this goal by utilizing nanomaterials for

[1] Encapsulation work is in collaboration with Dr. Wei Fan. Particle synthesis and characterization developed by Dr. Fan.

manipulation of the intracellular and extracellular milieu of islet cells. The background and prior work utilizing these nanomaterials is covered in Chapter 2. Additionally, islet transplantation, the problems associated with it, and interventional strategies are also covered in Chapter 2.

The first strategy we discuss for modulating islet cell survival is a drug delivery approach using a targeted liposome system. The liposomes are decorated with a fibronectin-mimetic peptide bullet, PR_b, which binds specifically to the $\alpha_5\beta_1$ integrin (Craig, Rexeisen, Mardilovich, Shroff, & Kokkoli, 2008; Mardilovich, Craig, McCammon, Garg, & Kokkoli, 2006). By decorating the liposomes with PR_b we are able to increase the binding and internalization of the cargo loaded liposomes to $\alpha_5\beta_1$ expressing cells. Chapter 3 is a study investigating the utility of this peptide with porcine islet cells. We demonstrate the expression of $\alpha_5\beta_1$ on the freshly isolated porcine islet cells and the ability of PR_b functionalized liposomes to bind and internalize into the cells in a PR_b concentration dependent manner (Atchison et al., 2010). In Chapter 4 we extend this study to investigate the delivery of a therapeutic load to insulin producing β cells via the PR_b functionalized liposomes. In this study we use a model β cell line, INS-1, that expresses $\alpha_5\beta_1$ and is capable of secreting insulin in response to a glucose challenge (Asfari et al., 1992). Liposomal delivery of ATP is shown to protect β cells from an ischemic insult in a two-fold manner. We find that both the lipids composing the liposomes and the encapsulated ATP both provide a benefit to the stressed β cells. We monitor the transfer of rhodamine-labeled lipids to the β cell membrane as well as the PR_b mediated internalization of liposomes loaded with a fluorescent aqueous cargo. We show that β cells treated with ATP liposomes retain higher

cell viability compared to their untreated and empty liposome treated counterparts. This study demonstrates the utility of PR_b functionalized liposomes for delivering therapeutic loads to insulin producing β cells.

Chapter 5 presents work on the cell encapsulation approach. In this chapter the synthesis of the silica nanoparticles, including the addition of fluorescent molecules and surface modifications, is introduced. These particles are then utilized for a layer-by-layer encapsulation strategy on the surface of both INS-1 β cells and porcine islet cells. Using scanning electron and laser scanning confocal microscopies we demonstrate the adsorption of the 20 nm particles on the surface of the cell membranes. We show silica nanoparticle coatings that can be assembled in various conditions and remain stable for hours. Additionally, we confirm that porcine islets coated with silica nanoparticles are capable of secreting insulin in response to a glucose challenge (Atchison et al., 2011). This work presents proof of concept and is currently being extended to improve stability of the coatings and investigate the ability of the coatings to protect from immunological insults. The complete work is concluded and future directions discussed in Chapter 6.

CHAPTER 2

BACKGROUND

The essential concepts pertaining to modulation of islet cell death with nanomaterials are reviewed here. Topics include type 1 diabetes; islet transplantation: protocols, issues, and interventional strategies; targeted drug delivery system: previous applications and current system design; and background information on silica nanoparticles.

2.1 TYPE 1 DIABETES

Type 1 diabetes (T1D) accounts for about 5% of diagnosed cases of diabetes in adults. In 2011, approximately 18.8 million Americans had been diagnosed with diabetes and about one million being patients had T1D (CDC, 2011). T1D is characterized by immune-mediated destruction of the insulin-producing, pancreatic β cells (Willcox, Richardson, Bone, Foulis, & Morgan, 2009). Clinical onset of T1D occurs when the majority of the β cells have been destroyed. This is preceded by insulitis, an influx of lymphocytes into the islet which can occur years before the clinical onset (Homo-Delarche & Boitard, 1996; Wicker et al., 1987; Z. J. Zhang, Davidson, Eisenbarth, & Weiner, 1991). Patients with T1D must rely on exogenous sources of insulin to maintain normal blood glucose levels, leading to the threat of hyperglycemia or hypoglycemia which can both be dangerous. Other complications are also associated with diabetes including heart disease and stroke, high blood pressure, blindness, kidney disease, nervous system disease, dental disease, and birth defects. These complications, as well as the threat of hyperglycemia or hypoglycemia, about double the

risk of death for people with diabetes compared to people of the same age without diabetes (CDC, 2011). Treatments for T1D include exogenous insulin injections, insulin pumps, strict diet control and exercise, pancreas transplantations, islet allograft transplantations, or a combination of these treatments.

2.1.1 Mechanisms of Type 1 Diabetes

T cells are a primary culprit for the destruction of β cells in T1D. Naive T cells mature in the thymus and utilize their broad diversity of T cell receptors to recognize foreign antigen (M. M. Davis & Bjorkman, 1988). T cells can mature into helper, cytotoxic, or regulatory T cells which can mount an attack on invading foreign antigen. However, the diversity of the T cell receptors inevitably leads to T cell receptors that recognize and react to autoantigens (antigens normally expressed by the host) (Anderson et al., 2002). Tolerance to autoantigens is accomplished by host presentation of the antigens in the thymus. Naive T cells that interact strongly with autoantigens presented in the thymus will be negatively selected (anergy or deletion) from the T cell repertoire (Derbinski, Schulte, Kyewski, & Klein, 2001; Hudrisier, Feau, Bonnet, Romagnoli, & Van Meerwijk, 2003). The presentation of otherwise tissue specific antigens (e.g. insulin) in the thymus is accomplished by medullary epithelial cells which express the autoimmune regulator (AIRE) protein (Anderson et al., 2002; Derbinski et al., 2001). If the AIRE protein is mutated, expression of tissue specific antigens in the thymus is affected and T cells specific to these autoantigens are allowed to mature and undergo clonal expansion (Liston et al., 2004). The breakdown of this self-tolerance mechanism plays a primary role in the development of T1D (Geenen, 2012; Liston et al., 2004; Pugliese et al., 1997; Pugliese, 1998; Vafiadis et al., 1997; Wucherpfennig & Eisenbarth, 2001).

2.1.2 Treatments for Type 1 Diabetes

Insulin therapy is the common treatment for T1D. While this therapy can help the patients achieve normal blood glucose levels, it is not a cure for the disease. Insulin injections lead to the risk of a series of chronic complications. In order to prevent these complications the patient must maintain extremely strict metabolic control which is not an easy undertaking. The severe risk of hypoglycemia makes it difficult for the patient to achieve normoglycemia with insulin therapy. Insulin analogs that are faster adsorbing have made the use of insulin pumps more prominent but the real-time analysis of blood glucose is still not ideal for these treatments to work most efficiently (Atkinson & Eisenbarth, 2001). Whole pancreas transplantation has been shown to be an effective therapy for T1D (R P Robertson, 1999; White, Shaw, & Sutherland, 2009). However, the surgical risks, donor availability, and harsh immunosuppression therapy make this therapy an option primarily for patients receiving a kidney graft or who have abnormal difficulty with the complications associated with insulin therapy. Since the success of the Edmonton protocol (Shapiro et al., 2000) islet transplantation has shown promise as a treatment for T1D (Hering et al., 2005; Shapiro et al., 2000, 2006; Tiwari, Schneider, Barton, & Anderson, 2012). This treatment is advantageous because it delivers the necessary endocrine cells to control the blood glucose level while minimizing the associated surgical risks. However, issues regarding immunosuppression and lack of available donors are still relevant (Pileggi et al., 2006; Ryan, Paty, Senior, & Shapiro, 2004).

2.2 Islet Transplantation

Islet transplantation is a promising treatment for T1D due to the ability of the graft to return normal glycemic control to the patients with a minimally invasive procedure

(Kenyon, Ranuncoli, Masetti, Chatzipetrou, & Ricordi, 1998; Shapiro et al., 2000; Sutherland et al., 1974). However, the risks associated with the procedure and the necessary immunosuppression must be weighed against the benefits. Many times, especially in children, the risks associated with immunosuppression are too great to warrant this procedure. However, if there is a need for another organ graft (i.e. kidney) and an immunosuppression regimen will already be in place, islet transplantation may be a good option (Kenyon et al., 1998). Since 2000 over 750 patients with T1D have received islet transplants at sites all over the world (McCall & Shapiro, 2012). The initial report in 2000 demonstrated 100% insulin independence in seven patients receiving multiple islet transplants (Shapiro et al., 2000) however, cumulative results from the international trial by the Immune Tolerance Network have less encouraging results (Shapiro et al., 2006). The trial demonstrated that although the same protocol was used, prior experience in islet isolation and handling of posttransplant immunosuppression had considerable effect on the outcome (Shapiro et al., 2006). Currently, insulin independence at two years posttransplant is >27% with significant decline thereafter (McCall & Shapiro, 2012). One persistent problem is the use of multiple islet transplants from multiple donors (McCall & Shapiro, 2012; Shapiro et al., 2000, 2006; Shapiro & Ricordi, 2004). The necessity of multiple donors limits the number of transplants that can ultimately occur. Donor pancreas procurement for islet transplantations is extremely low. It is estimated that 70% of available cadaveric pancreata are not recovered and those procured are first offered to centers for whole pancreas transplantations (Shapiro & Ricordi, 2004). Therefore, it is important that an islet transplantation protocol can be established which utilizes a single donor. This has been demonstrated in a limited number of cases, notably at the University of Minnesota (Hering

et al., 2004, 2005) and the University of California, San Francisco (Posselt, Bellin, et al., 2010; Posselt, Szot, et al., 2010). The success of these centers in single donor insulin independence achievement might be due to the donor selection criteria and limited ischemia periods (McCall & Shapiro, 2012).

2.2.1 ISLET ARCHITECTURE

Islets of Langerhans make up about 1-2% of the total mass of the pancreas (Homo-Delarche & Boitard, 1996). They are clusters of α, β, δ, and pp endocrine cells, which contain glucagon, insulin, somatostatin and pancreatic polypeptide granules respectively, and other nonendocrine cells (Elayat, El-Naggar, & Tahir, 1995). The architecture and composition of islets varies widely among species(Steiner, Kim, Miller, & Hara, 2010). In mouse, rat, and to some extent pig islets the β cells make up the core of the islet while the α, δ, and pp cells are located at the periphery (Crowther, Gotfredsen, Moody, & Green, 1989; Jay, Heald, Carless, Topham, & Downing, 1999; Steiner et al., 2010). However, in human islets the α and δ cells are dispersed throughout the islets and intermingle with β cells located in both the core and the periphery of the islets (Brissova et al., 2005; Elayat et al., 1995). In regards to composition, β cells make up between 28% and 75% of human islets, 61% to 88% of mouse islets, and around 82% of porcine islets (Brissova et al., 2005; Dufrane, Goebbels, Fdilat, Guiot, & Gianello, 2005). Another important aspect of the islet architecture is the degree and arrangement of the vascular (Bonner-Weir & Orci, 1982). Although islets make up roughly 1-2% of the mass of the pancreas, 5-15% of the blood perfused into the pancreas goes to the islets (Jansson & Carlsson, 2002). The blood flow is controlled by nervous, endocrine, and metabolic mechanisms. The arrangement of the different endocrine cells

may play a role in the blood flow control, however this is not completely understood (Ballian & Brunicardi, 2007; M. D. Menger, Yamauchi, & Vollmar, 2001).

2.2.2 Complications in Islet Isolation and Transplantation

Whole pancreas transplantations are capable of reversing diabetes with only one donor pancreas, but successful islet transplants often require two or more donor pancreata (McCall & Shapiro, 2012; Shapiro et al., 2000, 2006; Shapiro & Ricordi, 2004). This discrepancy between whole graft and isolated islets is thought to occur due to apoptosis of the β cells in the isolated islets (Contreras et al., 2001; Emamaullee, Rajotte, et al., 2005; Emamaullee, Liston, Korneluk, Shapiro, & Elliott, 2005; Emamaullee & Shapiro, 2006; Giuliani et al., 2005; Rosenberg et al., 1999; F. T. Thomas et al., 1999; R. Wang & Rosenberg, 1999). The isolation process, culture, and posttransplant period all exert stresses on the islets that can lead to cell death (Bennet et al., 2000; Emamaullee & Shapiro, 2006; Papas, Hering, et al., 2005; Paraskevas et al., 2000; Rosenberg et al., 1999; R. Wang & Rosenberg, 1999). The death of the islet cells, especially the β cells, leads to an increase in the mass of islets required per transplant and therefore decreases the ratio of treated patients per donor. Methods to evade the eventual loss of islet cell viability resulting from the incurred stresses are necessary to lower the number of islets needed per transplantation and eventually make single donor transplants the standard.

Figure 2.1 reviews the basic procedure for islet transplantation into the portal vein. The procedure can be broken down into four basic parts: donor pancreas preservation, islet isolation, islet culture (not shown in figure), and posttransplant. Each stage of this procedure has an effect on the outcome of the transplant (J. R. T. Lakey, Burridge, & Shapiro, 2003).

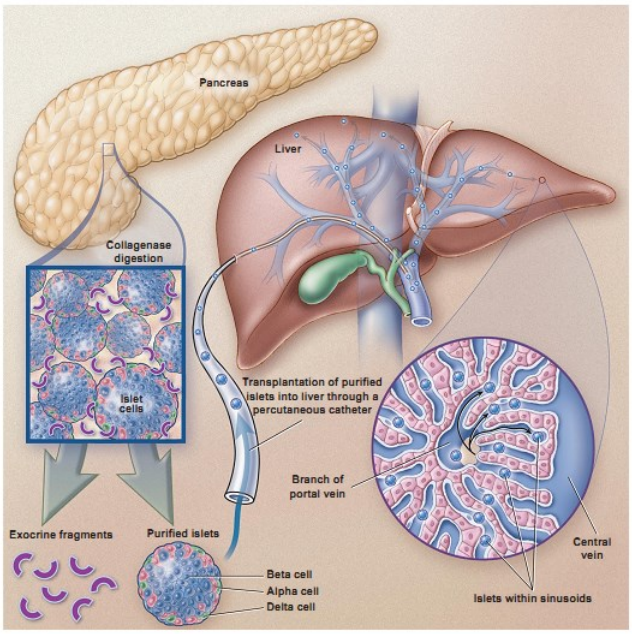

Figure 2.1: General protocol for islet transplantation. Islets are removed from the donor pancreas by a collengase digestion, followed by purification to separate the islets from the exocrin tissue. Purified islets are infused through the portal vein into the patient's liver. Reproduced with permission from R.P. Robertson, *The New England Journal of Medicine,* 2004, 350, 694-705. Copyright Massachusetts Medical Society.

2.2.2.1 Preservation

Periods of cold and warm ischemia during pancreas preservation are known to negatively affect the yield and viability of isolated islets (Daniel Brandhorst, Iken, Bretzel, & Brandhorst, 2006). The length of cold ischemia was shown to directly affect the quality of isolated human islets when pancreata were flushed with University of Wisconsin (UW) solution (a standard organ preservation solution) (J. R. Lakey, Rajotte, Warnock, & Kneteman, 1995). To improve the oxygenation of the organ, Kuroda et al. developed a two-layer method (TLM). This method incorporates a layer of UW solution and a layer of a perfluorochemical into which oxygen is bubbled (PFC) (Y Kuroda et al., 1988). The PFC is

lipophilic and has a higher density than UW solution, so two distinct layers can form. The pancreas is then floated between the two solutions. The TLM was shown to increase the ATP content of human pancreata preserved for up to 72 hours compared to preservation in UW solution alone (Yoshikazu Kuroda et al., 1992). Additionally, the TLM improved the recovery and function of canine islets subjected to 3 or 24 hours of cold ischemia (Tanioka et al., 1997) and human islets subjected to short or long periods of ischemia (Matsumoto et al., 2002). However, although the TLM shows improved results, there is evidence that large portions of the pancreas are not oxygenated during the cold ischemia time (Papas, Hering, et al., 2005). Persufflation has been used to increase the ATP levels of preserved pancreata over the levels achieved with the TLM (W E Scott III et al., 2011; William E Scott III et al., 2010; Thomas M Suszynski et al., 2012) but the TLM remains the standard in pancreas preservation prior to islet isolation. Islets exposed to prolonged periods of ischemia develop areas of necrosis within the islet, possibly contributing to early graft loss (Giuliani et al., 2005).

2.2.2.2 Isolation

Islets are released from the pancreatic tissue using an enzymatic digestion. Improvements in the protocols, enzyme preparations, and dissociation temperatures have increased isolated islet yields (Bottino et al., 2007; H. Brandhorst, Brandhorst, Hering, & Bretzel, 1999) but the digestion still imposes many stresses on the islets that can affect viability (Bottino et al., 2004; Paraskevas et al., 2000; Rosenberg et al., 1999; R. Wang & Rosenberg, 1999). The digestion process releases the islets from the surrounding tissue and increases the preparation purity by removing excess exocrine tissue. An enzyme cocktail is used to dissociate the islets from the tissue and extracellular matrix (ECM) proteins, however loss

of these interactions can decrease cell survival (Ilieva et al., 1999; Pinkse et al., 2006; Ris et al., 2002; Rosenberg et al., 1999). The isolation is imprecise and the variation of islet ECM compositions between species requires the digestion process to be tailored for each species (Brissova et al., 2005; Elayat et al., 1995; Steiner et al., 2010; R. Wang, Paraskevas, & Rosenberg, 1999). Cells bind to ECM through heterodimeric integrin receptors located on the surface of the cell (Meredith & Schwartz, 1997; Schwartz & Ingber, 1994). The interaction between integrins and ECM leads to signaling cascades which regulate cell survival and differentiation (Aplin, Stewart, Assoian, & Juliano, 2001; Giancotti, 1999; Z. Zhang, Vuori, Reed, & Ruoslahti, 1995). Loss of these connections triggers a form of apoptosis known as anoikis (Frisch & Screaton, 2001). Several techniques have been applied to modulate the apoptotic signaling series, such as culturing islets on ECM substrates to provide the ligands for the integrin receptors or providing soluble factors that bind to the receptors (i.e. antibodies, peptides, proteins) (Pinkse et al., 2006; R. Wang & Rosenberg, 1999). Due to the decrease in viability after isolation, assessment of islet function after isolation is extremely important, though difficult. Only with accurate assessment can the ability of the islet preparation to reverse diabetes be approximated correctly (Boyd, Cholewa, & Papas, 2010; Papas, Suszynski, & Colton, 2009; Ricordi, Gray, et al., 1990).

2.2.2.3 Culture

Culturing islets before they are transplanted allows the patient to start an immunosuppression regime to hopefully decrease posttransplant graft loss occurring through immunity (Hering et al., 2004). However, this period can also further stress isolated islets. After isolation, the vasculature of the islets is destroyed and they must rely on

diffusion for oxygen and nutrient transfer (Jansson & Carlsson, 2002). This can further the development of necrotic cores (Giuliani et al., 2005; Thomas M Suszynski, Papas, & Avgoustiniatos, n.d.).

2.2.2.4 Transplantation

Isolated islets are injected into the portal vein where they travel until they become lodged in liver sinusoids. Until complete revascularization, the islet suffers from ischemic conditions where oxygen and nutrients are limited (Carlsson, Liss, Andersson, & Jansson, 1998; Thomas M Suszynski et al., n.d.). The combination of ischemic conditions (Moritz et al., 2002), proinflammatory cytokines (Rabinovitch, 1998; Rabinovitch & Suarez-Pinzon, 2007) and immune rejection lead to an estimated loss of 70% of the transplanted β cell mass (Emamaullee & Shapiro, 2006; Ryan et al., 2005). This loss of β cell mass can lead to graft failure and the need for multiple transplantations. Immunosuppression is necessary to protect the transplanted islet from host recognition, but the regimen can further damage the islets, as well as increase risks for the patient (Emamaullee & Shapiro, 2006; Ryan et al., 2004). Strategies to lower the necessary immunosuppression and decrease the number of islets needed per transplant are discussed in the following sections.

2.2.3 Porcine Islets

One solution to the limited supply of human islets is the use of xenografts. Porcine islets are a promising alternative to human islets (Davalli et al., 1995) and provide numerous benefits including the on-demand availability of young, healthy, living, pathogen-free donors, the ease of breeding (Bottino et al., 2007; Rood et al., 2006), and the previous use of porcine insulin. Porcine insulin differs from human insulin by only a single amino acid (Schernthaner, 1993; Z. J. Zhang et al., 1991). Porcine islets have recently been shown to

reverse diabetes in a non-human primate model (Hering et al., 2006; Kirchhof et al., 2004), highlighting their potential. Porcine islets are inherently fragile (Deijnen, Hulstaert, Wolters, & Schilfgaarde, 1992; Ricordi, Socci, et al., 1990) and suffer from the same stresses as human islets during preservation, isolation, culture, and transplantation. Therefore, strategies to protect the islets from these stresses could be beneficial in both islet transplantation models.

2.2.4 Molecular Strategies for Increased Islet Survival

Due to the myriad of stresses islets encounter during the transplantation protocol, many strategies exist to increase cell survival (Narang & Mahato, 2006). In this work, we focus on strategies that use nanomaterials to improve islet transplantation.

2.2.4.1 Gene delivery

A review by Emamaullee and Shapiro (2006) details the different molecular approaches for evading apoptosis in islet cells, highlighting the potential benefits and drawbacks of each technique. Overexpression of genes intended to promote revascularization (Narang et al., 2004), molecules that mediate reactive oxygen species (ROS) generation and destruction (Lepore et al., 2004), or strategies that prevent coagulation and thus instant blood-mediated inflammatory reaction (Contreras et al., 2004; Van der Windt et al., 2007) are all techniques that have met with limited success. These strategies target steps late in the death cascade and it is proposed that the marginal success is due to the fact that the islets are already fairly stressed at the points of intervention and cannot recover (Emamaullee & Shapiro, 2006). Therefore, many researchers have focused on directly inhibiting the apoptosis signaling cascade in the islet cells. The most promising molecular therapies have involved Bcl-2 (Contreras et al., 2001; Rabinovitch et al., 1999), A20 (Grey et

al., 2003; Grey, Arvelo, Hasenkamp, Bach, & Ferran, 1999), or X-linked inhibitor of apoptosis protein (XIAP) (Emamaullee, Rajotte, et al., 2005; Emamaullee, Liston, et al., 2005). Transfection of these genes has most commonly been accomplished using adenovirus and other viral vectors. Viral vectors are advantageous because they are highly efficient for transduction and delivery of cargo to the nucleus and work for a wide variety of tissues. However, the risk of immunogenicity is a major concern (S. S. Davis, 1997; C. E. Thomas, Ehrhardt, & Kay, 2003). Adenoviruses are the most immunogenic of the viral vectors. They can induce a cytokine mediated inflammatory reaction and activate cytotoxic T-cells against viral gene products produced by the transfected cells (Khalil, Kogure, Akita, & Harashima, 2006; C. E. Thomas et al., 2003). These immunogenic responses to adenoviruses are the major limiting factor for their use in gene transduction.

Nonviral vectors are an exciting alternative to viral vectors in part because of their efficient gene delivery (Pelisek et al., 2006), ease of scale up (Mustapa et al., 2007), and circumvention of the immunological risks. Lipopolyplexes are one subset of nonviral vectors that have interesting properties (R. J. Lee & Huang, 1996). A lipopolyplex is polycation condensed DNA entrapped within (or complexed with) anionic, neutral, or cation peptide-modified liposomes. These vectors combine the advantages of the two separate systems, lipoplexes and polyplexes (L. Yu, Suh, Koh, & Kim, 2001). Lipoplexes are cationic lipids mixed with DNA that are able to escape the endosome by fusing with the lipid membrane. Polyplexes use cationic polymer to condense the DNA (higher compaction than with lipoplexes) and can accomplish endosomal escape if polyethyleneimine (PEI) is used as the polymer. However, these polyplexes can be toxic and encapsulating them into a liposome shields their toxic effects. Additionally, peptides can be incorporated into the

liposomes to increase their ability to target specific cells (Mustapa et al., 2007) and polyethylene glycol (PEG) can be used to increase the circulation time of the liposomes (Klibanov, Maruyama, Torchilin, & Huang, 1990). The complete entrapment of polyplexes within liposomes is difficult to demonstrate but is currently being studied in the Kokkoli lab (Adil et al., n.d.). Improvements in nonviral gene delivery could enhance the implementation of these options in future islet transplantation protocols.

2.2.4.2 Re-establishment of ECM connections

Loss of the ECM has been shown to cause islet cell apoptosis and researchers have investigated methods of re-establishing these integrin/ECM connections. Culturing rat islets on ECM substrates (collagen IV, laminin, and fibronectin) or incubating with Arg-Gly-Asp (RGD) peptide or anti-β1 antibody was shown to increase survival after 24 hours of culture (Pinkse et al., 2006). In another study, investigators monitored the apoptosis of canine islets cultured normally, supplemented with soluble fibronectin, or cultured on a rat-tail collagen substrate for the first six days of culture (R. Wang & Rosenberg, 1999). They found a significant decrease in apoptosis in the latter two conditions compared to the control but there was an overall increase in apoptosis over the course of the six days in all samples. Although culturing islets on ECM substrates was shown to decrease apoptosis, adhered islets are not advantageous for later transplantation. Islets left free floating during the culture period avoid the need for subsequent enzymatic digestion steps. Entrapment in hydrogels has been investigated as a means to create an encapsulation barrier around the islets (Weber, Hayda, Haskins, & Anseth, 2007). Islets entrapped in hydrogels had better viability and function when the hydrogels were functionalized with ECM components

(Nagata, Asuka, Inoue, & Tabata, 2002; Weber & Anseth, 2008). From these examples it is clear that the matrix interactions are crucial for islet cell survival and function.

2.2.4.3 Protection from posttransplant ischemic stress

After transplantation, islets are exposed to conditions that can lead to cell death (Davalli et al., 1996). Hypoxia causes impairment of mitochondrial function, leading to depletion of high energy phosphate bond molecules such as ATP. ATP drives most energy-requiring processes within the cell and is required for the cell to maintain homeostasis. ATP controls many ion pumps that maintain the cell intracellular environment. When this control breaks down due to lack of ATP, cell swelling, hydrolysis of cell components, and cell necrosis occurs (Michiels, 2004). In the β cell, hypoxia has the additional effect of altering the glucose stimulated insulin secretion response.

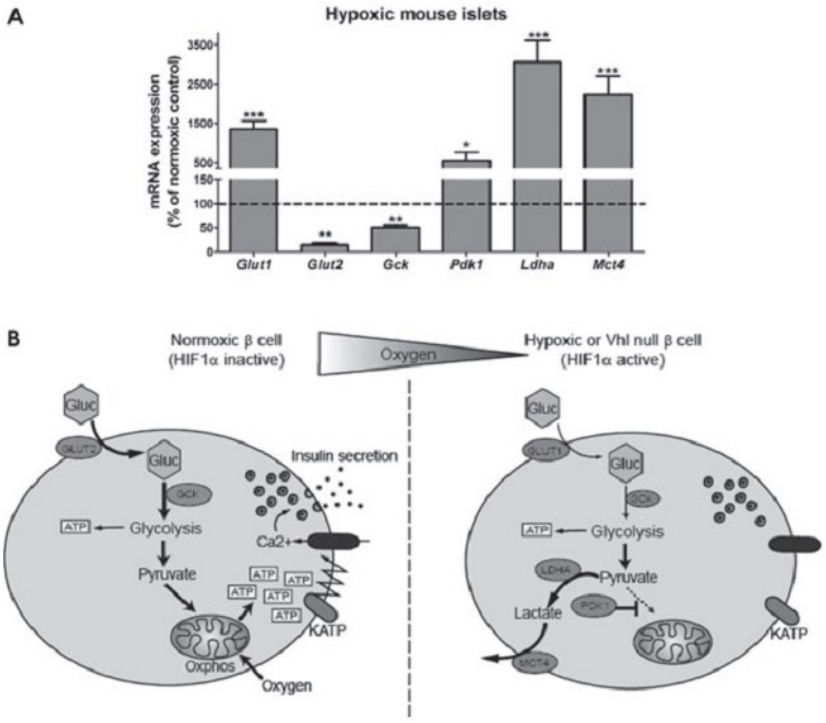

Figure 2.2: Response of islets to hypoxic conditions. A) Changes in gene expression resulting from 16 hours of culture in a hypoxic environment (1% O_2). B) Hypoxic culture conditions affect the ability of β cells to secrete insulin. Reproduced with permission from Cantley et al. 2010.

As demonstrated in Figure 2.2, hypoxia leads to changes in gene expression and breakdown of cellular metabolism. This leads to a reduction in ATP production. Closure of ATP dependent potassium channels leads to insulin secretion, but in a hypoxic environment these channels remain open. Studies have demonstrated the inhibitory effect of hypoxia on β cell function (Dionne, Colton, & Yarmush, 1993; Papas, Long Jr., Constantinidis, & Sambanis, 1996). Papas et al. investigated the effect of different oxygen tensions on the insulin secretion from transformed β cells and found significant reduction in insulin secretion happened at lower oxygen tension (7 mmHg) than in islets (50% secretion compared to normoxic control occurred at 27 mmHg O_2) (Dionne et al., 1993). This may be due to the size of the islet creating gradients in oxygen tension within the islet (Papas et al., 1996; Thomas M Suszynski et al., n.d.). Protocols which provide better oxygenation during pancreas preservation (William E Scott III et al., 2010) or islet cell transport (Avgoustiniatos et al., 2008), increase revascularization (H. A. Kim et al., 2009; Narang et al., 2004), or deliver agents to protect from hypoxia (Ah Kim et al., 2009; C. Chen et al., 2011; Emamaullee, Rajotte, et al., 2005) have attempted to address the issue of prevailing hypoxia before and after islet transplantation.

In addition to the issues above, hypoxia combined with reoxygenation of the tissue can injure cells through reactive oxygen species (ROS) and reactive nitrogen species (RNS) (C. Li & Jackson, 2002). To improve survival rates of the stressed islet cells, researchers have investigated various interventional strategies. Delivery or overexpression of different antioxidants has been one area of investigation. Islet cells have naturally low levels of many

of these antioxidants, increasing their susceptibility to oxidative stress (Benhamou et al., 1998; Lenzen, Drinkgern, & Tiedge, 1996). The stable overexpression of glutathione peroxidase, catalase, and copper-zinc superoxide dismutase have all been shown to protect insulin-producing β cells from the effects of different ROS *in vitro* (Lepore et al., 2004; Tiedge, Lortz, Munday, & Lenzen, 1998, 1999). Vitamin E analogs have also been shown to protect islets from periods of anoxia (Oz, Wildey, Kendir, & Papas, 2007). Antioxidants capable of scavenging more than one species of ROS are favored for islet protection. Metallothionein is a cysteine-rich protein that binds heavy metals and functions as an antioxidant. It has been demonstrated to scavenge a wide variety of ROS in islets and improve allotransplantation results in mice receiving treated versus non treated islets (X. Li, Chen, & Epstein, 2004). While many of these therapies do improve islet cell viability *in vitro* and some have demonstrated efficacy *in vivo*, the problem that persists is the activation the death responses occurring during the isolation. Therefore, a strategy to counter the stress induced death mechanisms before isolation may be beneficiary (Bottino et al., 2004).

2.2.5 Islet Encapsulation

The harsh side effects of immunosuppression therapy on both the transplanted islets and the patient limit the potential use of islet transplantation. Encapsulating islets in a semi-permeable membrane has been used as a strategy to protect the islets from recognition by the host's immune system and therefore decrease, or even rid, the need for immunosuppression therapy. Additionally, encapsulation may promote the application of alternative cells sources, including xenografts (T. Wang et al., 2008). The first effort at encapsulation was accomplished by Lim and Sun in 1980. They encapsulated islets in a

polylysine alginate microcapsule and were able to reverse diabetes in non-immunosuppressed mice for 3 weeks (Lim & Sun, 1980). This technique has since been studied by many investigators (Reviewed by Beck et al. (2007) and Rabanel et al. (2009)) and has included use of biopolymers (i.e. alginate, agarose) (Cui et al., 2004; Gazda et al., 2007; Kobayashi et al., 2003; Safley, Kapp, & Weber, 2002; Teramura & Iwata, 2010a; T. Wang et al., 2008), polyelectrolyte multilayers (Miura, Teramura, & Iwata, 2006; Wilson et al., 2011; Wilson, Cui, & Chaikof, 2008), silica sol-gels (Carturan, Toso, Dal, & Monte, 2004; Snyder et al., 2009), and live cells (Teramura & Iwata, 2009a; Teramura, Minh, Kawamoto, & Iwata, 2010). Including PEG as either a base layer or as part of a layer-by-layer strategy is a popular approach to increase the biocompatibility of the encapsulation (Cruise, Hegre, Scharp, & Hubbell, 1998; Miura et al., 2006; Sawhney, Pathak, & Hubbell, 1994; Teramura & Iwata, 2009b; Teramura, Kaneda, & Iwata, 2007; Teramura et al., 2010; Wilson et al., 2008; Xie et al., 2005). However, the polymer does not remain stably on the surface of the cells unless it is covalently bonded (Inui, Teramura, & Iwata, 2010). All microcapsules must allow sufficient transport of nutrients and hormones to the cell and secretory and waste products away from the cell. At the same time, large proteins and immunogenic molecules (i.e. antibodies, lymphocytes) must be excluded. While the aforementioned systems all boast the ability to protect the islets from cell-mediated immune destruction, inhibiting the flux of smaller factors such as cytokines, chemokines, and small antigens is much more difficult. Small molecules released from the transplanted islets can be taken up by resident antigen presenting cells and activate the immune system (Gray, 2001). Although T cells and B cells cannot directly act on the encapsulated cells, once activated they secrete proinflammatory molecules which further promote the release of factors such as nitric oxide (NO) (Groot et

al., 2003). The smaller proinflammatory molecules and NO can then diffuse through the capsule leading to damage or death of the islet cells.

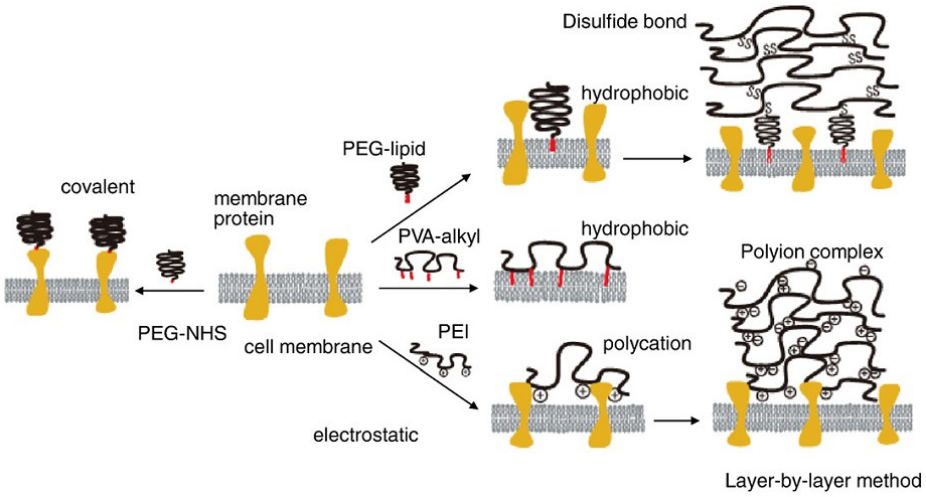

Figure 2.3: Conformal encapsulation strategies. Cells are encapsulated by harnessing covalent bonding, hydrophobic interactions, or layer-by-layer using oppositely charged polyions. Reproduced from Teramura and Iwata 2010a with permission from Elsevier.

Layer-by-layer strategies are advantageous due to the ability to better control the size exclusion properties by tailoring the materials and number of coatings, while retaining a thin, conformal coating. Many of the other microencapsulation techniques dramatically increase the total volume of the encapsulated islets (Groot et al., 2003; Kobayashi et al., 2003; Safley et al., 2002). The increased size increases the total transplanted volume, therefore limiting certain transplant sites, including the portal vein. Additionally, the increased size can inhibit oxygen and nutrient diffusion, further promoting a hypoxic environment. Therefore, a promising microcapsule would be thin and biocompatible, have precise pore size control, exclude antibodies, large proteins, immune cells, chemokines, and cytokines, allow transport of nutrients and hormones to and from the cells, and allow modifications to provide enhanced immunomodulation.

2.3 Targeted Drug Delivery

In this work, we demonstrate the utility of a targeted drug delivery system for protection of β cells from ischemic insult. The study is documented in Chapters 3 and 4. Each chapter is accompanied by a brief introduction of relevant literature. The following sections will provide background information on targeted drug delivery and previous applications of ATP liposomes.

2.3.1 Liposomes for Drug Delivery

Liposomes have been used for a wide variety of applications in the last few decades with many reviews devoted to this research field. One predominant area of research is the application of liposomes for anticancer drug delivery. Drugs encapsulated in larger particles tend to accumulate in the tumor via the enhanced permeability and retention (EPR) effect (reviewed by Maeda et al. 2000). In this way the nanoparticles can increase the ability of the drug to reach the tumor site. Functionalizing the nanoparticles with a ligand that recognizes a cell surface receptor enhances the transport of the nanoparticle into the tumor cells once it has reached the tumor environment. Peptides are the most commonly used targeting ligand due in part to their ability to recognize many different cell targets. The current status of peptide targeted lipid nanoparticles is reviewed by Pearce et al. (2012).

While liposomes are most widely known for targeting cancer cells, they are also used in other applications including gene delivery, antifungal treatments, ischemia-reperfusion treatment, insulin delivery, and diagnostics (Reviewed in Torchilin 2005). In this work we are investigating the delivery of ATP to β cells exposed to ischemic conditions.

2.3.2 ATP LIPOSOMES

ATP is the most abundant source of energy in cells. As mentioned previously, ischemic conditions deplete cells' ATP levels, leading to a series of events that ultimately ends in cell necrosis (Michiels, 2004). Hydrolysis of ATP *in vivo* makes direct delivery of the ATP to the ischemic tissues (Korb et al., 2008; Tep et al., 2009) difficult.To increase delivery of ATP to the tissues and protect from degradation, encapsulation in liposomes has been proposed and demonstrated in various models of ischemia (Verma, Levchenko, et al., 2005). Studies on myocardial (Hartner et al., 2009; Levchenko et al., 2010; Verma, Hartner, Levchenko, Bernstein, & Torchilin, 2005; Verma, Levchenko, et al., 2005), liver (Hayashi et al., 1997; Korb et al., 2008; Neveux et al., 2002; Tep et al., 2009), retina (Dvoriantchikova, Barakat, Hernandez, Shestopalov, & Ivanov, 2010), and wound healing(Chiang et al., 2007; Chien, 2010; J. Wang et al., 2010) ischemia have shown the ability of liposomal encapsulated ATP (ATPL) to prevent cell death and tissue dysfunction following ischemic events. Liposome encapsulation protects the ATP from enzymatic degradation and enhances ATP penetration into the cells.

Liang et al. (2004) evaluated different methods of formulating ATPL. They looked at lipid film hydration, pH gradient, reverse phase evaporation, and freeze-thawing. They found that the freeze-thawing method (lipid film hydration plus freeze-thawing) led to the highest encapsulation of ATP. They also evaluated different separation processes and found that gel filtration, centrifugation, and dialysis all lead to similar outcomes. By using the freeze-thaw method combined with gel filtration for separation, the ATP encapsulation efficiency was 0.38 μmole ATP per μmole lipid. This group has harnessed ATPL for protection of myocardial cells from ischemic conditions (Figure 2.4) (Hartner et al., 2009; Levchenko et

al., 2010; Wei Liang, Levchenko, Khaw, & Torchilin, 2004; Verma, Hartner, et al., 2005; Verma, Levchenko, et al., 2005). Additionally, ATPL functionalized with an anti-myosin antibody had an additional improvement over nonfunctionalized ATPL in an isolated ischemic heart model. The antibody allows the liposomes to target myosin exposed in cells with compromised membranes. The authors found that in the isolated heart model, free ATP had a beneficial effect on left ventricular developed and diastolic pressure (measurement of contractile function) but preincubation with ATPase ameliorated most of the benefit from free ATP while retaining that from ATPL (Hartner et al., 2009). *In vivo* the benefit of the free ATP would be unexpected because it is hydrolyzed by extracellular enzymes.

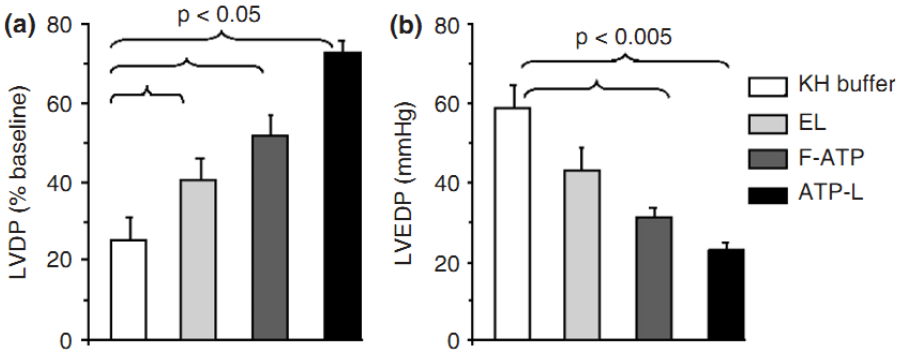

Figure 2.4: Protection of isolated rat heart by ATP liposomes. Treatments were delivered for one minute prior to ischemia onset. Ischemia was achieved by decreasing perfusion pressure to zero for 25 minutes and then the hearts were reperfused for 30 minutes. Left ventricular developed (LVDP) and left ventricular end diastolic pressure (LVEDP) was measured as an indicator of contractile function. ATP liposomes (ATP-L) had the best recovery of contractile function compared to empty liposomes (EL), free ATP (F-ATP), and buffer (KH buffer). Reproduced with permission from (Hartner et al., 2009).

ATPL have also been used in other applications. ATP content in hepatocytes is decreased during hypoxia, affecting viability and function of the cells (Hayashi et al., 1997). ATPL were used to benefit cold-stored livers by increasing the energy status and preserving cell volume (Neveux et al., 2000, 2002). To increase the uptake of ATPL to hepatocytes,

liposomes were decorated with an original ligand, ASGPr, which interacts with the asialoglycoprotein receptors. However, incorporation of this ligand did not improve the internalization of liposomes, which was demonstrated by fluorescent labeling as well as by a lack of increase in intracellular ATP in cells treated with liposome formulations (Tep et al., 2009). The use of ATPL with liver applications has been reviewed by Korb et al. (2008). ATPL have also been used in wound healing applications. Fusogenic ATP liposomes decreased the healing time for full thickness skin wounds compared to empty liposomes in mice (Chiang et al., 2007) and rabbits (J. Wang et al., 2010). The ATPL effect on healing time was investigated for both ischemic and non-ischemic rabbit tissue wounds and found to significantly decrease the healing time in both conditions.

These applications demonstrate the promise of ATP liposomes for ischemic insults. Efforts to increase internalization by adding ligands or changes to liposome composition have indicated that one of the primary barriers to ATP delivery is getting the liposome and cargo into the cell. In this work we demonstrate the application of ATPL to ischemic β cells and incorporate a targeting ligand to facilitate internalization of the liposomes.

2.3.3 Fibronectin-Mimetic Peptide, PR_b

As mentioned earlier, peptides are a common ligand used to increased liposome binding and internalization into cells. The Arg-Gly-Asp (RGD) peptide is a common peptide ligand used to target integrins present on the cell surface (Kokkoli et al., 2006; Ruoslahti, 1996). RGD is the primary binding site for the fibronectin protein to the $\alpha_5\beta_1$ integrin (Leahy, Aukhil, & Erickson, 1996). Although RGD is fibronectin's primary binding domain, it lacks the binding strength and affinity to $\alpha_5\beta_1$ of native fibronectin (García, Schwarzbauer, &

Boettiger, 2002). Native fibronectin's high affinity to the $\alpha_5\beta_1$ integrin is due to the presence of both the RGD binding domain and the Pro-His-Ser-Arg-Asn (PHSRN) synergy domain (Burrows, Clark, Mould, & Humphries, 1999; Redick, Settles, Briscoe, & Erickson, 2000). These two domains are separated by approximately 35 Å (Leahy et al., 1996). The Kokkoli group previously hypothesized that by mimicking the distance and hydrophobicity/ hydrophilicity between RGD and PHSRN, a peptide could be developed with increased binding strength and specificity for $\alpha_5\beta_1$. The fibronectin-mimetic peptide designed, termed PR_b, is composed of a spacer (KSS) at the N terminus, the fibronectin synergy sequence (PHSRN), a linker ($(SG)_5$), and the primary binding sequence (RGDSP) (Mardilovich et al., 2006). The linker is 37 Å in length and has a 1:1 hydrophobicity/ hydrophilicity ratio, similar to that of native fibronectin (Mardilovich & Kokkoli, 2004). To create a peptide-amphiphile, PR_b can be conjugated to a dialkyl tail. The PR_b peptide-amphiphile is composed of a C_{16} dialkyl ester tail with a glutamic acid (Glu) tail linker and $-(CH_2)_2-$ tail spacer connected to the N terminus of the PR_b peptide ($(C_{16})_2$-Glu-C_2-KSSPHSRN$(SG)_5$RGDSP).

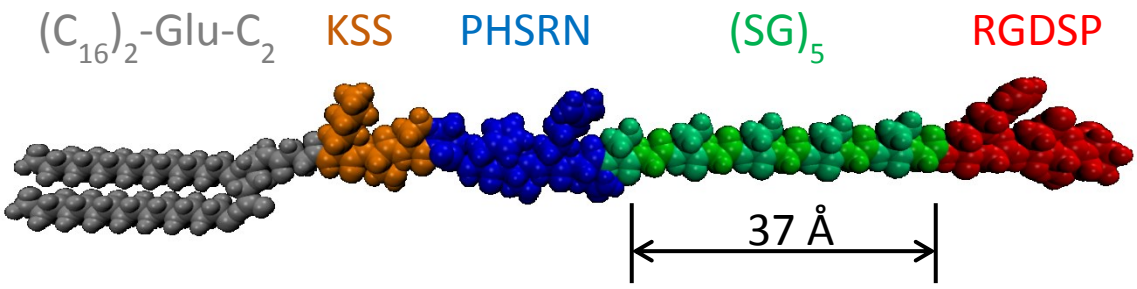

Figure 2.5: Design of PR_b peptide-amphiphile.

The degree of hydrophobicity/ hydrophilicity of the linker region affects the peptide's binding strength to $\alpha_5\beta_1$. Surfaces functionalized with the PR_b peptide-amphiphile were

compared to surfaces functionalized with peptide-amphiphiles containing both the RGD and PHSRN domains spanned by either purely hydrophobic or purely hydrophilic linkers (Craig et al., 2008). PR_b outperformed the other sequences in both binding strength and endothelial cell adhesion. PR_b surfaces were also compared to surfaces functionalized with GRGDSP, 50 mol% GRGDSP-50 mol% PHSRN randomly presented at the interface, and native fibronectin. PR_b outperformed fibronectin and other peptide surfaces in terms of cell adhesion, cell spreading, $\alpha_5\beta_1$ specificity, cytoskeleton organization, and ECM fibronectin production (Mardilovich et al., 2006; Shroff, Pearce, & Kokkoli, 2012). Single tailed versions of the peptide-amphiphile (PR_g) have been used to form nanofiber hydrogels (Rexeisen et al., 2010; Shroff, Rexeisen, Arunagirinathan, & Kokkoli, 2010). These PR_g hydrogels were compared to control gels and shown to increase cell adhesion, cytoskeleton organization, and ECM production.

2.3.4 Drug Delivery with PR_b Functionalized Vesicles

PR_b has also been used to functionalize liposomes and polymersomes for drug delivery to cancer cells expressing the $\alpha_5\beta_1$ integrin. PR_b functionalized stealth nanoparticles have shown PR_b concentration dependent binding to prostate cancer (Demirgöz et al., 2008), colon cancer (Garg et al., 2009), and breast cancer cells (Pangburn, Bates, & Kokkoli, 2012; Pangburn, Georgiou, Bates, & Kokkoli, 2012; Shroff & Kokkoli, 2012). Additionally, these studies demonstrated increased efficacy of PR_b functionalized stealth nanoparticles compared to nanoparticles functionalized with GRGDSP. The specificity of PR_b to $\alpha_5\beta_1$ has been demonstrated with blocking experiments using antibodies (Pangburn, Bates, et al., 2012) or free peptide (Garg et al., 2009; Pangburn, Georgiou, et al., 2012; Shroff & Kokkoli, 2012) to block the cell surface $\alpha_5\beta_1$ integrin receptors. These studies indicate that the

binding and uptake of the PR_b functionalized nanoparticles is through interactions with the $\alpha_5\beta_1$ integrins. Studies on PR_b functionalized nanoparticle internalization and trafficking have demonstrated that the nanoparticles are internalized through receptor-mediated endocytosis and colocalize with early and late endosomes after internalization (Shroff & Kokkoli, 2012).

CHAPTER 3

BINDING OF THE FIBRONECTIN-MIMETIC PEPTIDE, PR_B, TO $\alpha_5\beta_1$ ON PIG ISLET CELLS INCREASES FIBRONECTIN PRODUCTION AND FACILITATES INTERNALIZATION OF PR_B FUNCTIONALIZED LIPOSOMES

3. 1 SYNOPSIS

Islet transplantation is a promising treatment for type 1 diabetes. Recent studies have demonstrated that human islet allografts can restore insulin independence to patients with this disease. As islet isolation and immunotherapeutic techniques improve, the demand for this cell-based therapy will dictate the need for other sources of islets. Pig islets could provide an unlimited supply for xenotransplantation and have shown promise as an alternative to human islet allografts. However, stresses imposed during islet isolation and transplantation decrease islet viability, leading to loss of graft function. In this study, we investigated the ability of a fibronectin-mimetic peptide, PR_b, which specifically binds to the $\alpha_5\beta_1$ integrin, to reestablish lost extracellular matrix (ECM) around isolated pig islets and increase internalization of liposomes. Confocal microscopy was used to show the presence of the integrin $\alpha_5\beta_1$ on the pig islets on days 0 (day of isolation), 1, 2, 3, 7, and 11 of culture. Islets cultured in medium supplemented with free PR_b for 48 hours were found to have increased levels of ECM fibronectin secretion compared to islets in normal culture conditions. Using confocal microscopy and flow cytometry we found that PR_b peptide-amphiphile functionalized liposomes delivered to the pig islets internalized into the cells in a PR_b concentration dependent manner, and non-functionalized liposomes showed no

internalization. These studies proved that the fibronectin-mimetic peptide, PR_b, is an appropriate peptide bullet for applications involving $\alpha_5\beta_1$ expressing pig islet cells. Fibronectin production stimulated through $\alpha_5\beta_1$ PR_b binding may decrease apoptosis and therefore increase islet viability in culture. In addition, PR_b peptide-amphiphile functionalized liposomes may be used for targeted delivery of different agents to pig islet cells.

3.2 INTRODUCTION

Type 1 diabetes continues to present therapeutic challenges. Recent results have shown the potential of islet transplantation as an alternative to whole pancreas transplantation for diabetes treatment (Hogan, Pileggi, & Ricordi, 2008). Several programs have reported successful restoration of normoglycemia and insulin independence in immunosuppressed patients who received human islet allografts (Froud et al., 2005; Hering et al., 2005; Shapiro et al., 2000, 2006). As of 2005, 82% of patients receiving human islet allografts at the three leading islet transplantation centers were insulin independent at one year post islet transplant completion (Shapiro et al., 2005; Shapiro & Ricordi, 2004). As this cell-based therapy benefits from improved isolation and immunotherapeutic techniques, the demand for islet replacement therapy will increase, straining the already short supply of human islet donors (Rood et al., 2006). Porcine islets could provide an unlimited supply for islet transplantation and have shown promise as a successful alternative to human islet allografts (Cardona et al., 2006; Cozzi & Bosio, 2008; Dufrane & Gianello, 2008; Hering et al., 2006; Hering & Walawalkar, 2009; Kin, Korbutt, Kobayashi, Dufour, & Rajotte, 2005; Rood et al., 2006). Porcine islets are advantageous due in part to the on-demand availability of young, healthy, living, pathogen-free donors, and the ease of breeding (Bottino et al., 2007;

Rood et al., 2006). Additionally, porcine islets respond to blood glucose concentration similarly to human islets and porcine insulin has been used for daily injections, differing from human insulin by only one amino acid (Rother & Harlan, 2004; Schernthaner, 1993; Sutherland et al., 1974; Z. J. Zhang et al., 1991).

The isolation process affects both human and porcine islet cell viability (Paraskevas et al., 2000; Rosenberg et al., 1999). The loss of viability stems, at least in part, from the loss of extracellular matrix (ECM) from the islets' environment (Ris et al., 2002; Rosenberg et al., 1999; R. Wang & Rosenberg, 1999). Adhesion to ECM is mediated through integrin receptors. $\alpha_5\beta_1$ is an important integrin for promoting cell adherence, spreading, survival, and angiogenesis (S. Kim, Bell, Mousa, & Varner, 2000; J. W. Lee & Juliano, 2000; Meredith & Schwartz, 1997; O'Brien, Frisch, & Juliano, 1996; Z. Zhang et al., 1995). It binds the Arg-Gly-Asp (RGD) sequence of ECM proteins including fibronectin, vitronectin, and fibrinogen (Danen & Yamada, 2001; Pierschbacher & Ruoslahti, 1984). Fibronectin also contains a synergy sequence Pro-His-Ser-Arg-Asn (PHSRN) that contributes to the high affinity of the $\alpha_5\beta_1$ integrin to fibronectin (Burrows et al., 1999; Kokkoli, Ochsenhirt, & Tirrell, 2004; Mould, Askari, & Humphries, 2000; Takagi, 2004). Regarding islets, various integrins have been studied to determine their role in the development of the pancreas and in islet survival (Pinkse et al., 2006; Ris et al., 2002; Rosenberg et al., 1999; R. Wang et al., 2005, 1999; R. Wang & Rosenberg, 1999). The integrin repertoire displayed on islets from human (R. Wang et al., 2005, 1999), hamster, porcine (R. Wang et al., 1999), canine (R. Wang & Rosenberg, 1999), and rat (Pinkse et al., 2006) lines have been investigated by various groups. Wang et al. (R. Wang et al., 1999) studied porcine islets and found expression of integrin subunits α_2, α_3, α_5, and α_v but not β_1.

RGD peptides are commonly used as bullets for targeting integrins including $\alpha_5\beta_1$ (Kokkoli et al., 2006; Ruoslahti, 1996). However, RGD peptides do not have the same binding strength and affinity as native fibronectin (García et al., 2002; Pangburn et al., 2009) thus limiting their therapeutic use. Previously, we hypothesized that a peptide mimicking both the distance and hydrophilicity/hydrophobicity between the primary binding RGD domain and the PHSRN synergy site on fibronectin could increase the peptide's binding affinity and specificity to $\alpha_5\beta_1$ (Mardilovich et al., 2006; Mardilovich & Kokkoli, 2004). In native fibronectin the distance between RGD and PHSRN is 30-40 Å (Leahy et al., 1996). We sought to mimic this distance and the relative hydrophilicity/hydrophobicity of the region spanning the two sequences. We designed a peptide, PR_b, composed of a spacer (KSS) at the N terminus, the fibronectin synergy site sequence (PHSRN), a linker ($(SG)_5$) and the primary binding sequence (RGDSP) (Mardilovich et al., 2006). The length of the linker is 37 Å and the hydrophilicity/hydrophobicity ratio is 1:1; one hydrophobic glycine (G) to one hydrophilic serine (S) amino acid, reflecting the approximate ratio found in native fibronectin (Mardilovich et al., 2006; Mardilovich & Kokkoli, 2004). PR_b was synthesized as a peptide-amphiphile by conjugating it to a dialkyl tail (Figure 3.1). The design features the PR_b headgroup, a C_{16} dialkyl ester tail with a glutamic acid (Glu) tail linker and $-(CH_2)_2-$ tail spacer. The $(C_{16})_2$-Glu-C_2 was connected to the N terminus of PR_b. Our original hypothesis stated that the degree of hydrophilicity/hydrophobicity is an important design parameter for a fibronectin-mimetic peptide. We compared the PR_b peptide-amphiphile to similar peptide-amphiphiles containing the RGD and PHSRN sequences spanned by a purely hydrophobic or purely hydrophilic region (Craig et al., 2008). We found that PR_b outperformed the other peptide sequences in binding strength and human umbilical vein endothelial cell (HUVEC) adhesion. We have also compared surfaces functionalized with

PR_b to surfaces functionalized with GRGDSP, 50 mol% GRGDSP- 50 mol% PHSRN randomly presented at the interface, and native fibronectin. We demonstrated that the PR_b functionalized surfaces outperformed fibronectin and other peptide surfaces in terms of HUVEC cell adhesion, cell spreading, $\alpha_5\beta_1$-specificity, cytoskeleton organization, and ECM fibronectin production (Mardilovich et al., 2006). The PR_b peptide-amphiphile (PR_b PA) was also used for targeted drug delivery (Demirgöz et al., 2009, 2008; Garg et al., 2009) and tissue engineering applications (Rexeisen et al., 2010). PR_b PA functionalized conventional and stealth liposomes (liposomes covered with polyethylene glycol, PEG) showed improved cell binding and internalization as compared to non-targeted liposomes or liposomes functionalized with GRGDSP in prostate cancer cells (Demirgöz et al., 2008) and colon cancer cells (Garg et al., 2009). We have demonstrated specificity of PR_b to $\alpha_5\beta_1$ by blocking cell adhesion with antibodies(Mardilovich et al., 2006) and liposomal cell internalization with free PR_b (Garg et al., 2009).

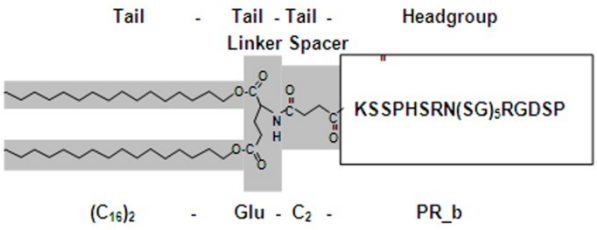

Figure 3.1: Schematic of PR_b peptide-amphiphile

Losses of porcine islet viability during isolation and after transplantation are major problems in xenotransplantation of the fresh porcine islets. The goal of this study was to examine $\alpha_5\beta_1$ expression on porcine islet cells and determine if PR_b is an appropriate peptide for targeting islets in culture. We hypothesized that the PR_b peptide could increase the production of ECM proteins, such as fibronectin, in cultured islets, thus reestablishing

the ECM that was lost during digestion. We also hypothesized that PR_b PA functionalized liposomes would show increased internalization into porcine islet cells thus providing a possible mechanism for enhanced delivery of encapsulated agents of interest for cytoprotecting, immunomodulating, as well as imaging of cultured porcine islets after transplantation. We envision a scenario in which PR_b could be used in a multi-faceted approach to protecting and maintaining islet viability. Free PR_b peptide would be used to target islets soon after isolation to prevent apoptosis and increase islet yield. Then, PR_b PA functionalized liposomes would be targeted to islets *ex vivo* to deliver molecules that could protect the islets from hypoxic and other stresses encountered after transplantation or allow for monitoring viability and imaging islets after transplantation. Therefore in this study we first present evidence of $\alpha_5\beta_1$ integrin expression on the porcine islet cells on the days following islet isolation for the first time in literature. We go on to show increased fibronectin production from porcine islets cultured with supplemented PR_b. Finally, our data show that PR_b PA functionalized liposomes internalize into porcine islets in a concentration dependent manner while non-targeted liposomes do not internalize.

3.3 Materials and Methods

3.3.1 Porcine Islet Isolation and Oxygen Consumption Rate Analysis

Porcine islets were isolated and cultured free-floating as previously described (H. Brandhorst et al., 1999; Kirchhof et al., 2004; Ricordi, Socci, et al., 1990; Van der Burg, Basir, & Bouwman, 1998). Islet quality control (Ricordi, Gray, et al., 1990) revealed 1,789 ± 1,194 islet equivalents (IE)/g pancreas, corresponding to an average islet yield of 92% ± 35% IE. IE is a spherical aggregate of cells with a 150 μm mean diameter (Colton et al., 2007). The purity of the islet graft as assessed by the percentage of dithizone-positive cells was >90%

(mean, 94%). For all experiments, the number of IE was determined based on IE availability and number of IE required to perform the experiment. Oxygen consumption rate (OCR) analysis was used to determine islet viability and was performed as described previously (Papas, Colton, et al., 2007; Papas, Pisania, Wu, Weir, & Colton, 2007). The OCR/DNA on day 7 ranged from 71-276 nmol/min-mg DNA. OCR analysis was also used to evaluate PR_b cytotoxicity. The OCR/DNA ratio of islets exposed to 0.1 mg/mL PR_b for 24 or 72 hours of culture was compared to control islets at those time points. Data were obtained from nine pig isolations.

3.3.2 Integrin Expression.

Approximately 100 IE were removed from culture for each sample, pelleted in microcentrifuge tubes by centrifugation at 800 rpm for one minute in a tabletop centrifuge, and washed twice with phosphate buffered saline (PBS). Samples were incubated at 4°C with primary antibodies to $\alpha_5\beta_1$ (JBS5), α_5 (P1D6), and β_1 (HB1.1) (Millipore, Temecula, CA) at a 1:33 dilution over a rotary shaker for one hour. Islets were pelleted and washed twice in PBS, incubated at 4°C with secondary antibody, anti-mouse IgG FITC-conjugated (Millipore), at a 1:33 dilution over a rotary shaker for one hour, pelleted and washed twice. Nuclear staining was performed using a cell membrane permeable blue-fluorescent Hoechst 33342 dye (Molecular Probes, Eugene, OR) at a concentration of 2.0 μM and membrane staining was performed using a cell-impermeable red-fluorescent Alexa Fluor 594 wheat germ agglutinin (WGA; Molecular Probes) at 5.0 μM in PBS for 45 minutes at room temperature over a rotary shaker. Islets were washed twice, resuspended in PBS and prepared for immediate confocal microscopy analysis. The Olympus Fluoview FV1000 confocal laser scanning microscope at the Biomedical Image Processing Laboratory at the

University of Minnesota was used for all confocal studies. 10 to 15 z-scans (horizontal cross-section of the islet at a particular z height) were taken for each islet. Images shown are z-scans from the middle of the islet. The $\alpha_5\beta_1$ expression was analyzed on the specified days of culture for at least two different porcine islet isolations.

Integrin expression was also determined using western blot. Protein lysate from multiple isolated islet lots were received from the Schulze Diabetes Institute. Protein concentration was determined by the BCA™ Protein Assay Kit (Thermo Scientific, Waltham, MA) following the manufacturer's protocols. Samples were separated by 7.5% SDS-PAGE under non-reducing conditions, transferred to a polyvinylidene fluoride (PVDF) membrane (Bio-Rad), and analyzed by western blotting. Antibodies to α_5 (AB1949) and β_1 (AB1952), and the secondary antibody anti-rabbit horseradish peroxidase (HRP) conjugate (12-348) were purchased from Millipore. Blots were developed using a TMB (3,3',5,5'-tetramethylbenzidene) Stabilized Substrate for Horseradish Peroxidase (Promega, Madison, WI).

3.3.3 Fibronectin Production

Approximately 100 IE were removed from culture for each sample and suspended in 2 mL of warm culture medium (Medium 199 (Sigma) supplemented with 10% donor pig serum and ciprofloxacin) in disposable plastic dishes (BD Biosciences, San Jose, CA). Free PR_b peptide (received from the BioMedical Genomics Center at the University of Minnesota) dissolved in PBS was delivered to the islets at specific theoretical excesses as determined by the following calculation: Assuming an upper limit of 50,000 $\alpha_5\beta_1$ integrins per cell (Neff et al., 1982) and approximately 1,500 cells per IE (Colton et al., 2007), there are a total of $7.5*10^7$ $\alpha_5\beta_1$ integrins per IE. Therefore $1.25*10^{-16}$ moles of PR_b is necessary per islet for a

1:1 ratio of $\alpha_5\beta_1$ to PR_b. We gave concentrations of PR_b peptide at 5,000 (5Kx; 133 ng PR_b), 10,000 (10Kx; 267 ng), 20,000 (20Kx; 534 ng), and 100,000 (100Kx; 2,670 ng) times excess this theoretical 1:1 amount. The PR_b was added to the culture medium on the indicated day and allowed to incubate for 48 hours. After 48 hours the islets were stained with anti-fibronectin primary antibody specific for secreted fibronectin (P1H11, 1:133 dilution, Millipore) for 1 hour at 4°C over a rotary shaker and then stained with a secondary antibody (anti-mouse IgG FITC conjugated; 1:133 dilution) for one hour at 4°C. Nuclear and membrane staining were performed as described in the integrin expression section. Confocal images were taken immediately after sample preparation. 10 to 15 z-scans were taken for each islet. The FluoView software was used to create 2D z-projections of the optical sections. This image analysis technique projects the fluorescent features in each z-scan of the islet onto a common image plane positioned parallel to the source slices. The result is a single 2D composite representation of the fluorescent features from all slices included in the projection.

Fibronectin production was also analyzed using western blotting. After incubation for 48 hours with or without free PR_b in serum-free medium, the islet medium was collected and filtered three times for 30 minutes each with a 10KD centrifugal filter device (Millipore) at 4 °C. Filtration was necessary to remove excess free PR_b peptide present in the medium. Protein concentration was determined as above and 20 μg of protein was loaded into the gels. The samples were separated by SDS-PAGE under reducing conditions and transferred to a PVDF membrane. Fibronectin was detected with an anti-fibronectin antibody (AB1945, Millipore), followed by an anti-rabbit HRP conjugate secondary antibody. Membranes were

developed using TMB Stabilized Substrate for HRP and quantified using Quantity One software (Bio-Rad).

3.3.4 Liposome Preparation and Characterization

The PR_b peptide-amphiphile (PR_b PA) ($(C_{16})_2$-Glu-C_2-KSSPHSRN$(SG)_5$RGDSP) (PR_b headgroup KSSPHSRN$(SG)_5$RGDSP was purchased in crude form from the BioMedical Genomics Center at the University of Minnesota) was synthesized as described previously (Mardilovich & Kokkoli, 2004). Liposomes composed of 1,2-dipalmitoyl-*sn*-glycero-3-phophocholine (DPPC), cholesterol (Avanti Polar Lipids Inc., Alabaster, AL), and PR_b PA were prepared as described elsewhere (Fenske, Maurer, & Cullis, 2003). Briefly, DPPC, cholesterol, and PR_b PA solutions were combined at concentrations of *x* mol% PR_b PA, 35 mol% cholesterol, and (65-*x*) mol% DPPC. The liposomes were hydrated with 2 mM of calcein (excitation 494, emission 517) (Invitrogen, Carlsbad, CA) in HBSE buffer (10 mM HEPES, 150 mM NaCl, 0.1 mM EDTA, pH 7.4) at 65°C and at a final lipid concentration of 10 mM. The hydrated lipids were freeze-thawed five times and then extruded through two stacked 100 nm polycarbonate membranes (Avestin Inc., Ottawa, Canada) 21 times using a hand-held extruder (Avestin). Liposomes were filtered over a Sepharose CL-4B gel filtration column. Filtered liposomes were stored at 4-8°C for up to 2 weeks before use. Phospholipid concentration was determined using the phosphorus colorimetric assay described elsewhere (P. S. Chen, Toribara, & Warner, 1956) and total PR_b PA concentration (on the inside and outside of the liposomes) was determined using the BCA assay according to the manufacturer's protocol. The ZetaPALS Zeta Potential Analyzer (Brookhaven Instruments, Holtsville, NY) was used to determine both the zeta potential (electric potential at the interfacial double layer of the liposome) and diameter of the liposomes by dynamic light scattering (DLS). Cyrogenic-transmission electron microscopy (Cryo-TEM) was used for

direct imaging of PR_b functionalized liposomes. Vitrobot (FEI Company) was used to prepare the Cryo-TEM samples. 3μL of liposome solution was put on lacey Formavar/Carbon grid. The grid was blotted for 1 second with an offset of -2. The specimen was immediately immersed into liquid ethane cooled close to its freezing point. The vitrified specimen was transferred, without rewarming, into a Gatan 613.DH cooling holder and observed on a JEOL 1210 TEM operated at 120 kV.

3.3.5 Liposome Internalization and Binding

For analysis of liposome internalization, approximately 150 IE were used per sample. The islets were removed from culture on the indicated day and suspended in 0.5 mL of culture medium. Liposomes were added at 250 μM lipid concentration and the islets were incubated at 37°C over a rotary shaker for the specified periods (24 or 48 hours). After incubation, the islets were pelleted and washed twice. The islets were then fixed in 4% paraformaldehyde in PBS (pH 7.4) for 15 minutes at 37°C. Cell nucleus and membrane staining were performed as described in the integrin expression section. Confocal images were taken immediately after sample preparation. 10 to 15 z-scans were taken for each islet. The FluoView software was used to create 2D z-projections of the optical sections as described above. Each treatment (day removed from culture, mol% PR_b PA, and length of incubation) was examined for at least two different islet isolations. For flow cytometry analysis, approximately 800 IE were used per sample. The islets were suspended in 1.5 mL of culture medium. Liposomes were added at 250 μM lipid concentration and the islets were incubated at 37°C over a rotary shaker for 24 hours. After incubation, the islets were pelleted and washed twice with Buffer A (0.5% bovine serum albumin (BSA) (Sigma), 2mM ethylenediaminetetraacetic acid (EDTA) in PBS). The islets were dissociated into a single

cell suspension by incubating at 37°C with 1 mL of cell dissociation buffer (Sigma) over a rotary shaker, pelleted and washed twice with Buffer A. The dissociated islets were resuspended in PBS and flow cytometry analysis was carried out immediately on a FACS Calibur instrument located at the Flow Cytometry Core facility in the Cancer Research Center of the University of Minnesota.

3.4 Results and Discussion

3.4.1 Integrin Expression

Porcine islet cells were stained for integrin subunits α_5 and β_1 and the $\alpha_5\beta_1$ complex on day 0 (day of isolation), day 1, day 2, day 3, day 7 and day 11 of culture. Intact islets were examined by confocal microscopy with 10-15 z-scans per islet. The images shown in Figures 3.2 and 3.3 are z-scans taken from the middle of the islet. Figure 3.2 A-F shows expression of $\alpha_5\beta_1$ on all days examined with no apparent trend in expression. Figure 3.3 shows expression of the individual α_5 (A, C) and β_1 (B, D) subunits on days 0 and 11 of culture. Protein lysates from porcine islets during days 0, 2, and 7 or 8 of culture were used to confirm the expression of the α_5 and β_1 subunits via Western blotting. These results are shown in Figure 3.3E. Under non-reducing condition α_5 runs at 155 kDa and β_1 at 110 kDa. These bands are apparent on the respective blots. The 220 kDa band on the β_1 blot represents a dimer of the β_1 subunits (Belkin, Kozlova, Bychkova, & Shekhonin, 1996), while the band at 150 kDa represent the β_1 chain associated with an α chain, seen previously in other reports (Paños et al., 2004; Richard et al., 1998). The α_5 and β_1 subunits have been shown to be expressed on islet cells from different species (Pinkse et al., 2006; R. Wang et al., 2005, 1999; R. Wang & Rosenberg, 1999), and α_5 has been shown to be expressed on

porcine islets (R. Wang et al., 1999), but we are the first to show the presence of β_1 on porcine islet cells.

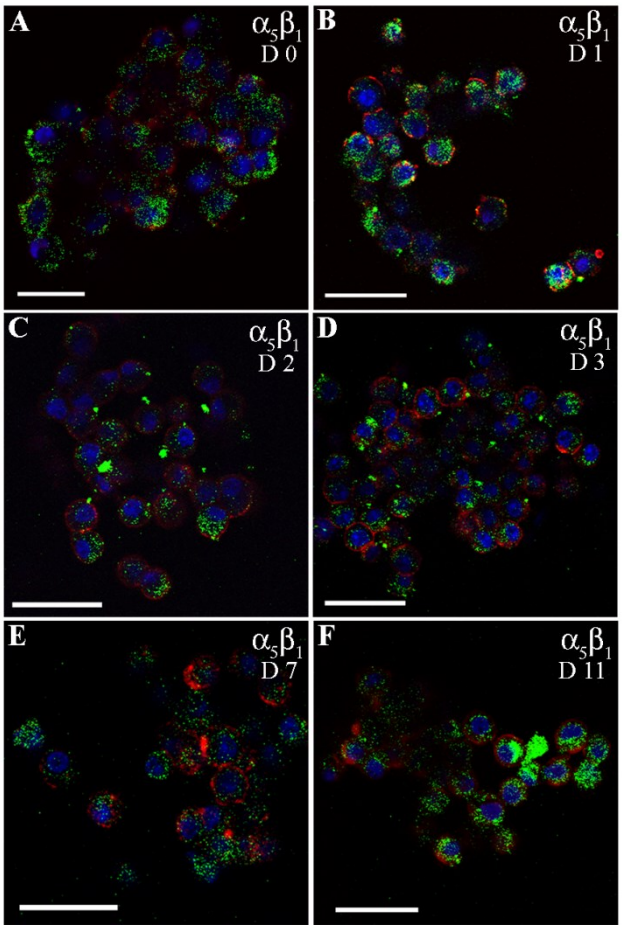

Figure 3.2: $\alpha_5\beta_1$ expression on porcine islets. Islets stained for $\alpha5\beta1$ (green), nucleus (blue), and cell membrane (red) on different days. $\alpha_5\beta_1$ was stained on A the day of isolation (D 0), B day 1 of culture (D 1), C day 2 of culture (D 2), D day 3 of culture (D 3), E day 7 of culture (D 7), and F day 11 of culture (D 11). The images are z-scans from the middle of the islet. All scale bars are 20 μm.

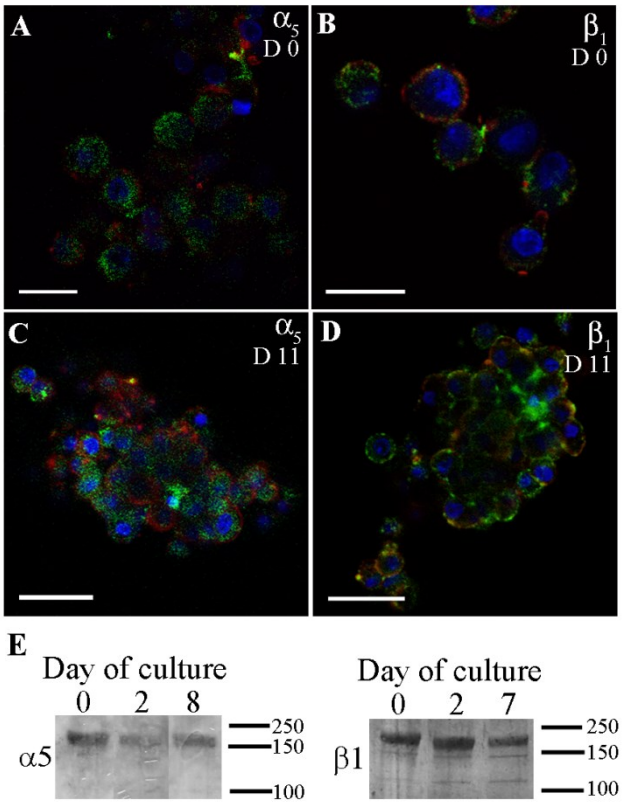

Figure 3.3: Expression of α_5 and β_1 on porcine islets of Langerhans characterized by confocal microscopy and Western blotting. Porcine islets were stained for α_5 or β_1 (green), nucleus (blue), and cell membrane (red) on different days of culture and imaged by confocal microscopy. α_5 was stained on A day 0 and C day 11 of culture. β_1 was also stained on B day 0 and D day 11 of culture. Separate islet samples were used to stain α_5 and β_1 so there is no colocalization of the subunits in the images. The images are z-scans from the middle of the islet. All scale bars are 20 μm. E Western blots showing expression of the integrin subunits α_5 and β_1 in porcine islet cells on days 0, 2, and 7 or 8 of culture. The molecular weight marker is shown to the right of each image.

3.4.2 Fibronectin Production

Incorporating ECM mimetic peptides into cellular environments has been shown to increase matrix production and cell viability (Hwang, Varghese, Zhang, & Elisseeff, 2006; Kisiday et al., 2002; H. J. Lee et al., 2006; Pinkse et al., 2006). Since $\alpha_5\beta_1$ was constitutively expressed on the cultured islet cells, PR_b (a fibronectin-mimetic peptide that specifically binds to $\alpha_5\beta_1$) was an excellent candidate for targeting these integrins. Our previous research demonstrated that PR_b has stronger adhesion to $\alpha_5\beta_1$ than the commonly used GRGDSP

peptide or other fibronectin-mimetic peptides (Craig et al., 2008; Mardilovich et al., 2006). Additionally, we found HUVECs attached to surfaces fully functionalized with PR_b had increased fibronectin production compared to other peptide and protein surfaces (Mardilovich et al., 2006). Therefore, we hypothesized that the addition of free PR_b peptide to the islet culture would increase ECM production, restoring the matrix lost during the isolation process. To ensure that PR_b is not cytotoxic to the islet cells OCR analysis was performed on islets isolated from nine different pigs that were cultured with or without 0.1 mg/mL PR_b for 24 or 72 hours. The presence of dead cells lowers the OCR/DNA ratio. Figure 3.4 shows that the OCR/DNA ratio was similar for islet cells cultured with or without PR_b at both time points demonstrating that PR_b is not cytotoxic to the islet cells.

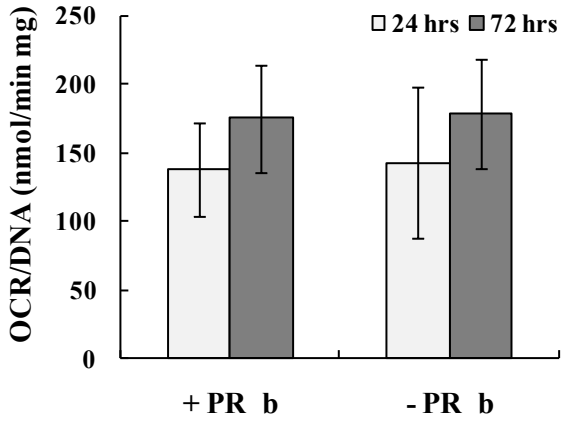

Figure 3.4: Oxygen consumption rate (OCR) per mg DNA for porcine islet cells incubated with 0.1 mg/mL free PR_b (+ PR_b) or without PR_b (-PR_b) for 24 or 72 hours of culture. The experiment was performed on islets from nine isolations (n=9). Data are expressed as the mean ± standard deviation. Data provided by the Schulze Diabetes Institute.

To determine if PR_b can reestablish the production of ECM after islet isolation we added free PR_b to islet samples during the culture period. Porcine islets do not attach to the culture flask so integrin binding is dependent only on ligands present in the medium. The

concentrations of PR_b employed were determined by calculating a hypothetical amount of PR_b necessary to bind to a theoretical number of $\alpha_5\beta_1$ integrins on the islet cells, assuming one molecule of PR_b binds to one integrin. PR_b was added to the culture medium in amounts excess of this 1:1 concentration. PR_b was supplemented at 5,000 (5Kx), 10,000 (10Kx), 20,000 (20Kx), and 100,000 (100Kx) times excess this theoretical concentration to the culture medium of the islet samples on day 2 of culture after isolation (day 0) and allowed to incubate for 48 hours before the islets were analyzed with confocal microscopy. The results are shown in Figure 3.5 and are 2D z-projections of all the fluorescent features from the multiple layers of the islet that were captured. Islets incubated with 5Kx (Figure 3.5B), 10Kx (Figure 3.5C), and 20Kx (Figure 3.5D) free PR_b showed fibronectin production within the core of the islet as well as at the periphery, while control samples (Figure 3.5A) showed minimal fibronectin production primarily at the periphery of the islet. This result is representative of all samples analyzed. 20Kx of PR_b promoted the highest level of fibronectin production. Adding 100Kx (Figure 3.10) did not further increase the fibronectin production levels possibly because the $\alpha_5\beta_1$ integrins were fully saturated. Free PR_b at the same concentrations was also added to islets on day 0 and allowed to incubate for 48 hours for western blotting analysis. The medium from these samples was analyzed to quantify the amount of fibronectin present. The blot shown in Figure 3.6 demonstrates that increasing PR_b leads to more fibronectin production, and that 20Kx produces significantly ($p < 0.05$) more fibronectin than the control or 5Kx samples. These trends are similar to the trends found by quantifying confocal images of PR_b supplemented islets (Figure 3.11). Together these results show that the PR_b peptide induces increased fibronectin production in free floating islets. Fibronectin production is beneficial for islets because it reestablishes integrin-matrix interactions which provide survival signals to the cell (Danen & Yamada,

2001; Meredith & Schwartz, 1997). Analyzing the effects of this increased fibronectin production on the viability of the porcine islets in culture is the subject of future work.

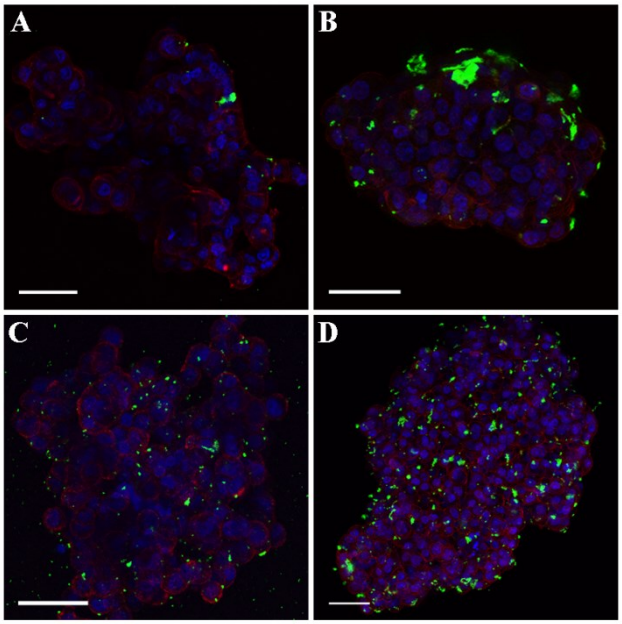

Figure 3.5: Fibronectin production. PR_b was added to the culture medium on day 2 of culture and the islets were imaged 48 hours later by confocal microscopy. Images show the cell membrane (red), nucleus (blue), and secreted fibronectin (green). The images are 2D z-projections of the fluorescent features from the multiple layers of the islet that were captured. The amount of PR_b added to the culture medium is as follows: A Control- no PR_b was added to the culture medium, B 5Kx (133 ng), C 10Kx (267 ng), D 20Kx (534 ng). All scale bars are 20 μm.

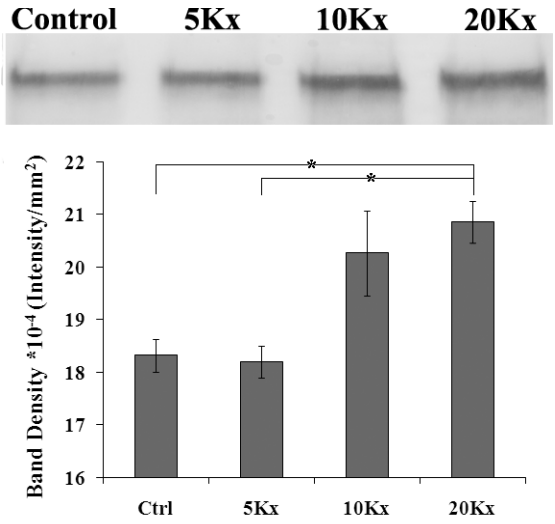

Figure 3.6: Western blot of fibronectin production. PR_b was added to serum-free culture medium on day 0 of islet culture and allowed to incubate for 48 hours. The resulting medium was analyzed by western blotting. The amount of PR_b added to the culture medium is as follows: Ctrl (no PR_b was added to the culture medium), 5Kx (133 ng), 10Kx (267 ng), and 20Kx (534 ng). The graph represents band density for *n*=2 replicates. Student t-test statistical analysis shows a significant difference between both the control and 5Kx samples compared to the 20Kx samples (*, $p < 0.05$).

3.4.3 Liposome Characterization and Internalization

Targeted drug delivery has many applications from disease treatment to imaging applications (Pangburn et al., 2009). We investigated the ability of PR_b PA functionalized conventional liposomes to bind and internalize into porcine islet cells. The use of liposomes to deliver agents of interest to islet cells in culture before transplantation could increase the delivery efficiency and lower the total amount of agent needed for the specific application. We hypothesized that by functionalizing the liposomes with PR_b PA we could increase internalization of conventional liposomes. We investigated whether conventional liposomes with no peptide or functionalized with different amounts of PR_b PA could bind and internalize in porcine islet cells in culture. Liposomes were characterized via DLS, zeta potential measurements, and cryo-TEM. We studied liposome internalization for a variety of liposome formulations, days of culture for islets, and incubation periods for liposomes. Since PR_b PA is the targeting bullet, the final mole percent of PR_b PA in the liposomes is

used to distinguish the different liposome formulations. The liposome formulations used in this study are shown in Table 3.1 in the Supplementary Information. Differences in size and zeta potential don't seem to play a role in the level of liposome internalization, therefore any differences in binding and internalization should stem from the amount of PR_b PA functionalized on the liposomes. Figure 3.7 shows a cryo-TEM image of liposomes functionalized with 1.6 mol% PR_b PA. The image shows a mean diameter of about 100 nm which is consistent with DLS data shown in Table 3.1 (Supporting Information).

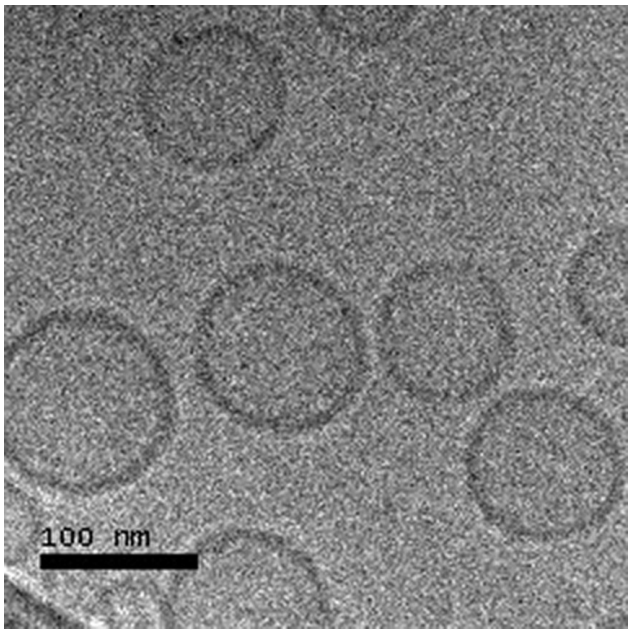

Figure 3.7: Cryo-TEM image of liposomes functionalized with 1.6 mol% PR_b PA. Image acquired by Dr. Wei Fan.

The liposomes were delivered to islets on the day of isolation (day 0) or on day 2 of culture and incubated for 24 or 48 hours. Figure 3.8 shows representative images of the liposome and time combinations. Liposomes with no PR_b PA (0% PR_b PA) showed no internalization in the islet cells. With 0.6 mol% of PR_b PA functionalization there was increased internalization and even more seen for the 1.6 mol% and 3.2 mol% PR_b PA

formulations. Liposomes functionalized with 3.2 mol% PR_b PA had the greatest level of internalization after 48 hours of incubation. As shown in the figure, the internalization efficiencies depended on the PR_b PA concentration and the time of incubation which has been seen previously in the targeted delivery of PR_b PA functionalized liposomes to cancer cells (Demirgöz et al., 2008; Garg et al., 2009). Greater internalization was also seen after 48 hours of incubation as compared to 24 hours. The images are 2D z-projections of the fluorescent features from the multiple layers of the islet that were captured with the confocal microscope.

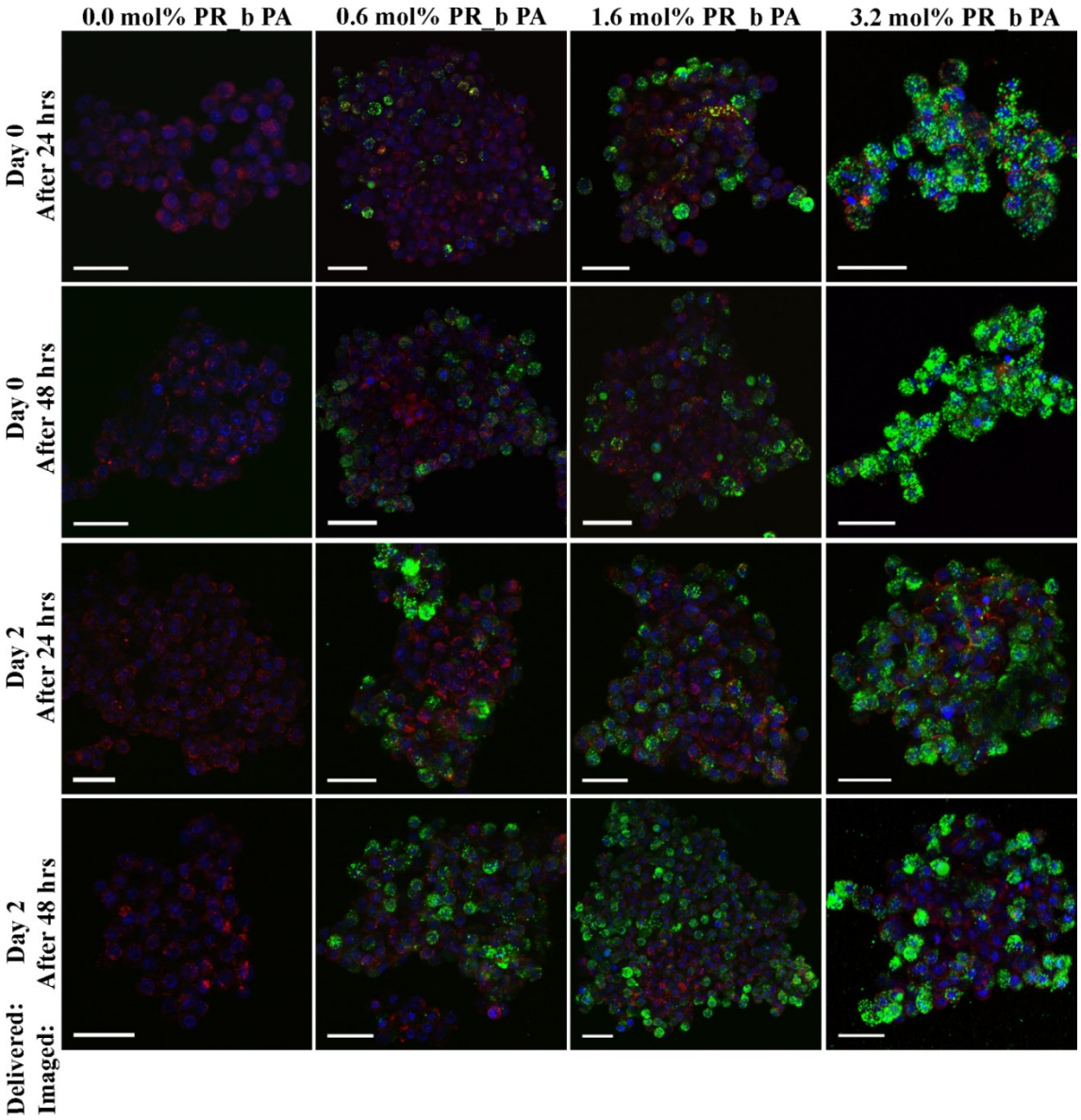

Figure 3.8: Liposome internalization into porcine islets. Liposomes functionalized with PR_b PA or with no peptide were delivered to islets on the day of isolation (row 1 and 2) or day 2 of culture (row 3 and 4) and allowed to internalize for 24 (row 1 and 3) or 48 (row 2 and 4) hours. Confocal images show the cell membrane (red), nucleus (blue), and the liposomes (green). The images are 2D z-projections of the fluorescent features from the multiple layers of the islet that were captured. At least 2 different pig isolations were tested for each time point and images are shown from a single experiment. All scale bars are 20 μm.

Flow cytometry was used to quantify the level of binding and internalization of the PR_b PA functionalized and nonfunctionalized liposomes. The flow cytometry data shown in Figure

3.9 are from liposomes delivered on day 0 of IE culture and analyzed after 24 hours of incubation. The figure shows a concentration dependent effect, where liposomes without PR_b PA show minimal binding to the islet cells and liposomes functionalized with 0.6, 1.0, and 3.2 mol% PR_b PA showed increased levels of fluorescence. The table in Figure 3.9 shows the percentage of islet cells with a positive shift in fluorescence compared to the control samples. From the data, the PR_b PA concentration dependent increase in cell binding is clear; higher PR_b PA functionalization leads to a greater percentage of cells with a positive shift in fluorescence. This trend was also seen for liposomes delivered to IE on days 7 and 12 of culture (Figure 3.12). Data show that PR_b PA functionalized liposomes have improved cell binding and internalization ability compared to nonfunctionalized liposomes when delivered to porcine islets of Langerhans. These results confirm that PR_b PA functionalized liposomes could be used to deliver agents of interest to the porcine islets in culture.

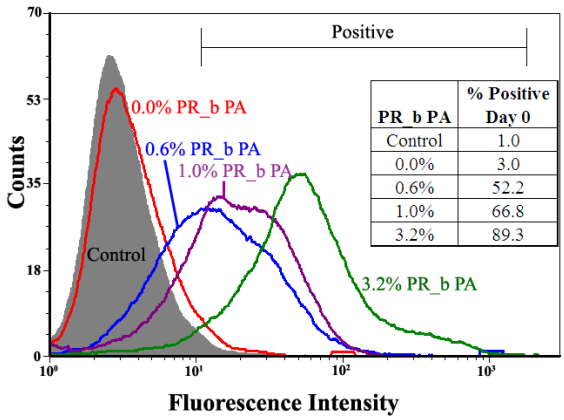

Figure 3.9: Flow cytometry analysis of liposome internalization. Liposomes were added to the culture on day 0 and allowed to incubate with the islets for 24 hours before analysis. The percentages of cells with a positive fluorescent shift compared to the control are shown in the inset table. A positive shift in fluorescence represents binding and/or internalization of calcein loaded liposomes into the islet cells. The results are representative for *n*=2. Results shown are from a single experiment and the other experiment is shown in the Supporting Information (Figure 3.12).

3.5 CONCLUSIONS

In this study we demonstrated the presence of the $\alpha_5\beta_1$ integrin on porcine islet cells. These studies also show that the fibronectin-mimetic peptide, PR_b, is an appropriate peptide bullet for applications involving porcine islets. The free peptide was shown to stimulate ECM production from isolated islet cells, reestablishing integrin-matrix connections lost during isolation. PR_b PA was also shown to increase internalization of conventional liposomes into islet cells, potentiating their use for delivering agents of interest *ex vivo* to porcine islet cells. Our lab is currently investigating a number of methodologies for which PR_b may play a critical role in protecting, maintaining, and tracking porcine islets during isolation, the culture period, and after transplantation. These studies will be the subject of future work.

3.6 SUPPORTING INFORMATION

Table 3.1: Characterization of actual liposome formulations used in each experiment. Data are expressed as the mean ± standard error of the mean (n=1, 3 measurements).

mol% PR_b	Diameter (nm)	Zeta Potential (mV)
0.0[a]	98.0 ± 1.4	-6.0 ± 3.9
0.0[b]	83.6 ± 0.4	13.2 ± 14.8
0.0[c]	112.3 ± 0.3	-9.6 ± 5.5
0.3	123.4 ± 0.3	7.1 ± 8.7
0.6	122.7 ± 0.6	-8.1 ± 2.9
0.8	112.4 ± 0.3	-2.3 ± 10.5
1.0	181.4 ± 4.8	-10.5 ± 3.3
1.6	99.9 ± 0.2	-5.1 ± 2.5
3.2	157.1 ± 4.0	-4.8 ± 0.7
4.2	113.7 ± 0.1	-20.4 ± 4.6
5.4	100.9 ± 0.4	-6.5 ± 3.6

a: formulation for confocal studies (Figure 3.8) and day 0 flow study (Figure 3.9)

b: formulation for day 7 flow study (Figure 3.12)

c: formulation for day 0 and day 12 flow studies (Figure 3.12)

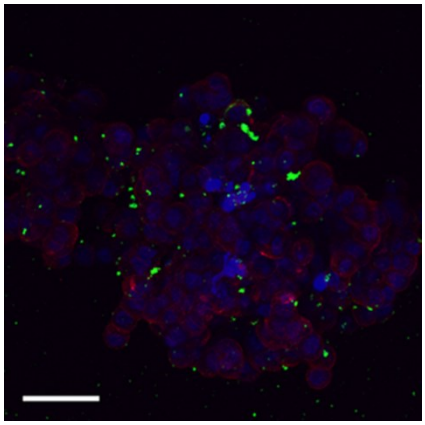

Figure 3.10: 100Kx Fibronectin production **sample. PR_b was added to the culture medium on day 2 of culture and the islets were imaged 48 hours later by confocal microscopy. Images show the cell membrane (red), nucleus (blue), and secreted fibronectin (green). The image is a 2D z-projections of the**

fluorescent features from the multiple layers of the islet that were captured. 2670 ng of PR_b (100Kx) was added to the culture medium. The scale bar is 20 μm.

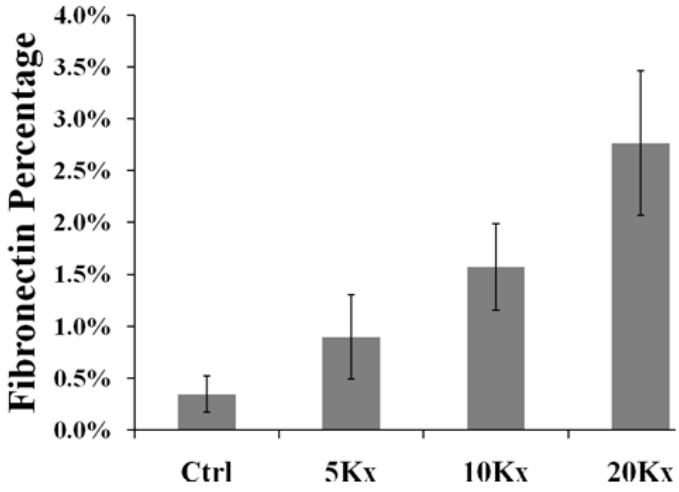

Figure 3.11 Percent of fibronectin intensity in islets.Quantification of confocal images of fibronectin production from islets stimulated with free PR_b. Values obtained by summing total fibronectin pixels of each confocal slice together and dividing by the sum of the total pixels of the cell area from each confocal slice. These results are similar to those obtained from the fibronectin western blot. Supplementing free PR_b to the islets increases fibronectin production from the islets. n=2

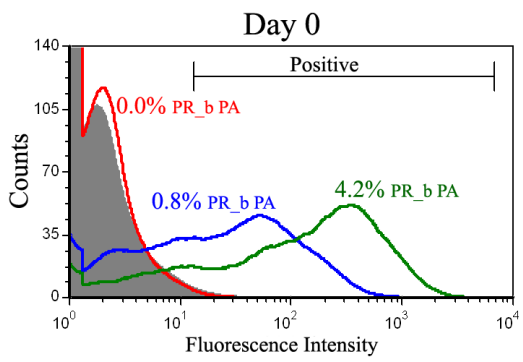

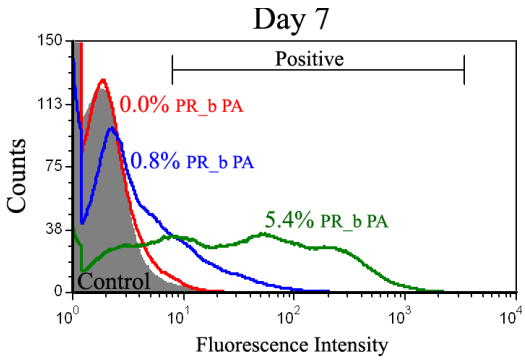

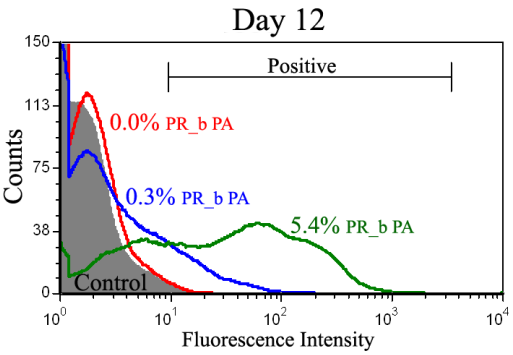

PR_b PA	% Positive Day 0	Day 7	Day 12
Control	1.1	1.0	1.0
0.00%	0.8	1.9	1.3
0.30%	-	-	15.9
0.80%	63.4	19.4	-
4.20%	86.9	-	-
5.40%	-	68.3	65.5

Figure 3.12: Flow cytometry data of liposomes added to islet culture on day 0, 7, and 12 and allowed to incubate for 24 hours. Liposomes were functionalized with various amounts of PR_b PA or not functionalized. The percentages of cells with a fluorescent shift are listed in the table. A shift in fluorescence represents binding and/or internalization of calcein loaded liposomes to the cell. Each graph represents one experiment.

CHAPTER 4

PROTECTION OF ISCHEMIC β CELLS THROUGH DELIVERY OF LIPIDS AND ATP BY TARGETED LIPOSOMES

4.1 SYNOPSIS

Islet transplantation is a promising treatment for type 1 diabetes, but despite the successes, existing challenges prevent widespread application. Ischemia, occurring during pancreas preservation and isolation, as well as after islet transplantation, decreases islet viability and function. We hypothesized that the liposomal delivery of adenosine triphosphate (ATP) could prevent the loss of cell viability during an ischemic insult. In the following work we use a model β cell line, INS-1to probe the liposome/cell interactions and examined the ability of liposomes functionalized with the fibronectin-mimetic peptide PR_b to facilitate the delivery of ATP to ischemic β cells. We demonstrate that PR_b increases the binding and internalization of liposomes to the β cells. Unexpectedly, when comparing the ability of PR_b liposomes with and without ATP to protect INS-1 cells from ischemia we found that both formulations increased cell survival. By probing the functional activity of ischemic cells treated with PR_b functionalized liposomes with and without ATP we find that both lipids and ATP play a role in maintaining cell viability after an ischemic insult. This approach may be beneficial for preventing ischemia related damage to islet cells, especially in the organ preservation stage.

4.2 INTRODUCTION

An explosion of studies involving islet transplantation was seen after Shapiro et al. (2000) demonstrated insulin independence in seven patients receiving islet transplantations. However, despite the successes, (Hering et al., 2004, 2005; R Paul Robertson, 2010; Ryan et al., 2005) this cell based therapy must still overcome many challenges before it can become a widespread option for patients with type 1 diabetes. Some of the primary complications include the shortage of available islets for transplantation and the loss of islet viability before and after transplantation (Beck et al., 2007; Emamaullee & Shapiro, 2006; Rother & Harlan, 2004; Ryan et al., 2005; Shapiro & Ricordi, 2004). Ischemia (deprivation of oxygen and nutrients) has been linked to the poor islet viability and function during organ preservation and isolation, as well as after the islets have been transplanted (Emamaullee, Liston, et al., 2005; Lazard, Vardi, & Bloch, 2012; Linn et al., 2006; Moritz et al., 2002; Nadithe, Mishra, & Bae, 2012). Pancreas preservation prior to islet isolation has been demonstrated to play a large role in islet isolation outcomes (Tanioka et al., 1997). The periods of warm and cold ischemia during the organ storage directly affect the quality of the retrieved islets and therefore the function of the transplanted graft (D Brandhorst, Brandhorst, Hering, Federlin, & Bretzel, 1999; Hering et al., 2004; Shapiro & Ricordi, 2004). Strategies to improve the preservation conditions aim to increase the adenosine triphosphate (ATP) content of the organ and have demonstrated improved islet isolation outcomes (Hering et al., 2002; J. R. T. Lakey, Tsujimura, Shapiro, & Kuroda, 2002; Matsuda et al., 2003; W E Scott III et al., 2011; William E Scott III et al., 2010; Thomas M Suszynski et al., 2012; Tanioka et al., 1997). However, loss of islet yield and viability during isolation remains a problem. Additionally, ischemia negatively affects islets after transplantation. Isolation disrupts the native vasculature of the islets, which require 7-10 days post-

transplant for complete revascularization (M. Menger et al., 1989). During this period the islets must rely on diffusion for nutrients and oxygen supply, compromising islet viability and function (Dionne et al., 1993; Giuliani et al., 2005; Ryu et al., 2009; T M Suszynski et al., 2011).

Ischemic conditions deplete cells' ATP levels, leading to a series of events that ultimately end in cell necrosis (Michiels, 2004). In β cells, the insulin secreting cells of the islets, ischemic conditions also impair the secretion of insulin (Cantley et al., 2010; Dionne et al., 1993). While direct delivery of ATP to ischemic tissues is an appealing idea, the hydrolysis of ATP in vivo necessitates a delivery mechanism (Korb et al., 2008; Tep et al., 2009). Previous studies on myocardial (Hartner et al., 2009; Levchenko et al., 2010; Verma, Hartner, et al., 2005; Verma, Levchenko, et al., 2005), liver (Hayashi et al., 1997; Korb et al., 2008; Neveux et al., 2002; Tep et al., 2009), retina (Dvoriantchikova et al., 2010), and wound healing (Chiang et al., 2007; Chien, 2010; J. Wang et al., 2010) ischemia models have demonstrated the application of liposomal encapsulated ATP (ATPL) for maintaining cell viability. Liposome encapsulation protects the ATP from enzymatic degradation and enhances ATP penetration into the cells. Though much effort has gone into improving the ATP level in preserved pancreata and transplanted islet cells, ATPL delivery has not been attempted. Currently strategies primarily involve improved oxygenation techniques (Hering et al., 2002; Nadithe et al., 2012; W E Scott III et al., 2011; Witkowski et al., 2005) and anti-apoptosis strategies (Ah Kim et al., 2009). Given the multiple ischemia conditions that β cells are exposed to, ATPL delivery could provide a flexible and beneficial approach for improving preservation and isolation protocols, as well as a treatment option following islet transplantation.

As demonstrated in the drug delivery literature (Levine, Scott, & Kokkoli, 2012; Pangburn et al., 2009; Pearce et al., 2012), functionalizing liposomes with a cell binding ligand improves delivery of the cargo into the cells. Previously, we demonstrated that functionalization with the fibronectin-mimetic peptide PR_b (KSSPHSRN$(SG)_5$RGDSP) facilitates the binding and internalization of liposomes into porcine islet cells (Atchison et al., 2010). While nontargeted liposomes had little to no internalization into the porcine islet cells, PR_b functionalized liposome internalization was PR_b concentration dependent. The design of PR_b peptide includes a KSS spacer, the RGDSP integrin binding motif, and the $\alpha_5\beta_1$ integrin synergy binding domain, PHSRN (García et al., 2002; Mardilovich & Kokkoli, 2004). The two binding domains are separated by a linker $(SG)_5$ that mimics both the length and hydrophobicity/hydrophilicity ratio found in the amino acids in the native protein (Craig et al., 2008; Mardilovich et al., 2006). Addition of a 16 carbon dialkyl tail forms the PR_b peptide-amphiphile ($(C_{16})_2$-Glu-C_2-KSSPHSRN$(SG)_5$RGDSP) (Mardilovich et al., 2006). PR_b peptide binds specifically to the $\alpha_5\beta_1$ integrin with a K_D = 76.3 ± 6.3 nM (Mardilovich et al., 2006; Pangburn, Bates, et al., 2012; Shroff et al., 2012) and has outperformed the ubiquitous RGD peptide (Kokkoli et al., 2006) in terms of specificity, cell adhesion, cell signaling, and extracellular matrix production (Mardilovich et al., 2006; Shroff et al., 2012). Additionally, PR_b has proven to be an effective peptide bullet in the delivery of chemotherapeutic loads to $\alpha_5\beta_1$ expressing cancer cells, outperforming both nontargeted and GRGDSP functionalized particles (Demirgöz et al., 2009, 2008; Garg & Kokkoli, 2011; Garg et al., 2009; Pangburn, Bates, et al., 2012; Pangburn, Georgiou, et al., 2012; Shroff & Kokkoli, 2012). PR_b peptide has also been used in the development of tissue constructs, promoting better cell adhesion, proliferation, and signaling (Rexeisen et al., 2010; Shroff et al., 2010).

In this work our goal is to target insulin-producing β cells with PR_b functionalized ATPL under ischemic conditions. Initially we attempted to evaluate the system on porcine islet cells, but the variability in islet viability from batch-to-batch made accessing the function of the materials difficult. Therefore, to better understand the material/cell interactions, a β cell line, INS-1, was used for the studies. Preliminary work with porcine islets can be found in Appendix 2. INS-1 cells have previously been shown to express the α_5 and β_1 integrins (Krishnamurthy, Li, Al-Masri, & Wang, 2008), and are capable of secreting insulin in response to a glucose challenge (Asfari et al., 1992; Cline, Pongratz, Zhao, & Papas, 2011). First, we evaluate the binding and internalization of liposomes containing polyethylene glycol (PEG2000) and functionalized with PR_b into INS-1 cells. The interactions between the liposomes and the cells are investigated for both PR_b functionalized and nontargeted liposomes using flow cytometry and microscopy. The effect of liposomal delivery of ATP to INS-1 cells in an ischemic environment is probed using metabolic and functional assays. We demonstrate that PR_b targeted liposomes provide protection from ischemia through delivery of ATP as well as by supplementing lipids to the compromised cells.

4.3 Materials and Methods

4.3.1 Materials

The PR_b peptide sequence (KSSPHSRN$(SG)_5$RGDSP) was purchased in crude form from the Oligonucleotide and Peptide Synthesis Facility at the University of Minnesota. The PR_b peptide-amphiphile $(C_{16})_2$-Glu-C_2-KSSPHSRN$(SG)_5$RGDSP (referred to as PR_b throughout) was synthesized as described previously (Berndt, Fields, & Tirrell, 1995; Mardilovich et al., 2006; Mardilovich & Kokkoli, 2004, 2005). Lipids 1,2-dipalmitoyl-*sn*-glycero-3-phosphocholine (DPPC), 1,2-dipalmitoyl-*sn*-glycero-2-phosphoethanolamine-N-(methoxy(polyethylene glycol)-2000) (ammonium salt) (DPPE-PEG2000, referred to as

PEG2000), 1,2-dipalmitoyl-*sn*-glycer-3-phosphoethanolamine-N-(lissamine rhodamine B sulfonyl) (ammonium salt) (DPPE-RHOD, referred to as RHOD), 1,2-bis(10,12-tricosadiynoyl)-*sn*-glycero-3-phosphocholine (DC(8,9)PC), and cholesterol were purchased from Avanti Polar Lipids Inc. (Alabaster, AL). Extrusion assembly and 100 nm polycarbonate membranes were obtained from Avestin, Inc. (Ottawa, Canada). WST-1 assay was purchased from Clontech Laboratories, Inc. (Mountain View, CA). Calcein (excitation, 494; emission, 517), Hoechst 33342 nucleic acid stain, and Prolong Gold Antifade reagent were purchased from Invitrogen, Inc. (Carlsbad, CA). The bicinchoninic acid (BCA) protein assay kit was purchased from Thermo Fischer Scientific (Rockford, IL). Fetal bovine serum (FBS) was purchased from Atlas Biologicals, Inc. (Fort Collins, CO). The insulin ELISA was purchased from Mercodia Inc. (Uppsala, Sweden). All other reagents were purchased from Sigma-Aldrich (St. Louis, MO).

4.3.2 Liposome Preparation and Characterization

Liposomes composed of DPPC, cholesterol, PEG2000, and PR_b were prepared as described previously (Atchison et al., 2010; Demirgöz et al., 2008; Fenske et al., 2003; Garg et al., 2009; Shroff & Kokkoli, 2012). Briefly, solutions of lipids, amphiphiles, and cholesterol were mixed in a round bottom flask and dried under argon to create a thin film. Solutions were combined at concentrations of *x* mol% PR_b, 35 mol% cholesterol, 3 mol% PEG2000, *y* mol% RHOD and (62-*x*-y) mol% DPPC. DC(8,9)PC-PEG liposomes were made by combining 99 mol% DC(8,9)PC and 1 mol% PEG2000. The lipid films were hydrated with 2 mM calcein in HBSE buffer (10 mM HEPES, 150 mM NaCl, 0.1 mM EDTA, pH 7.4), HBSE buffer, Tris buffer (10 mM Tris, 136.4 mM KCl, 13.6 mM NaCl, pH 7.4), or 400 mM adenosine triphosphate (ATP) in HBSE buffer, freeze-thawed five times, and then extruded 21 times through two stacked 100 nm polycarbonate membranes. Liposomes were filtered over a

Sepharose CL-4B gel filtration column to remove unencapsulated material and stored at 4-8°C. After gel filtration, DC(8,9)PC-PEG liposomes were cooled to 4 °C and placed in a precooled glass dish. The lipids were polymerized by crosslinking for 10 minutes in a CL-1000 UV Crosslinker (UVP LLC, Upland, CA). Polymerization was monitored by a change in absorbance spectrum and visual color change. The absorbance spectrum was acquired on a Synergy H1 plate reader (Biotek, Winooski, VT). Liposome phosphorous concentration was determined using the phosphorus colorimetric assay described elsewhere (P. S. Chen et al., 1956). PR_b concentration was determined using the BCA assay according to the manufacturer's protocol. The ZetaPALS zeta potential analyzer (Brookhaven Instruments, Holtsville, NY) was used to determine both zeta potential and diameter of the liposomes by dynamic light scattering (DLS). Encapsulated ATP concentration was determined using reversed phase high-performance liquid chromatography (HPLC). Liposomes were lysed with 0.4% (v/v) sodium dodecyl sulfate (SDS) in distilled water. The chromatography was performed on an Xterra Prep MS C_{18} 150*10 mm stainless steel column (Waters Corp., Milford, MA) packed with 5 μm beads. The isocratic elution was run at room temperature with the 96/4 (v/v) mixture of 0.1 M KH_2PO_4 buffer, pH 6.0, and methanol at a flow rate of 1 mL/min. The UV absorbance was detected at 254 nm on an Agilent 1100 series HPLC (Santa Clara, CA). ATP standards were run each time liposome formulations were evaluated.

4.3.3 Cell Culture

INS-1 cells were cultured in RPMI-1640 medium containing 11.1 mM glucose and supplemented with 10% FBS, 10 mM HEPES, 2 mM L-glutamine, 1 mM sodium pyruvate, 0.05 mM β-mercaptoethanol, 100 units/mL penicillin, and 100 μg/mL streptomycin. Cells were incubated at 37°C in a humidified 5% CO_2 environment until they were 80-100% confluent and subsequently passaged.

4.3.4 MICROSCOPY

INS-1 cells were plated at $5*10^5$ cells/well in 12 well plates containing poly-l-lysine coated coverslips and allowed to adhere overnight. Liposomes (containing 2 mM calcein or rhodamine-labeled lipid) were added at 250 μM lipid concentration in complete media at the indicated temperature and incubated for 1 hour. Cells were washed twice with phosphate buffered saline (PBS) and prepared for imaging. For calcein liposome imaging cells were fixed with 4% paraformaldehyde in PBS and the nuclei stained with 2 μM Hoechst 33342. Cells were then mounted with Prolong Gold Antifade reagent. INS-1 cells incubated with liposomes containing rhodamine-labeled lipids were stained with Hoechst 33342 immediately after washing with PBS and the coverslips inverted onto a glass slide containing a small amount of PBS. Cells were imaged immediately. The Olympus Fluoview FV1000 confocal laser scanning microscope at the University Imaging Center at the University of Minnesota was used for all confocal studies.

INS-1 cells treated with 2 mM calcein liposomes (as indicated above) were also imaged with fluorescence microscopy. Cells were processed as above, without fixation. Cells were immediately imaged using an $EVOS_{fl}$ microscope (AMG, Bothell, WA) equipped with DAPI, GFP and Texas-Red filter sets.

4.3.5 LIVE/DEAD IMAGING

INS-1 cells were seeded at $5*10^5$ cells/well of a 96 well plate and incubated for approximately 40 hours. Cells were washed twice with PBS followed by addition of medium and treatments. For ischemic conditions cells were incubated in serum free medium without glucose supplemented with 100 units/mL penicillin and 100 μg/mL streptomycin (referred to as glucose depleted minimal medium). Liposomes were added at a concentration of 250 μM lipids and free ATP was added at 200 μM. Cells were incubated for

6 hours under anoxic conditions (0% O_2). Anoxic conditions for all experiments were established by placing cells in a water jacketed chamber filled with 95% N_2, 5% CO_2 and connected to a circulating water bath maintained at 37°C. After the anoxic period the media was replaced with complete medium and the cells were stained with 1 μM calcein AM and 150 nM propidium iodide (PI). After 45 minute incubation the cells were imaged with a Nikon Eclipse TE 300 inverted light microscope (Nikon Inc., Tokyo, Japan) equipped with a Nikon high pressure mercury arc lamp. A FITC filter (excitation BP465-495, emission BP515-555; Nikon 96107M B-2E/C C12353) was used to collect calcein AM fluorescence and a rhodamine filter (excitation BP528-553, emission 590LP; Nikon DM575 G-2A) was used to collect PI fluorescence. Images were captured using a SPOT RT CCD camera (Diagnostic Instruments, Sterling Heights, MI) and Metamorph imaging software (Molecular Devices Corp., Sunnyvale, CA).

4.3.6 Flow Cytometry

For investigation of calcein liposome binding to INS-1 cells and temperature dependence of rhodamine-labeled lipid transfer, the INS-1 cells were trypsinized (0.25% trypsin +0.1% EDTA) and resuspended in complete medium at a concentration of $1*10^6$ cells/mL. Cells were incubated with liposomes at a lipid concentration of 250 μM on a rotary shaker for 1 hour at either 4 or 37°C. Following the incubation period cells were pelleted and washed twice with ice-cold PBS. Flow cytometry was carried out immediately. For blocking experiments, the same protocol was followed except the cells were incubated with 500 μg/mL free PR_b peptide for 30 minutes before the addition of liposomes.

For the time course studies of rhodamine-labeled lipid transfer from liposomes to INS-1 cells, cells were seeded in 24 well plates at $3*10^5$ cells/well and incubated overnight. Cells

were washed twice with PBS and incubated with liposomes at 250 μM total lipid in glucose depleted minimal medium. Plates were incubated in either normal conditions (normoxic, 21% O_2) or anoxic conditions (as described in the Live/Dead Imaging section) for the indicated period. The media was then removed and placed in a microcentrifuge tube and the cells were trypsinized and added to the microcentrifuge tube. The cells were pelleted and washed twice with ice-cold PBS. The cells were resuspended in ice-cold PBS and flow cytometry analysis carried out immediately. All flow cytometry analyses were performed at the flow cytometry core in the Cancer Research Center of the University of Minnesota.

4.3.7 METABOLIC ACTIVITY

To test the dependence of lipid concentration on the ability of liposomes to protect INS-1 cells from ischemia and to compare ATP liposomes to other liposome formulations, INS-1 cells were seeded at $5*10^5$ cells/mL in 96 well plates and incubated for approximately 40 hours. Cells were washed twice with PBS and incubated with with 3.6 μM free PR_b peptide, 120 μM free ATP, a combination of free PR_b and free ATP at 3.6 and 120 μM respectively, or liposomes at 300 μM lipid concentration in glucose depleted minimal medium. Free PR_b concentration was determined based on the average concentration of PR_b presented on the surface of PR_b-PEG liposomes. The plates were incubated for 6 hours in an anoxic environment. A normoxic control sample was prepared in the same fashion but was incubated in compete medium in the normal environment for the duration of the experiment. The media was replaced with 100 μL complete medium to provide substrates for metabolism (Takahashi, Abe, Gotoh, & Fukuuchi, 2002) and 10 μL of WST-1 reagent was added to each well. The plates were incubated for three hours under normal conditions. Metabolic activity was monitored by measuring the absorbance of the metabolized WST-1

reagent at 450 nm with a reference wavelength of 650 nm to account for background. The data is presented normalized to the normoxic sample using the following formulas:

$$mean\ OD_{sample} = OD_{450} - OD_{650}$$

$$\%Metabolic\ Activity = \frac{mean\ OD_{sample} - mean\ OD_{blank}}{mean\ OD_{normoxic\ control} - mean\ OD_{blank}} * 100$$

4.3.8 Glucose Stimulated Insulin Secretion

INS-1 cells were seeded at $5*10^5$ cells/well of a 96 well plate and incubated overnight. Wells were washed with PBS and incubated with liposomes at 300 μM lipid concentration or free ATP in glucose depleted minimal medium. Cells were then incubated in an anoxic environment for 6 hours. A normoxic control sample was collected by incubating in a normal environment (37°C, 5% CO_2) and using complete media during the 6 hour incubation. Following 6 hour incubation, the medium was replaced with complete medium and the cells were cultured under normal conditions for the 16 or 24 hours. After the culture period a glucose stimulated insulin secretion (GSIS) test was performed. The media was replaced with 2.8 mM glucose in Krebs buffer (25 mM HEPES, 115 mM NaCl, 24 mM $NaHCO_3$, 5 mM KCl, 1 mM $MgCl_2$-6 H_2O, 0.1% w/v BSA, 2.5 mM $CaCl_2$-2 H_2O, pH 7.4) and incubated for 30 minutes in a normal environment. Media was then replaced with either 2.8 mM or 15 mM glucose in Krebs buffer. Cells were incubated with glucose solutions for 1 hour in a normal environment. Following incubation, media was collected to measure insulin concentration via ELISA. Cells were lysed and total protein measured using the BCA assay. Data is displayed as the ratio of the insulin secretion (Ins, ng insulin/mg protein/hr) at 15 mM glucose to 2.8 mM glucose.

$$Stimulation\ Index = \frac{Ins_{15\ mM}}{Ins_{2.8\ mM}}$$

4.3.9 Statistical Analysis

Significance was determined using a Student's t test. Data analysis was performed using JMP Pro 9 software (SAS Institute Inc.). Significance was determined at $p < 0.05$. Significance is indicated throughout as * $p<0.05$, ** $p<0.01$, *** $p<0.001$, no significance compared to the control is indicated with the † symbol.

4.4 Results and Discussion

4.4.1 Liposome Binding and Internalization

In a previous report we demonstrated that PR_b functionalized liposomes showed effective binding and internalization into porcine islet cells and theorized that these functionalized liposomes could provide a benefit by delivering molecules of interest to insulin producing β cells (Atchison et al., 2010). In this study we are using a model β cell line, INS-1, to probe liposome-cell interactions and the delivery of ATP. By using a model cell line in this study we are able to avoid the convoluting effects of islet viability varying from batch to batch. First we investigated the effect of functionalizing liposomes with PR_b on the binding and internalization of the nanoparticles into INS-1 cells. We have previously demonstrated that the concentrations of both PR_b and PEG2000 affect the binding of the liposomes (Garg et al., 2009). PEG2000 imparts stealth properties of the liposomes and has been shown to decrease protein adsorption and increase circulation time (Wattendorf & Merkle, 2008). All liposomes in this study include 3 mol% PEG2000 and approximately 1.5-3.6 mol% PR_b on average in functionalized samples. Dynamic light scattering was used for characterization and demonstrates diameters ranging on average from 113-134 nm for the liposomes used in these studies. Full characterization and nomenclature information is shown in Table 4.1.

Table 4.1: Liposome characterization. Data is presented as the mean ± standard deviation from n = 3 – 8 samples. Samples marked with * contain 1 mol% lissamine rhodamine B labeled DPPE.

Liposome formulation	Encapsulate	Diameter (nm)	Zeta potential (mV)	PR_b (mol%)	ATP Encapsulation % (mole ATP/mole lipid)
PEG CAL	Calcein	117.4 ± 2.0	-2.9 ± 6.2	-	-
PEG CAL*	Calcein	128.4 ± 4.5	-5.4 ± 2.0	-	-
PEG HBSE*	HBSE buffer	134.2 ± 6.8	-2.6 ± 3.1	-	-
PEG HBSE	HBSE buffer	113.0 ± 5.4	-1.1 ± 2.1	-	-
PEG Tris	Tris buffer	122.7 ± 6.6	0.0 ± 2.1	-	-
PEG ATPL	ATP	126.0 ± 13.8	-4.7 ± 5.5	-	27 ± 12
PR_b-PEG CAL	Calcein	119.9 ± 6.4	0.2 ± 1.7	1.8 ± 0.7	-
PR_b-PEG CAL*	Calcein	127.6 ± 0.7	0.3 ± 4.6	1.4 ± 1.0	-
PR_b-PEG HBSE*	HBSE buffer	118.6 ± 9.0	-2.9 ± 4.3	3.6 ± 1.8	-
PR_b-PEG HBSE	HBSE buffer	122.8 ± 9.3	1.3 ± 0.3	1.6 ± 1.0	-
PR_b-PEG Tris	Tris buffer	117.8 ± 8.1	-3.5 ± 5.0	2.4 ± 0.2	-
PR_b-PEG ATPL	ATP	126.6 ± 8.0	-1.3 ± 3.5	1.5 ± 0.5	33 ± 11

To investigate the effect of PR_b functionalization on liposome binding, liposomes containing 2 mM calcein functionalized with or without PR_b were incubated with INS-1 cells for 1 hour at either 4°C or 37 °C and imaged with confocal or fluorescent microscopy. The cell viability is not affected at 4°C. As shown in the confocal micrographs of Figure 4.1A, when liposomes without PR_b (PEG CAL) are incubated at 4°C or 37°C, there is no detectable binding to the INS-1 cells. However, liposomes functionalized with PR_b (PR_b-PEG CAL) (Figure 4.1A, bottom row) show binding to the outside of the cells at 4°C and are internalized inside the cells at 37°C. The lack of binding by PEG CAL liposomes represents the stealth ability imparted by the PEG2000. These results are in agreement with other studies that suggest PR_b improves the binding capability of stealth liposomes compared to nontargeted liposomes (Demirgöz et al., 2008; Garg et al., 2009; Shroff & Kokkoli, 2012). Additionally, previous studies by our lab on PR_b functionalized stealth nanoparticle trafficking have indicated uptake through an $\alpha_5\beta_1$ mediated endocytosis pathway rather than fusion or non-specific binding (Pangburn, Bates, et al., 2012; Shroff & Kokkoli, 2012). This is in agreement with Figure 4.1A, which shows that liposomes merely adhered to the

cells when incubated at 4°C, a temperature at which endocytosis is mostly inhibited while fusion is still possible (Wileman, Harding, & Stahl, 1985) but are internalized at 37°C. To demonstrate the widespread difference between binding and internalization of PR_b-PEG CAL and PEG CAL liposomes, fluorescent images were taken at a lower magnification. Figure 4.1B demonstrates that at 37°C the PR_b-PEG CAL liposomes have much higher binding and internalization than the PEG CAL liposomes throughout the sample.

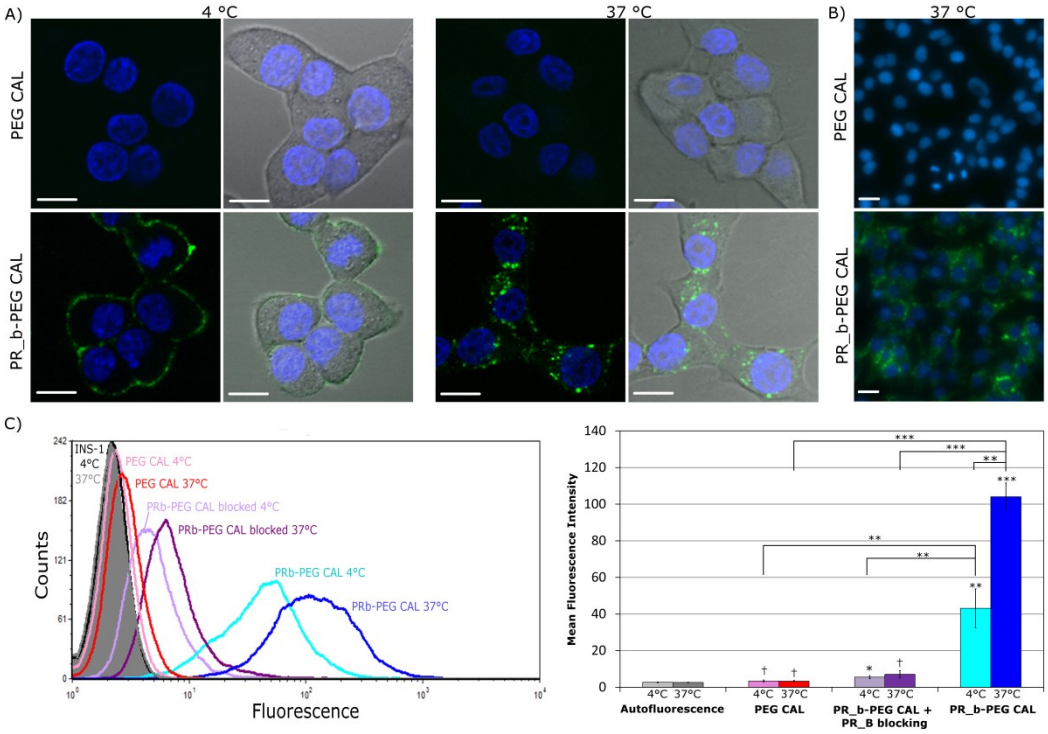

Figure 4.1: Binding and internalization of PR_b functionalized liposomes. A) Confocal micrographs of INS-1 cells treated with PEG CAL or PR_b-PEG CAL liposome for 1 hour at 4 or 37 °C. Nuclei are shown as blue and liposomes with encapsulated calcein appear green. The second column shows the image overlain onto the bright field image so cell boundaries can be discerned. Scale bars are 20 μm. B) Fluorescent images of INS-1 cells treated with PEG CAL or PR_b-PEG CAL liposomes for 1 hour at 37 °C. Scale bars are 20 μm. C) Representative flow cytometry data. INS-1 cells were incubated with liposomes for 1 hour prior to analysis. Blocked samples were incubated with 500 μg free PR_b peptide for 30 minutes prior to liposome addition. D) Flow cytometry cumulative analysis. The first column represents the autofluorescence of the INS-1 cells. Data is presented as mean ± SE of n=3-5 experiments. Symbols directly above each bar represent the significance compared to the autofluorescence at the same temperature. †, no significance; **, p<0.01; ***, p<0.001.

Further, flow cytometry was used to get a quantitative assessment of liposome binding and to probe PR_b specificity. In addition to incubating PEG CAL and PR_b-PEG CAL liposomes

for 1 hour at 4°C and 37°C, cells were also incubated with 500 μg/mL free PR_b peptide for 30 minutes prior to PR_b-PEG CAL addition to block the integrin binding sites. Figure 4.1C displays the histograms from a typical flow cytometry analysis. The histograms for the PR_b functionalized liposome samples are shifted farther to the right than the other samples. This indicates a higher level of fluorescence, and therefore liposome binding, in these samples. The mean fluorescence intensities from the histograms of multiple experiments are combined in Figure 4.1D. A higher intensity represents increased calcein liposome binding to the cells. As demonstrated in the confocal micrographs, samples treated with PR_b-PEG CAL liposomes have a significantly higher fluorescent intensity at both 4°C and 37°C than PEG CAL liposomes, which show virtually no binding at either temperature. Cells that are blocked with free PR_b peptide prior to liposome addition show significantly less binding compared to the unblocked PR_b-PEG CAL liposomes at both 4°C or 37°C. This indicates that the free PR_b is blocking the binding of the PR_b-PEG CAL liposomes to the cells. This is in agreement with other work in our lab that has demonstrated that PR_b is specific to the $\alpha_5\beta_1$ integrin using both antibody and peptide blocking assays (Garg et al., 2009; Pangburn, Bates, et al., 2012; Pangburn, Georgiou, et al., 2012; Shroff & Kokkoli, 2012).

4.4.2 Lipid Mediated Protection of Ischemic β Cells

Having demonstrated that PR_b is necessary to internalize the liposomes into the INS-1 cells, we decided to investigate the ability of PR_b functionalized liposomes to delivery ATP to ischemic INS-1 cells and the effect of this delivery on cell viability. Ischemic conditions were achieved by incubating cells in glucose depleted minimal medium in a 37°C, 95% N_2, 5% CO_2 environment. Cells treated with buffer only (control), free ATP, PR_b-PEG HBSE, or PR_b-PEG ATPL were exposed to 6 hours of ischemia followed by live/dead staining. As shown in Figure 4.2, control samples (Figure 4.2A) showed the highest loss of cell viability,

followed by free ATP samples (Figure 4.2B). Unexpectedly, cells treated with PR_b-PEG liposomes containing both HBSE buffer (Figure 4.2C) and ATP (Figure 4.2D) had better cell viability and a more spread morphology than the control. Treatment with DPPC alone (not in preformed liposomes) did not show the same level of protection, Figure 4.16 in the Supporting Information. The ability of the liposomes containing only buffer to protect the cells from ischemia was surprising and warranted further investigation.

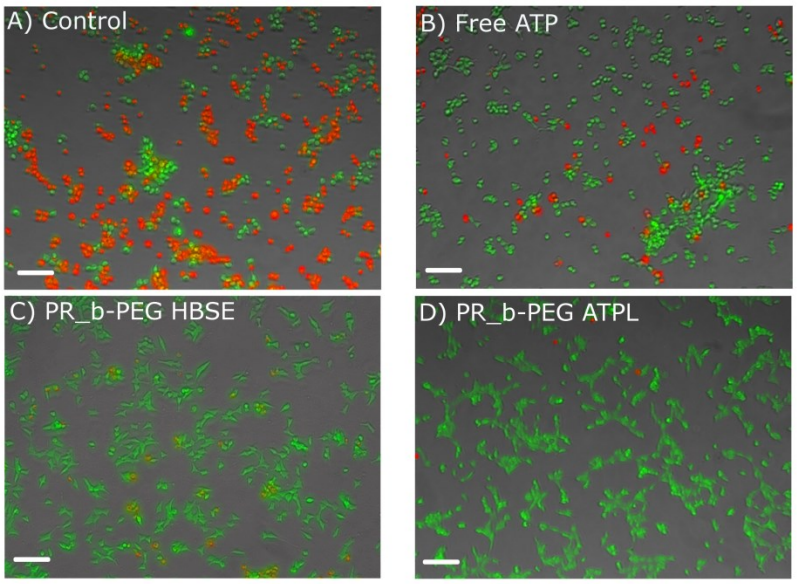

Figure 4.2: Live/dead staining of INS-1 cells exposed to ischemic conditions (glucose depleted minimal medium, 37 °C, 95% N_2, 5% CO_2) for 6 hours. Cells were treated with 200 μM free ATP or liposomes at 250 μM lipid concentration and stained with calcein AM (green-live) and propidium iodide (red-dead). Scale bars are 20 μm.

The live/dead assay gives a snapshot of the cells state but a metabolic assay, such as the WST-1 assay, provides a better understanding of their viability. This was used to investigate how the PR_b-PEG HBSE liposomes were providing protection to the ischemic INS-1 cells. Figure 4.1 demonstrates that nontargeted liposomes do not internalize into the INS-1 cells and that PR_b facilitates internalization. However, given that the PR_b-PEG HBSE liposomes used in Figure 4.2 are only delivering buffer, it was unclear what interaction provided the

benefit. Therefore, we compared nontargeted liposomes encapsulating only buffer (PEG HBSE) to PR_b-PEG HBSE liposomes. Liposomes were delivered to INS-1 cells at varying lipid concentrations and incubated in ischemic conditions for 6 hours. The WST-1 assay was used to probe their metabolic activity following this period. INS-1 cells treated with both liposome formulations had significantly higher metabolic activity than control cells treated only with buffer (Figure 4.3). Furthermore, metabolic activity increased with increasing amounts of added lipid for both the PR_b functionalized and nontargeted samples. There was no significant difference between the metabolic activities of samples treated with PEG HBSE or PR_b-PEG HBSE at each lipid concentration (100 μM $p=0.36$, 200 μM $p=0.36$, 300 μM $p=0.34$). While the liposome treatments do increase the metabolic activity over ischemic controls, the mean activity is still less than normal controls (100%). This is expected due to changes in gene expression and metabolism resulting from the period of ischemia (Cantley et al., 2010; Cheng et al., 2010). Considering that we have demonstrated that liposomes without PR_b do not internalize (Figure 4.1) it is possible that a mechanism that does not involve binding may be involved in the protection shown in Figure 4.3, as both PR_b-PEG HBSE (that internalize) and PEG HBSE liposomes (that do not internalize) show similar protection.

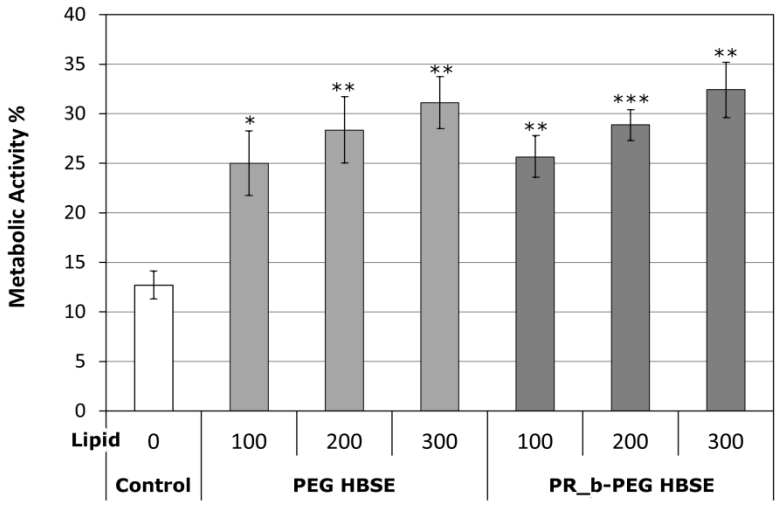

Figure 4.3: Metabolic activity of INS-1 cells treated with liposomes at various lipid concentrations (μM) and exposed to ischemic conditions for 6 hours at 37°C. Data is expressed as a percentage of the metabolic activity of INS-1 cells cultured in a normal environment (complete media, 37°C, 5% CO_2). Data represents the mean ± SE (n=4, 3 repetitions per n). Symbols directly above each bar represent the significance compared to the ischemic control (white bar).*, p<0.05; **, p<0.01; ***, p<0.001.

4.4.3 LIPID TRANSFER

Under ischemic conditions phosphatidylcholine degradation can lead to a loss in cell membrane integrity (Nachas & Pinson, 1992). We hypothesized that the liposomes provide excess lipids to the ischemic cells and maintain the membrane integrity to prolong cell survival. The liposomes could be working in the plug and seal method, originally proposed by Khaw et al. (1995). In this scheme, entire liposomes physically plug lesions created in the membrane during ischemia, maintaining the membrane integrity crucial for cell viability. In the work by Khaw et al., the liposomes were targeted to cytoskeletal myosin by functionalization with an anti-myosin antibody, allowing the liposomes to bind to myosin exposed by the membrane lesions. They found that anti-myosin targeted liposomes provided more protection than nontargeted liposomes. In the current work, the plug and seal theory seems unlikely as the cytoskeleton targeting capability is not included. Another

mechanism could include transfer of individual lipids from the liposomes to the cells during incubation. The transfer of lipids could supplement the ischemic cells with additional lipids to replace the degraded ones. Lipids have been shown to transfer from vesicles to the air/water interface (Schindler, 1979) and to cells (Sandra & Pagano, 1979). Perhaps a similar mechanism leads to transfer of lipids from the liposomes to the ischemic β cells. To investigate this theory, we included 1 mol% lissamine rhodamine B DPPE lipid (RHOD) in the liposome formulations and again encapsulated HBSE buffer (PEG HBSE* and PR_b-PEG HBSE*). These liposomes were then incubated with INS-1 cells in normoxic (21% O_2) or anoxic (0% O_2) environments at 37°C. The amount of fluorescent lipids transferred to the cells was monitored by measuring the fluorescence emitted from the cells after incubation and washing via flow cytometry. Figure 4.4 shows a representative data set for the anoxic environment (Figure 4.4A) and the cumulative mean fluorescence intensity data for both the anoxic (Figure 4.4B) and normoxic (Figure 4.4C) environments. The flow histogram for a normoxic environment experiment is shown in Figure 4.17 in the Supporting Information. From Figure 4.4 it is evident that the RHOD lipids are transferring to the INS-1 cells from both PEG-HBSE* and PR_b-PEG HBSE* liposomes. Under both conditions, and at each time point, the mean fluorescence from the cells is significantly greater than the autofluorescence of the cells. Additionally, the fluorescence transferred to the cells increases with longer incubation periods. Figure 4.1 indicates that PEG-HBSE liposomes do not bind or internalize into the INS-1 cells so the fluorescence transferred in the PEG HBSE* instance is not from binding of the liposomes to the cells. It is important to note that the fluorescence intensities measured in Figure 4.1 and Figure 4.4 are not directly comparable as they are different fluorescent markers.

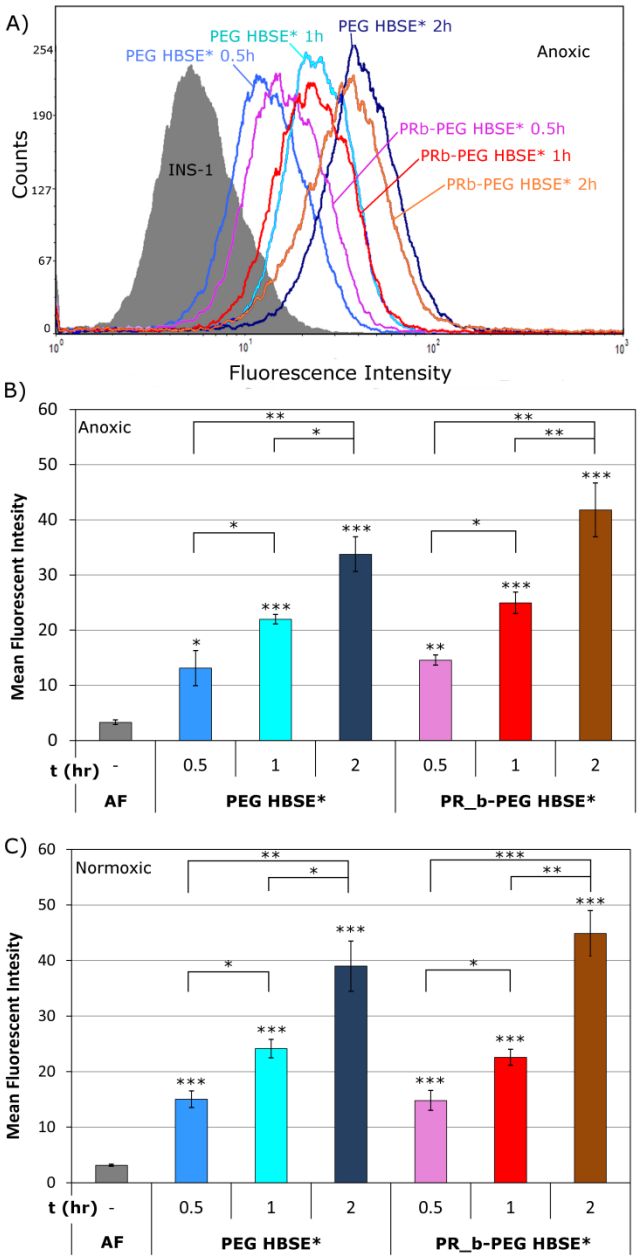

Figure 4.4: Transfer of rhodamine labeled lipids to INS-1 cells. A) Representative flow cytometry histogram for INS-1 cells incubated with PEG HBSE* and PR_b-PEG HBSE* liposomes in an anoxic environment at 37°C. Both liposome formulations contain 1 mol% lissamine rhodamine B DPPE. Liposomes were incubated for indicated times and after washing the fluorescence was monitored via flow cytometry. Cumulative flow cytometry data for anoxic (B) and normoxic (C) environments is displayed as the mean ± SE for n=3-4 experiments. Symbols directly over bars represent the significance compared to the autofluorescence (AF) of the INS-1 cells at the same temperature. *, p<0.05; **, p<0.01; ***, p<0.001.There is no statistical difference between PEG HBSE* and PR_b-PEG HBSE* samples at each time point for both conditions.

To further investigate this result we measured the temperature dependence of the RHOD lipid transfer. INS-1 cells were incubated with both PEG HBSE* and PR_b-PEG HBSE* for 1 hour at 4°C and 37°C. Cells were visualized by confocal microscopy and analyzed via flow cytometry. Cells were imaged without fixation due to artifacts appearing in the RHOD localization when samples were fixed (Fretz, Koning, Mastrobattista, Jiskoot, & Storm, 2004) (Figure 4.5).

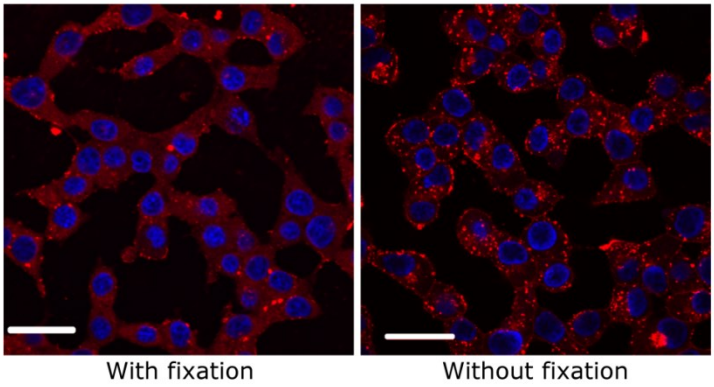

Figure 4.5: Fixation induced artifacts in lissamine rhodamine B DPPE labeling. Cells were incubated with PEG HBSE* liposomes for 1 hour at 37°C and imaged with or without fixation in 4% paraformaldehyde. Nuclei are shown in blue and rhodamine fluorescence in red. In samples that were fixed the rhodamine appeared diffuse within the cell while samples imaged without fixation showed rhodamine fluorescence primarily on the periphery of the cells and in a punctate pattern within the cells. Scale bar is 20 μm.

Figure 4.6A displays the confocal images and demonstrates that when cells were incubated with the liposomes at 4°C the fluorescence from the rhodamine labeled lipids (shown in red) was primarily on the periphery of the cells. When cells were incubated with the liposomes at 37°C the fluorescence was primarily located on the periphery and in a punctate pattern within the cell, most likely in the membranes of different cellular organelles. These images indicate that the rhodamine labeled lipids are likely located in the membrane components of the cells. Flow cytometry was used to quantify the fluorescence transfer (Figure 4.6B, representative experiment shown in Figure 4.18 in the Supporting

Information). The transfer of RHOD to the cells at 37°C was significantly greater than the transfer at 4°C for both formulations. At 4°C the lipids in the bilayer of the liposomes are closer to a gel state and therefore less likely to be able to escape the bilayer. There was no statistical difference in mean fluorescence intensities of the two formulations at both 4°C and 37°C (p=0.18 and 0.13, respectively).

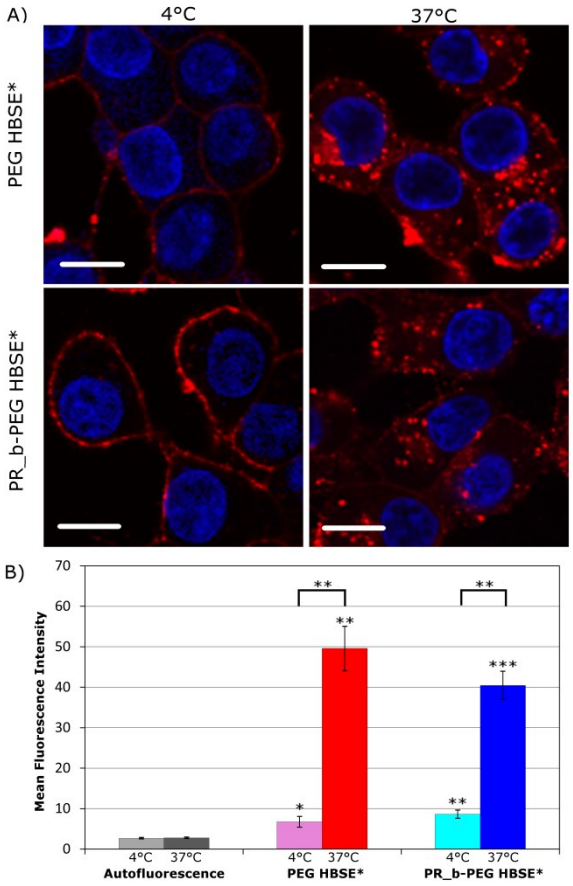

Figure 4.6: Temperature dependence of rhodamine labeled lipids. A) Confocal images of INS-1 cells incubated with PEG HBSE* and PR_b-PEG HBSE* liposomes. Liposomes were incubated for 1 hour at 4 and 37°C and imaged immediately. Nuclei are shown in blue and rhodamine labeled lipids are red. Scale bars are 20 μm. B) Cumulative flow cytometry data for INS-1 cells incubated for 1 hour with PEG HBSE* and PR_b-PEG HBSE* liposomes. Data is expressed as mean ± SE of n=3-4 experiments. Symbols directly over bars represent the significance compared to the autofluorescence of the INS-1 cells at the same temperature.*, p<0.05; **, p<0.01; ***, p<0.001. There is no statistical difference between PEG HBSE* and PR_b-PEG HBSE* at either temperature.

The lack of difference between the PEG HBSE* and PR_b-PEG HBSE* fluorescence transfer in both Figure 4.4 and Figure 4.6 indicates that binding of the liposomes is not necessary for lipid transfer. To confirm that nontargeted liposomes containing rhodamine labeled DPPE were not binding or internalizing, liposome containing the rhodamine labeled lipid were made with 2 mM calcein encapsulated inside (PEG CAL* and PR_b-PEG CAL*). These liposomes were incubated with the INS-1 cells for 1 hour and imaged with confocal microscopy. Samples treated with PEG CAL* liposomes demonstrate fluorescence from rhodamine but there is no detectable fluorescence from the calcein channel (Figure 4.7, top row) indicating that the rhodamine lipid transfer is happening without the binding and internalization of the liposomes. In contrast, samples treated with PR_b-PEG CAL* liposomes have significant fluorescence from the calcein and rhodamine fluorophores (Figure 4.7, bottom row), indicative of liposomes that have bound to the cells. Similar results were found in conditions with glucose depleted minimal medium (Figure 4.8). This figure confirms that inclusion of the rhodamine labeled DPPE lipid does not change the binding and internalization characteristics of the PR_b functionalized and nontargeted liposome formulations.

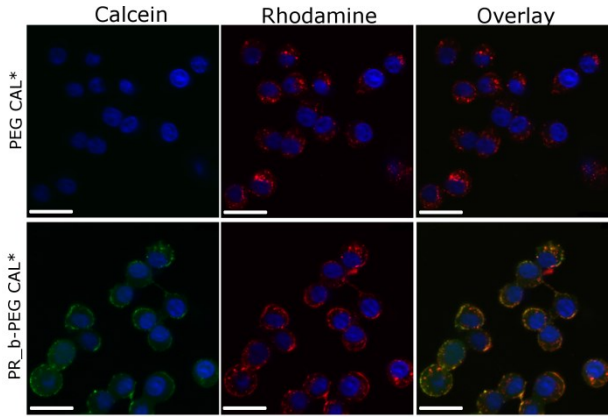

Figure 4.7: INS-1 cells treated with liposomes containing 1 mol% rhodamine labeled DPPE and encapsulating 2 mM calcein for 1 hour at 37°C, 5% CO_2. Confocal micrographs show the nucleus in blue, calcein in green, and rhodamine in red. Scale bars are 20 μm.

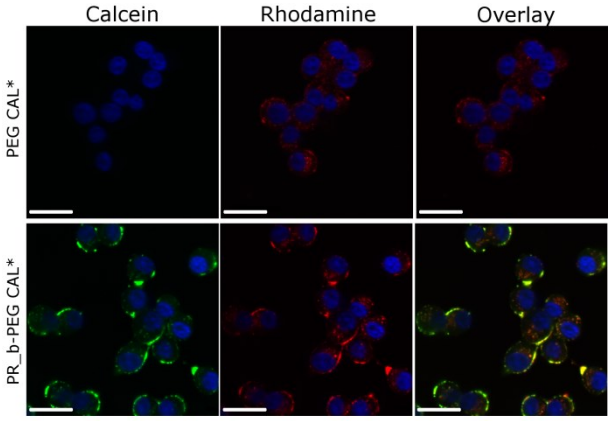

Figure 4.8: INS-1 cells treated with liposomes containing 1 mol% rhodamine labeled DPPE and encapsulating 2 mM calcein for 1 hour at 37°C, 5% CO_2 in glucose depleted minimal medium. Confocal micrographs show the nucleus in blue, calcein in green, and rhodamine in red. Scale bars are 20 μm.

When a lower concentration of RHOD (0.1 mol%) is included in the liposome formulations (PEG HBSE# and PR_b-PEG HBSE#), the effect of PR_b targeting becomes evident. Liposomes containing 0.1 mol% RHOD are characterized in Table 4.2. INS-1 cells incubated with PR_b-PEG HBSE# liposomes had significantly higher fluorescence intensity than cells incubated with PEG HBSE# liposomes at both 4 and 37°C as determined by confocal microscopy (Figure 4.9) and flow cytometry (Figure 4.10). This demonstrates that when a lower

concentration of rhodamine labeled lipid is used in the liposome preparation, the binding of the liposomes dominates the fluorescent labeling of the cells instead of lipid transfer.

Table 4.2: Characterization of liposomes containing 0.1 mol% RHOD.Data is presented as the mean ± standard deviation from n = 3 samples. Samples marked with # contain 0.1 mol% lissamine rhodamine B labeled DPPE.

Liposome formulation	Encapsulate	Diameter (nm)	Zeta potential (mV)	PR_b (mol%)
PEG HBSE#	HBSE buffer	119.7 ± 3.8	0.6 ± 0.8	-
PR_b-PEG HBSE#	HBSE buffer	111.9 ± 3.4	0.9 ± 0.3	2.9 ± 1.6

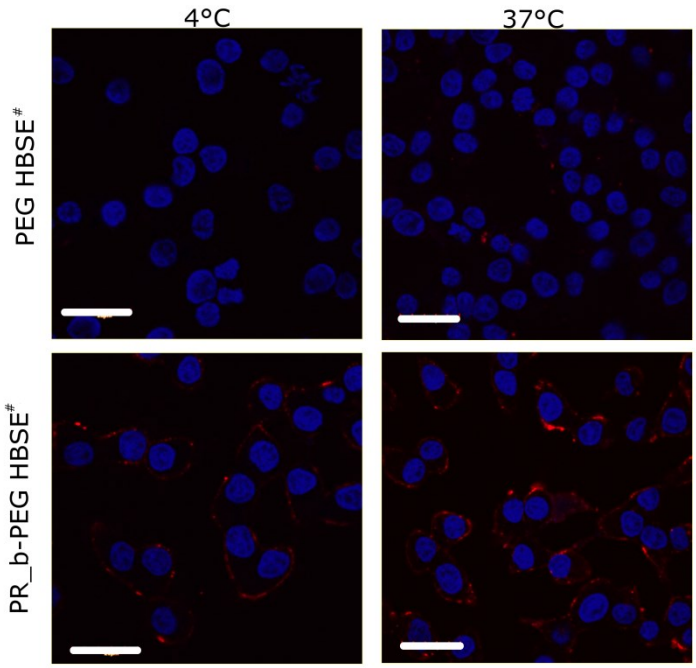

Figure 4.9: Confocal images of INS-1 cells incubated with PEG HBSE# and PR_b-PEG HBSE# liposomes. Both liposome formulations contain 0.1 mol% lissamine rhodamine B DPPE. Liposomes were incubated for 1 hour at 4 and 37°C and imaged immediately. Nuclei are shown in blue and rhodamine labeled lipids are red. Scale bars are 20 μm.

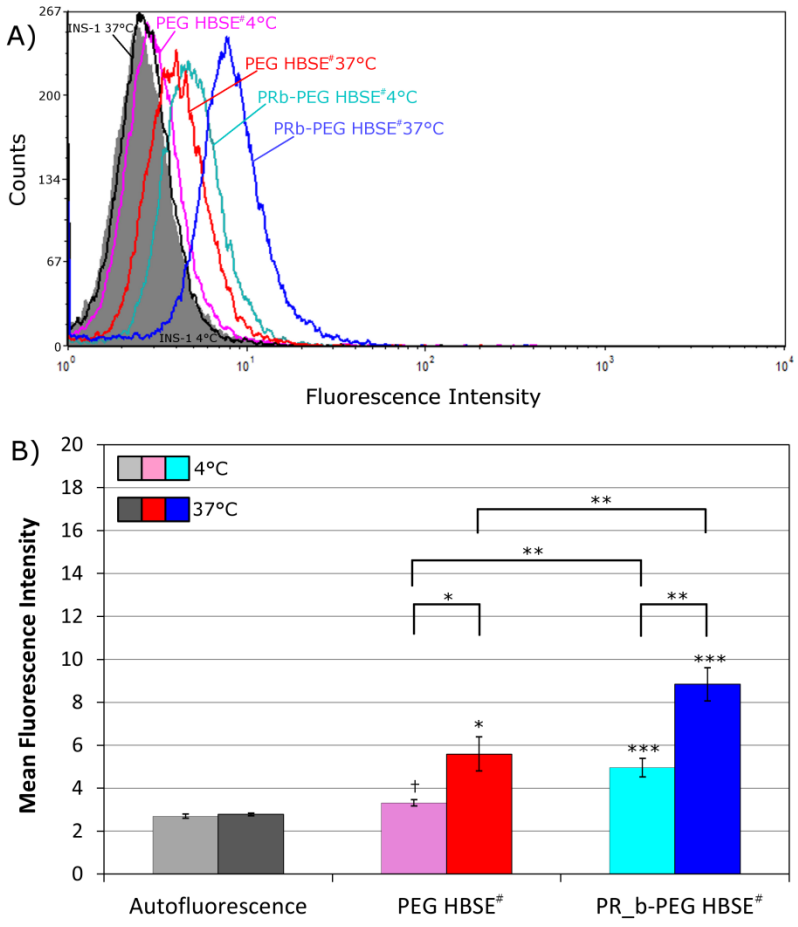

Figure 4.10: Transfer of rhodamine labeled lipids to INS-1 cells from liposomes containing 0.1 mol% RHOD. A) Representative flow cytometry histogram for INS-1 cells incubated with PEG HBSE# and PR_b-PEG HBSE# liposomes. Both liposome formulations contain 0.1 mol% lissamine rhodamine B DPPE. Liposomes were incubated for 1 hour at 4 and 37°C and the fluorescence monitored after washing via flow cytometry. B) Cumulative flow cytometry data for INS-1 cells incubated for 1 hour with PEG HBSE# and PR_b-PEG HBSE# liposomes. Data is expressed as mean ± SE of n=3-4 experiments. Symbols directly over bars represent the significance compared to the autofluorescence of the INS-1 cells at the same temperature. †, no significance; *, p<0.05; **, p<0.01; ***, p<0.001.

The data to this point seem to indicate that the lipids are playing a large role in protecting the β cells from ischemia. However, to strengthen this theory we used polymerizable liposomes as a negative control. These liposomes are composed of 99 mol% 1,2-bis(10,12-tricosadiynoyl)-*sn*-glycero-3-phosphocholine (DC(8,9)PC) and 1 mol% PEG2000. The

DC(8,9)PC-PEG liposomes contain HBSE buffer and are 144±65 nm in diameter. The DC(8,9)PC lipid is able to form crosslinks in the bilayer when exposed to UV light (Puri et al., 2011; Ramakers et al., 2012; Yavlovich et al., 2009; Yavlovich, Singh, Blumenthal, & Puri, 2011). Figure 4.11A demonstrates the schematic of the liposome formation and Figure 4.11B shows the absorbance and color change (inset images) indicative of liposome polymerization. The lipids in polymerized liposomes should have a greatly reduced ability to transfer to the cells during incubation. When the DC(8,9)PC-PEG liposomes are incubated with INS-1 cells exposed to ischemic conditions, there is no significant change in metabolic activity compared to the anoxic control (Figure 4.11C, $p=0.42$). This goes a step farther to demonstrate that the lipids themselves are imparting some protection to the ischemic β cells.

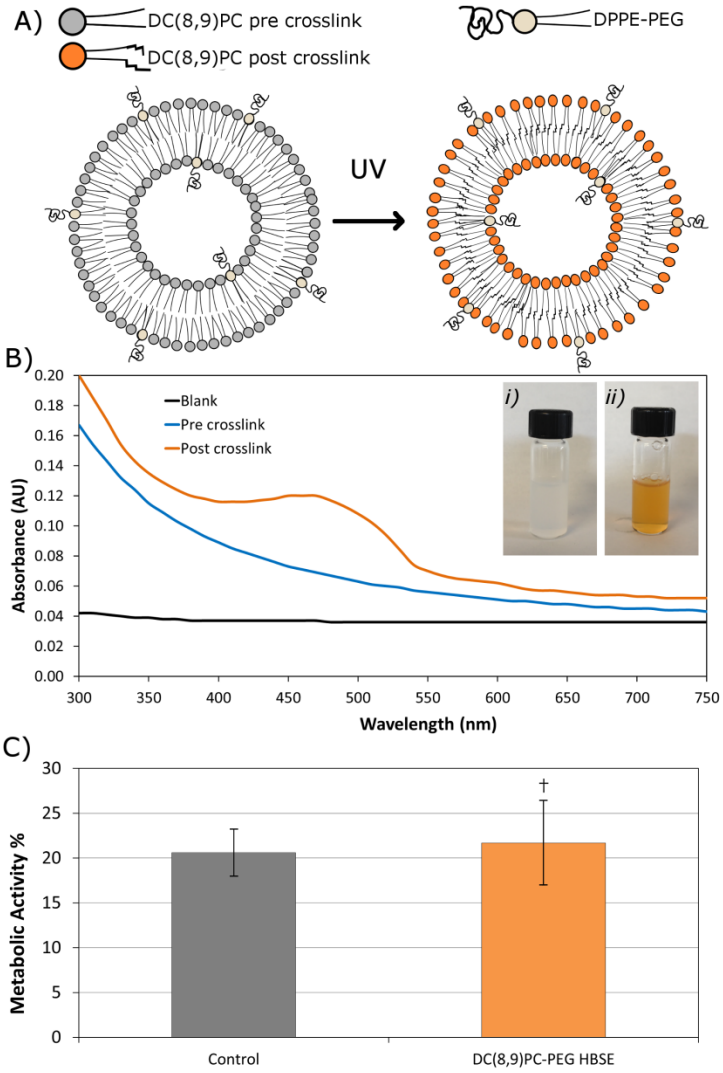

Figure 4.11: Polymerizable liposomes are formed by crosslinking lipids under UV light. A) Schematic of liposome formation. B) UV-vis absorbance spectrum of liposomes before and after polymerization. Blank refers to buffer only. Liposomes that are polymerized have an increase in absorbance and an indicative color change. Inset pictures represent liposomes i) before and ii) after polymerization. C) Polymerized liposomes do not significantly increase the metabolic activity of INS-1 cells exposed to 6 hours of ischemia at 37°C compared to the control. Data is presented as mean ± SE of n=7 experiments as a percentage of cells cultured in normal conditions (3 repetitions per experiment). †, no significance compared to control.

4.4.4 ATP Delivery Via Targeted Liposomes

While the lipids may be providing some protection from ischemia, we wanted to investigate if the ATP can provide additional functional benefits when compared to liposomes without a

payload. INS-1 cells were treated with free ATP, free PR_b peptide, a combination of free PR_b peptide and ATP, or different liposome formulations (PEG HBSE, PEG Tris, PEG ATPL, PR_b-PEG HBSE, PR_b-PEG Tris, and PR_b-PEG ATPL) and exposed to 6 hours of ischemic conditions. The metabolic activity of these cells was then compared to normally cultured cells (set as 100% metabolic activity). Figure 4.12 demonstrates that the metabolic activity of the cells is increased over the ischemic control sample for each treatment. Free PR_b peptide alone does not increase metabolic activity of the ischemic INS-1 cells over controls. Free ATP provides a similar benefit as the PEG HBSE, PEG Tris, PEG ATPL, PR_b-PEG HBSE and PR_b-PEG Tris treatments. Comparison between liposomes formulated with HBSE and Tris buffers only (PEG HBSE, PEG Tris, PR_b-PEG HBSE and PR_b-PEG Tris) demonstrates that the buffer encapsulated by the liposome does not impact the ability of the liposome formulation to increase metabolic activity, further implicating lipid transfer as the protective mechanism. Overall, the formulation functionalized with PR_b and encapsulating ATP (PR_b-PEG ATPL) performs significantly better than other liposome treatments. Though the effects of ATP and lipids do not appear to be additive, the liposomal delivery of ATP via the use of targeted stealth liposomes does increase the metabolic activity of the ischemic cells. The ability of PR_b functionalized liposomes to deliver ATP into cells, as well as transfer lipids, provides an additional benefit compared to nontargeted liposomes which can only transfer lipids to the ischemic cells.

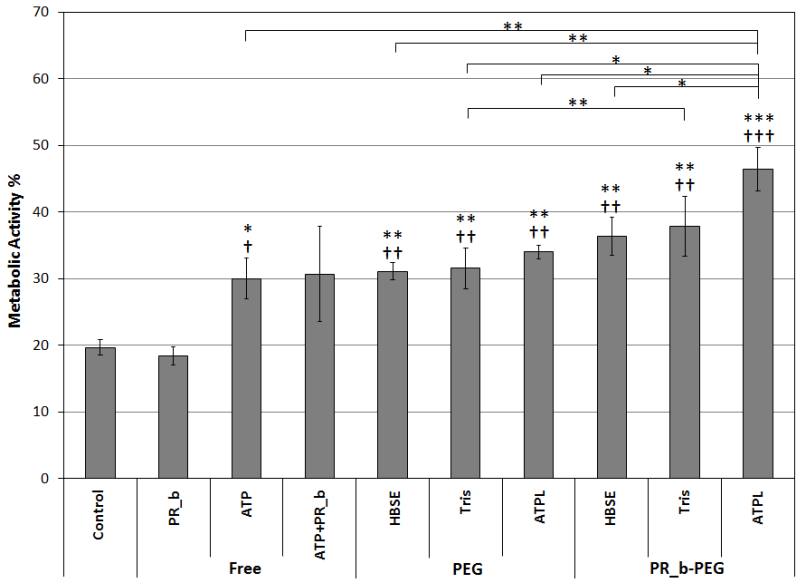

Figure 4.12: Metabolic activity of INS-1 cells treated with 3.6 μM free PR_b peptide, 120 μM free ATP, 3.6 μM free PR_b and 120 μM free ATP combined, or different liposomes (300 μM lipid concentration) and exposed to 6 hours of ischemia at 37 °C. PEG ATPL liposomes delivered 110 ± 29 μM ATP and PR_b-PEG ATPL liposomes delivered 122 ± 41 μM ATP. Data are expressed as a percentage of the metabolic activity of INS-1 cells cultured in a normal environment. Data shown as mean ± SE of n=3-11 experiments, 3-5 repetitions per n. * symbols directly over bars represent the significance compared to the ischemic control cells, † symbols directly over bars represent significance compared to free PR_b sample. *,† p<0.05; **,†† p<0.01; *,††† p<0.001 . If no symbol is displayed, there is no statistical significance for that pair.**

We also explored the effect of free ATP, PR_b-PEG HBSE, and PR_b-PEG ATPL treatments on the ability of INS-1 cells exposed to ischemia to secrete insulin in response to a glucose challenge. After the 6 hours of ischemic treatment, the cells were cultured normally and then tested for insulin secretion response. We tested the cells after both 4 and 8 hours of culture and did not see glucose stimulation (data not shown).

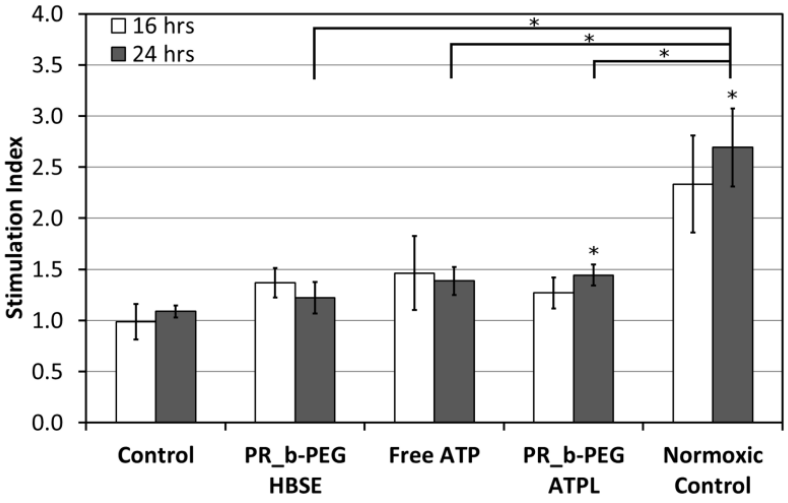

Figure 4.13: Functional activity of INS-1 cells treated with 150 μM free ATP or liposomes at a 300 μM lipid concentration and exposed to 6 hours of ischemia followed by 16 or 24 hours of normal culture (white and grey bars respectively). PR_b-PEG ATPL liposomes delivered 162 ± 16 μM ATP. Data is expressed as the ratio of insulin released at 15 mM glucose to the insulin released at 2.8 mM glucose. Data is expressed as mean ± SE of n=3-4 experiments. Symbols directly over bars represent the significance compared to the ischemic control cells.*, p<0.05

Based on previous reports, we decided to culture the cells longer before assessing their glucose responsiveness (Emamaullee, Liston, et al., 2005). As shown in Figure 4.13, normoxic control cells have between a 2 and 3 fold increase in insulin secretion when the glucose concentration changes from 2.8 to 15 mM. However, cells exposed to ischemic conditions have a reduced response to the increase in glucose concentration. Ischemic conditions lead to a change in gene expression which effects cell metabolism (Cantley et al., 2010) and therefore glucose responsiveness. Untreated cells have a stimulation index of about 1, meaning that the insulin secretion is the same at both 2.8 and 15 mM glucose. The liposome and free ATP treatments increase the stimulation index of the ischemic cells over the ischemic control, however only the PR_b-PEG ATPL sample after 24 hours of culture is significantly higher than the ischemic control at the same time point. Though each of the

treated samples has a lower stimulation index compared to the normoxic samples, the cells are capable of insulin secretion in response to a glucose challenge. Longer culture periods lead to a better recovery of glucose responsiveness, Figure 4.14. This data indicates that though the cells need time to recover from the ischemic insult, they are viable and regain their functional activity.

Though PR_b-PEG ATPL treatment slightly increases the insulin response of ischemic cells, the values are still well below normoxic controls. This is likely due to the changes in gene expression that occur in β cells exposed to ischemic environments (Cantley et al., 2010). Ischemia leads to activation of the hypoxia inducible factor 1alpha (HIF-1α) transcription factor which switches glucose metabolism from aerobic oxidative phosphorylation to anaerobic glycolysis in β cells (Cantley et al., 2010, Cheng et al., 2010, Cantley et al., 2009, Puri et al., 2009). This is accomplished through changes in genes controlling glucose uptake, glycolysis, and pyruvate utilization.[30] The delivery of ATP and lipids as shown in this work is able to maintain INS-1 cell viability during ischemic insult, however it does not appear sufficient to prevent the changes associated with HIF-1α expression. The ability of the ATP and lipid delivery to maintain viability and prevent the cells from undergoing necrosis could potentially allow the cells time to recover from the ischemic exposure in terms of glucose stimulated insulin secretion.

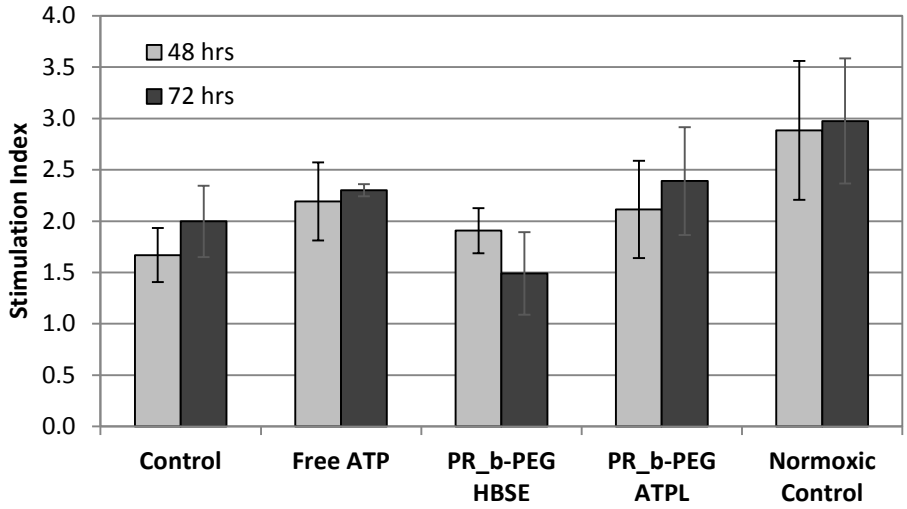

Figure 4.14: Functional activity of INS-1 cells treated with 150 μM free ATP or liposomes at a 300 μM lipid concentration and exposed to 6 hours of ischemia followed by 48 or 72 hours of normal culture. PR_b-PEG ATPL liposomes delivered 162 ± 16 μM ATP. Data is expressed as the ratio of insulin released at 15 mM glucose to the insulin released at 2.8 mM glucose. Data is expressed as mean ± SE of n=3-4 experiments.

Additionally, cells treated with PR_b-PEG ATPL or Free ATP had better control of basal insulin release levels than ischemic controls or samples treated with PR_b-PEG HBSE (Figure 4.15). This may indicate that although the cells have not regained their ability to increase insulin secretion, they are better able to regulate their cellular functions.

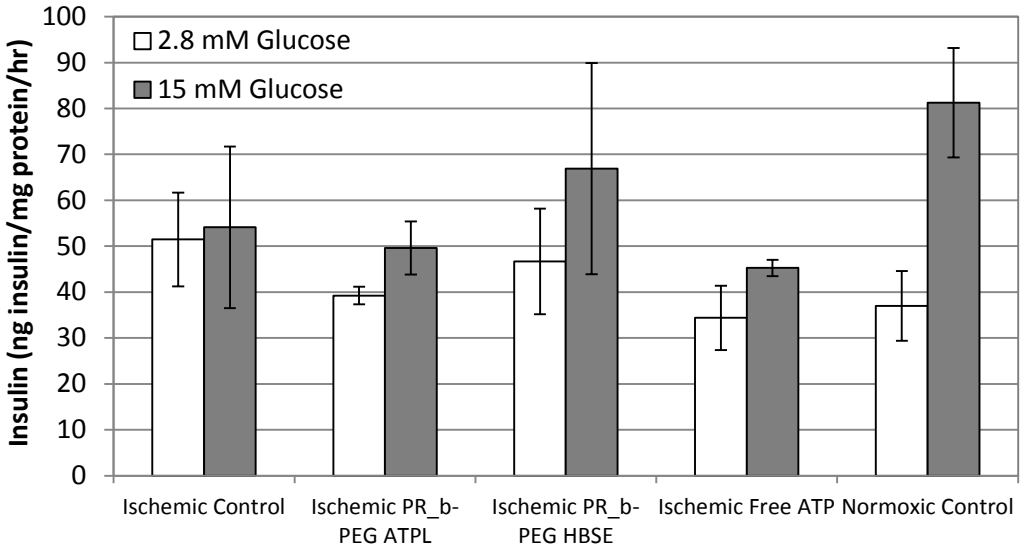

Figure 4.15: Glucose stimulated insulin release of INS-1 cells exposed to 6 hours of ischemia at 37°C followed by 16 hours of normal culture. Cells were treated with 150 mM free ATP or liposomes at 300 μM lipids. PR_b-PEG ATPL liposomes delivered 162 ± 16 μM ATP. Data is shown as the mean SE of n=3 experiments, 2 repetitions per n.

The results from the functional analyses demonstrate that both the lipids and the ATP provide benefits to the ischemic cells by maintaining cell viability, although they can only marginally improve insulin secretion. The delivery of ATP via PR_b functionalized stealth liposomes affords the best performance of all the treatments in terms of maintaining metabolic activity of β cells exposed to ischemia. Additionally, treatment with PR_b-PEG ATPL slightly improves the insulin secretion response after 24 hours of regular culture compared to the control. However, after longer culture times post ischemia all samples recover better glucose responsiveness but cells treated with PR_b-PEG ATPL and free ATP seem to recover slightly better than other samples. Also, cells treated with PR_b-PEG ATPL and free ATP have better regulation of insulin release at basal conditions after 16 hours of culture. In combination, these results demonstrate that the ATP delivery may be providing a

benefit in terms of cell function and control. The protection provided by free ATP in these experiments is promising; however in an *in vivo* setting these results would be unlikely due to the rapid degradation of free ATP *in vivo* (Chapat et al., 1991; Korb et al., 2008; Tep et al., 2009). Therefore, *in vivo* a bigger benefit would likely be seen for the PR_b-PEG ATPL compared to free ATP.

4.5 Conclusions

We have demonstrated the dual effect of treating ischemic β cells with PR_b targeted ATP liposomes. PR_b was shown to be necessary to internalized stealth liposomes into INS-1 cells and therefore could promote liposomal ATP delivery. Unexpectedly, INS-1 cells were partially protected from ischemic conditions by liposomes containing only buffer. Further investigation revealed that the lipids composing the liposomes play a role in maintaining cell membrane integrity. We hypothesize that the lipids are transferring from the liposomes to the cells, however an in depth analysis of this mechanism is outside the scope of the current work. PR_b targeted ATP liposomes were able to promote better cell metabolic activity than both free ATP and PR_b targeted liposomes containing only buffer, and increased the insulin secretion response compared to ischemic control cells. These results demonstrate that both the ATP and the lipids play a role in ischemic cell protection, however they cannot completely prevent the changes that result in decreased insulin secretion. We hypothesize that the activation of HIF-1α is leading to changes in gene expression that the ATP and lipids cannot prevent. However, by maintaining cell viability, these treatments may lead to better recovery of glucose responsiveness. Additionally, PR_b-PEG liposomes could be utilized to deliver alternative cargos specifically designed to interact with the HIF-1α cascade. The interactions of INS-1 β cells with the PR_b-PEG ATPL

described here will provide insight into the protection of islets from the myriad of ischemic conditions faced throughout isolation and transplantation. The ability of the PR_b targeted ATPL to prevent necrosis and maintain metabolic activity in ischemic β cells is promising for applications in pancreas preservation prior to islet isolation. As mentioned previously, current work in pancreas preservation is attempting to increase the ATP content of the organ. PR_b functionalized liposomes could facilitate the delivery of ATP and provide the additional benefit of lipid delivery. Improvement in preservation and isolation outcomes could lead to widespread application of islet transplants from a single donor, reducing both costs and risks associated with this procedure.

4.6 SUPPORTING INFORMATION

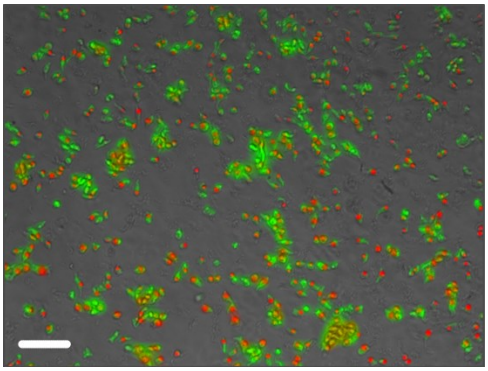

Figure 4.16: Live/dead staining of INS-1 cells exposed to ischemic conditions(glucose depleted minimal medium, 37 °C , 95% N_2, 5% CO_2) for 6 hours. Cells were treated with 250 μM DPPC and stained with calcein AM (green-live) and propidium iodide (red-dead). Scale bar is 20 μm.

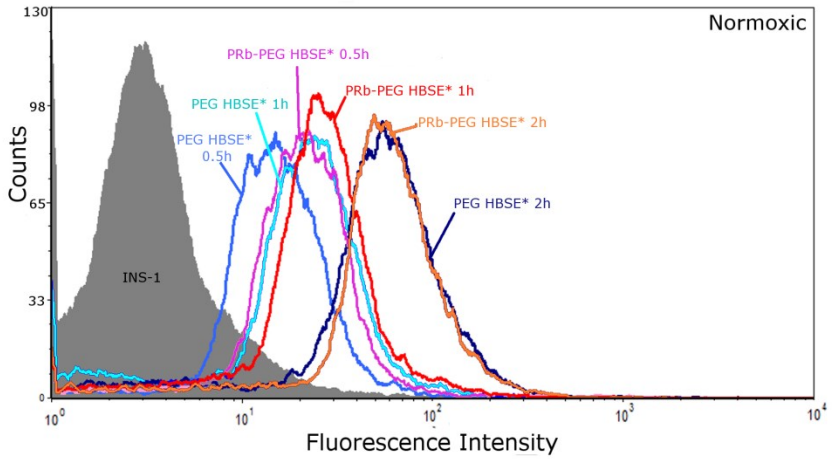

Figure 4.17: Representative flow cytometry histogram for INS-1 cells incubated with PEG HBSE* and PR_b-PEG HBSE* liposomes at 37°C. Both liposome formulations contain 1 mol% lissamine rhodamine B DPPE. Liposomes were incubated for indicated periods and the fluorescence monitored after washing via flow cytometry.

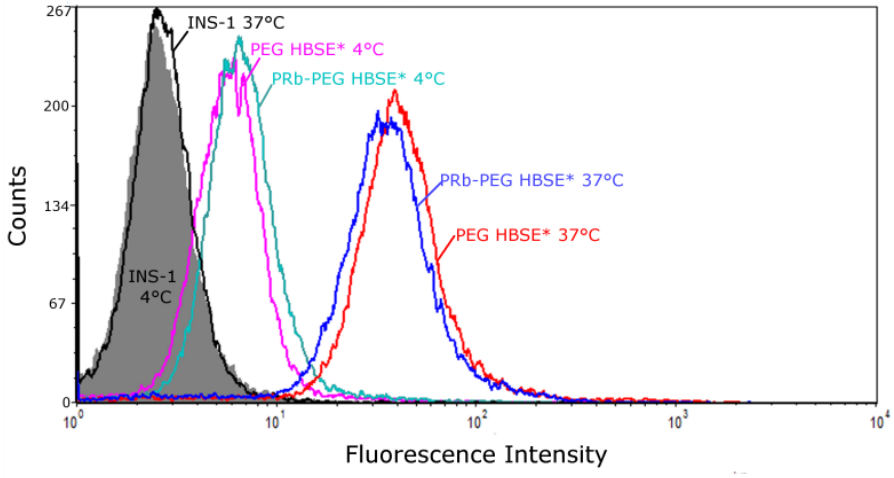

Figure 4.18: Flow cytometry histogram from a representative experiment monitoring the transfer of fluorescence from PEG HBSE* and PR_b-PEG HBSE* liposomes to INS-1 cells at 4°C and 37°C.Cells were incubated with liposomes for 1 hour. Both liposome formulations contain 1 mol% lissamine rhodamine B DPPE.

CHAPTER 5

SILICA NANOPARTICLE COATINGS BY ADSORPTION FROM LYS-SIL SOLS ON BIOLOGICAL SURFACES[2]

5.1 SYNOPSIS

Transplantation of islets of Langerhans is an attractive treatment for type I diabetes. However, human donor shortages, graft failure, and the necessity for life-long immunosuppression therapy are some of the issues affecting this therapy. Porcine islets have shown promise as an alternative islet supply to alleviate donor shortages but immunosuppression therapy is still necessary. It has been recognized that the encapsulation of living cells with permselective membranes could dramatically improve the viability of transplantation through immunoisolation and decrease the need for immunosuppression therapy. The ideal permselective membrane would simultaneously protect the cell from immunological attack, efficiently transport nutrients, and rapidly release therapeutic cell metabolites (e.g., insulin). Living cell encapsulation (e.g., islet) has included use of biopolymers (i.e. alginate, agarose), polyelectrolyte multilayers, silica sol-gels, poly (ethylene glycol) (PEG), and composites of these materials. However, many of the techniques lack pore size control and greatly increase the total volume of the transplanted graft. In this study, we first show the benign synthesis of small, fluorescent, and monodispersed silica nanoparticles with tunable surface potential. The relatively low cytotoxicity of silica nanoparticles has enabled their use in multiple biological applications. By tuning the surface potential of the silica nanoparticles to a positive charge, we show that

[2] Work performed in collaboration with Dr. Wei Fan

the particles are able to assemble on the surface of living cell membranes by simple adsorption. Utilizing layer-by-layer deposition, the particles are controllably assembled on the cell surface to build a thin nanoparticle membrane. Confocal and electron microscopy characterize the deposition of the nanoparticles on the surface of the cells and illustrate that, although the surface of the cell is dynamic and complex, the silica nanoparticles are deposited in a tunable and predictable fashion. The encapsulation protocol was shown to exhibit limited toxicity towards the cells, determined by a MTT viability assay. These findings highlight the potential of these nanoparticles for living cell encapsulation.

5.2 INTRODUCTION

Cell autotransplantation (same source) and allotransplantation (donor source) are attractive therapeutic approaches for treating diseased hosts that aim to employ cells for *in vivo*, autonomous release of metabolites. However, immunological rejection and controlled release capabilities still remain as challenges. For example, while transplantation of islets of Langerhans is an attractive therapy for treating type I diabetes,(Hering et al., 2004, 2006; Ricordi & Strom, 2004; Shapiro et al., 2000, 2006) both allografts and xenografts suffer from recognition by the host's immune system (Gray, 2001) and loss of graft function soon after transplantation (Emamaullee & Shapiro, 2006). It has been recognized that the encapsulation of living cells with permselective membranes could dramatically prolong the survival transplanted cells through immunoisolation (Ai, Fang, Jones, & Lvov, 2002; Gazda et al., 2007; Kobayashi et al., 2003; Lanza, Kuhtreiber, Ecker, Staruk, & Chick, 1995; Lim & Sun, 1980; Teramura & Iwata, 2009a, 2009b; Teramura et al., 2007). The ideal permselective membrane would simultaneously protect the cell from immunological attack, efficiently transport nutrients, and rapidly release therapeutic cell metabolites (e.g.,

insulin). Living cell encapsulation (e.g., islet) has included use of biopolymers (i.e. alginate, agarose) (Cui et al., 2004; Gazda et al., 2007; Kobayashi et al., 2003; Lim & Sun, 1980; Safley et al., 2002; T. Wang et al., 2008), polyelectrolyte multilayers (Miura et al., 2006), silica sol-gels (Pope, Braun, & Peterson, 1997; Snyder et al., 2009), poly (ethylene glycol) (PEG) (Miura et al., 2006; Sawhney et al., 1994; Teramura et al., 2007), and composites of these materials (Cui et al., 2004; Safley et al., 2002). These permselective materials must allow the flux of both nutrients and metabolites to ensure cell viability, while maintaining *in vivo* stability.

Silica nanoparticles have been used in a variety of applications and their low cytotoxicity (Fuller et al., 2008; Jin, Kannan, Wu, & Zhao, 2007; K. O. Yu et al., 2008) make these particles excellent candidates for multiple biological applications including cell imaging (Fuller et al., 2008; Jin et al., 2007; Larson et al., 2008; Law et al., 2008; Lin et al., 2005; Loo, Lowery, Halas, West, & Drezek, 2005; Park et al., 2009; Santra, Zhang, Wang, Tapec, & Tan, 2001), drug and DNA delivery (Fuller et al., 2008; Luo, Han, Belcheva, & Saltzman, 2004; Torney, Trewyn, Lin, & Wang, 2007), cell surface modification (Ai et al., 2002), cell membrane isolation (Chaney & Jacobson, 1983; Gkretsi et al., 2005; Stolz & Jacobson, 1992), and sol-gel cell encapsulation (Carturan et al., 2004; Pope et al., 1997; Snyder et al., 2009). The biocompatibility, chemical inertness, and mechanical strength of siliceous materials make them good candidates for encapsulation of biological materials, including mammalian cells (Carturan et al., 2004). Silica nanoparticles are synthesized predominantly using the Stöber method (Stöber, Fink, & Bohn, 1968), resulting in narrow distributions of large particles (>200 nm) but broad distributions of smaller particles. Recently, we (T. M. Davis et al., 2006; Fan et al., 2008; Snyder, Lee, Davis, Scriven, & Tsapatsis, 2007) and others (Hartlen, Athanasopoulos, & Kitaev, 2008; Yokoi et al., 2006) introduced a method for synthesizing

small, monodispersed silica nanoparticles in an aqueous environment in the presence of lysine or other basic amino acids. The approach allows for fine-tuning particle size by adjusting the multiple handles of the process, notably the silica content, lysine composition, stir rate during hydrolysis, pH, and hydrolysis and aging temperature, resulting in silica nanoparticle sols (hereafter referred to as lys-sil sols) that are stable for months, and also resist aggregation after being dispersed in other solvents including certain cell culture media(Fan et al., 2008; Snyder et al., 2009, 2007). It has also been demonstrated that lys-sil sols can form colloidal crystal arrays (Yokoi et al., 2006) and thin films by convective assembly (Snyder et al., 2007). In combination with their tuneable particle size, this

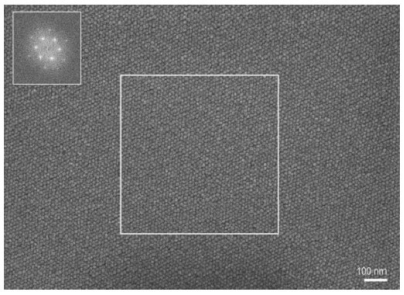

Figure 5.1: SEM image of lys-sil sol after evaporative drying. The insert depicts the Fourier transform pattern computed from the boxed area. Reproduced with permission from Snyder et al. (2007). Copyright 2007 American Chemical Society.

translates to capability for precise pore size control. However, convective methods, including evaporation-induced self-assembly (EISA), do not allow manipulation of deposit microstructure since they strongly favour close packing. Moreover, they are not compatible with applications where the substrate cannot be dried, such as living cell encapsulation. In this respect, it is desirable to develop functionalization techniques (Yoon, 2007) that enable deposition by adsorption. Here, we report new lys-sil sol syntheses that allow for adjustment of particle charge by surface functionalization. We also report on the inclusion of a fluorescent dye in the silica nanoparticles to be rendered observable by optical

microscopy. We then demonstrate layer-by-layer (LBL) assembly for living cell encapsulation. The findings reported here further establish lys-sil sols as a simple and flexible tool for precise colloidal assembly.

5.3 Materials and methods

5.3.1 Negatively Charged Lys-Sil Sols

Lys-sil sols were synthesized as described in refs (T. M. Davis et al., 2006; Yokoi et al., 2006) by hydrolysis of tetraethyl orthosilicate (TEOS,98%, Sigma-Aldrich) in aqueous solutions of L-lysine (Sigma-Aldrich). Aqueous solutions of prescribed lysine content were prepared using ultrapure water (resistivity of 18 MΩ cm by Millipore water purifier) and brought to 60^{o}C (for synthesis of 12 nm particles) or 90 ^{o}C (for synthesis of 20 nm particles), after which TEOS was added under magnetic stirring at 500 rpm. Hydrolysis was carried out under continued magnetic stirring for 48 h. The molar composition of the synthesis mixture described herein was 60 SiO_2 : 1.23 lysine : 9500 water : 240 ethanol.

5.3.2 Fluorophore Containing Lys-Sil Sols

Rhodamine 6G (Sigma-Aldrich, Dye content ~95 %) was incorporated to the silica nanoparticles of lys-sil sols through physical adsorption by nature of its amino groups and further seeded growth. 160 μL of 0.005 M Rhodamine 6G solution was introduced into 70 mL of 12 nm lys-sil sols (silica concentration of 0.031 wt%) under stirring at 500 rpm for 5 min at room temperature. Seeded growth was carried out by adding 0.29 g TEOS at 50 ^{o}C under stirring at 250 rpm for 12 h. To remove non-incorporated dye, the mixture was cleaned by centrifugation at 20000 rpm for 60 min and redispersed in water with a pH of 4.0 (The pH was adjusted to 4.0 with 0.25 M HCl). The process was repeated 3 times. Finally, the particles were dispersed in water with a pH of 4.0 and stored at 4 °C. Ultrapure water (resistivity of 18 MΩ cm by Millipore water purifier) was used in all experiments. The final

particle size of fluorophore containing lys-sil sols was 20 nm as determined by DLS and TEM.

5.3.3 Positively Charged Lys-Sil Sols

1. TMAPS functionalized lys-sil sols under acid condition

2.47 mL of 0.25 M HCl was added into 10 ml 20 nm lys-sil sols (1.84 wt%) made as described above. Then 100 μL N-trimethoxysilylpropyl-N,N,N-tri-methylammonium chloride (TMAPS, Gelest) was slowly added into the silica sol while stirring vigorously. The final pH of the solution was 1.2. The mixture was then heated at 60°C for 24 h with stirring at 500 rpm. The mixture was washed by centrifugation at 20000 rpm for 60 min followed by replacement of supernatant with water at a pH of 4.0 (the pH was adjusted by 0.25 M HCl). The process was repeated 3 times. Finally, the particles were dispersed in water with a pH of 4.0 and stored at 4°C. Ultrapure water (resistivity of 18 MΩ cm by Millipore water purifier) was used in all experiments..

2. TMAPS functionalized lys-sil sols under basic condition

10 mL of 0.1 wt% TMAPS was slowly added into 20 mL of 20 nm lys-sil sols (1.84 wt%, pH=9.2) made as described above while stirring vigorously. The final pH of the solution was 8.9. The reaction process and washing process were the same as the previously described surface modification under acid condition. Finally, the particles were dispersed in water with a pH of 4.0 and stored at 4°C.

3. Polyethyleneimine functionalized lys-sil sols under acid condition

3 mL of 1M HCl was added into 10 ml of 20 nm lys-sil sols (1.84 wt%) made as described above. Then 350 μL trimethoxysilylpropyl modified polyethyleneimine (Gelest) was slowly

added into the silica solution while stirring vigorously. The final pH of the solution was 1.2. The reaction process and washing process were the same as the previously described surface modification with TMAPS. Finally, the particles were dispersed in water with a pH of 4.0 and stored at 4 °C.

4. Fluorophore containing functionalized lys-sil sols (fluorescent positively charged particles)

For the surface modification of fluorophore containing lys-sil sols, 400 μL of 0.1 wt% TMAPS was slowly added into 10 mL of 20 nm fluorophore containing silica nanoparticles sol (0.16 wt%) made as described above while stirring vigorously. The reaction process and washing process were the same as the previously described surface modification of silica nanoparticles without dye. Finally, the particles were dispersed in water with a pH of 4.0 and stored at 4 °C. Zeta potential measurements indicate that positively charged fluorophore containing lys-sil sols have similar surface properties with the surface modified sols without dye.

5.3.4 Silica Nanoparticles Characterization

SEM images of silica nanoparticles were collected after sputter coating with platinum using a Denton VCR High Resolution Indirect Ion-Beam Sputtering System on a Hitachi S-900 Field Emission Gun Scanning Electron Microscope. TEM images were collected on a JEOL 1210. Cryo-TEM samples were prepared using FEI Vitrobot. The imaging was performed at -178 °C using an FEI Tecnai G2 F30 TEM operated at 300 kV. SAXS measurements of solid samples were taken on a home-built pinhole SAXS line with sample-to-detector distances of 369 cm using Cu Kα radiation. The sample was mounted in a brass block, and data were collected for 300 s. The UV–visible absorption spectra were measured with a Hewlett-Packard 8452A diode array spectrophotometer against a blank water reference. Zeta

potential titration curves and DLS were generated using a Brookhaven ZetaSizer 90 Plus. The pH of the solution is adjusted with 0.25 M HCl or 0.25 M NaOH. N_2 adsorption and desorption isotherms were measured at 77 K on an Autosorb-1 system. The specific surface area and the pore size distribution were calculated using the Brunauer–Emmett–Teller and BJH method, respectively. The Olympus Fluoview FV1000 confocal laser scanning microscope was used for confocal imaging.

5.3.5 INS-1 CELL COATING AT 4°C

INS-1 cells were cultured as described previously (Asfari et al., 1992). $5*10^5$ INS-1 cells were seeded onto poly-L-lysine (PLL, Sigma-Aldrich 0.1% in H_2O) coated glass substrates and allowed to incubate overnight at 37°C. PLL slides were made by incubating small glass coverslips in 2N NaOH for two hours, washing five times with DI H_20, one hour incubation in 0.01 wt% PLL in DI H_20, washing five time with DI H_20, rinsing with 100% EtOH, drying, and finally rinsing two times with sterile PBS. The substrates were washed twice with 4°C dextrose (pH 4.8) then incubated at 4°C for 30 minutes. Surface modified lys-sil sol (positively charged) was then suspended in dextrose at a concentration of 26.2 μg/mL and added to the substrates. The substrates were incubated for 30 minutes at 4°C with the nanoparticle solution followed by washing three times with 4°C dextrose. Unmodified lys-sil sol (negatively charged) in dextrose at a concentration of 26.2 μg/mL was then added to the substrates and incubated for 15 minutes at 4°C followed by washing three times in 4°C dextrose. This process was repeated 2 more times with 15 minute incubations each time resulting in six layers of alternating positive and negative silica nanoparticles.

5.3.6 INS-1 CELL COATING AT 37°C

INS-1 cells were cultured overnight on coverslips to allow for attachment. After cells attached, they were washed twice and incubated for 30 minutes with dextrose at 37 °C. Cells were washed one additional time and then incubated for 30 minutes with 26.2 μg/mL positive lys-sil sol in dextrose with 150 mM trehalose. After the incubation period, cells were washed three times and 26.2 μg/mL of negative lys-sil sol in dextrose with 150 mM trehalose was added to the culture and incubated for 15 minutes at 37°C. This process was repeated two more times with 15 minute incubations each time resulting in six layers of alternating positive and negative silica nanoparticles. After coating, the cells were washed three times and cultured for indicated times at 37°C. Coated INS-1 cells were cultured in RPMI-1640 with 11.1 mM glucose medium (Sigma) supplemented with 10% fetal bovine serum, 10 mM HEPES, 2 mM L-glutamine, 1 mM sodium pyruvate, 0.05 mM β-mercaptoethanol, 100 U/mL penicillin, 100 μg/mL streptomycin, and 150 mM trehalose. After the indicated incubation period, cells were washed three times with PBS, fixed with paraformaldehyde, and stained for nuclei as described in LSCM section below.

5.3.7 CELL VIABILITY

MTT assay was used to investigate cell viability via mitochondrial dehydrogenase activity. 3-(4,5-dimethylthiazol-2-yl)-2,5-diphenyl tetrazolium bromide or MTT (Sigma-Aldrich) is reduced to an insoluble purple formazan crystal by mitochondrial dehydrogenases showing intact functional mitochondria. After solubilization, the resulting solution is measured spectrophotometrically. INS-1 cells were seeded onto a 96 well plate at a density of $1*10^6$ cells/mL and incubated overnight in normal culture conditions. Samples were then coated with silica nanoparticle multilayers as described above. Control samples were processed identically as encapsulated samples omitting the silica nanoparticles. After the coating

process, MTT substrate in dextrose (1:10 dilution) was added to the samples and allowed to incubate overnight. Acidic isopropyl alcohol was used to dissolve the crystals. A SpectraMAX 384 spectrophotometer (Molecular Devices, Sunnyvale, CA) was used to determine the absorbance at 570 nm with a reference of 690 nm according to the manufacturer's protocol. The data were analyzed as mean ± SD of three independent experiments (n=5 replicates each) and further analyzed by a paired Student's t-test. Differences were considered significant when $p < 0.05$.

For trypan blue toxicity testing, approximately 1×10^6 (trypan blue) INS-1 cells were used per sample. The cells were removed from the culture flask by trypsinization and suspended in complete culture medium followed by incubation at 4 °C for 30 minutes. The cells were then centrifuged and washed with dextrose ((Baxter I.V. System 5 wt%) two times. Cells were incubated with 0 (control) and 26.2 μg/ml surface modified or unmodified silica nanoparticles in dextrose for 30 minutes at 4 or 37°C. The cells were then centrifuged and washed with dextrose, centrifuged again, and suspended in complete culture medium. Trypan blue dye was added to an aliquot of cell suspension at 50% v/v and analyzed by light microscopy.

5.3.8 INS-1 Cell Sample Preparation for SEM and LSCM

For preparing cell samples for SEM and laser scanning confocal microscopy (LSCM), cells were cultured and coated as described above. After coating the cell samples, LSCM samples were washed with cold dextrose and prepared for confocal microscopy by fixing with 4% paraformaldehyde in PBS, staining for nuclei using a cell membrane permeable blue-fluorescent Hoechst 33342 dye (Molecular Probes, Eugene, OR) at a concentration of 2.0 μM, and mounting on slides. The Olympus Fluoview FV1000 confocal laser scanning

microscope at the Biomedical Image Processing Laboratory at the University of Minnesota was used for all confocal studies. For SEM studies, after coating the cells with silica nanoparticles, the substrates were washed with 0.1 M cacodylate solution and placed in a gluteraldehyde fixative solution (0.1 M cacodylate, 2.5% gluteraldehyde) for one hour. Substrates were washed with 0.1 M cacodylate solution and added to a second osmium fixative solution (0.1 M cacodylate, 1% OsO_4) for 30 minutes in the dark, followed 0.1 M cacodylate rinses. The cells were then dehydrated through a series of ethanol solutions (20%, 50%, 70%, 80%, 2 x 95% and 4 x 100%) for five minutes each step, and dried with a critical point dryer (Tousimis Model 780A). The dry substrates were sputter coated with platinum using a Denton VCR High Resolution Indirect Ion-Beam Sputtering System.

5.3.9 Porcine Islet Coating
Porcine islets were cultured free floating as described previously (H. Brandhorst et al., 1999; Kirchhof et al., 2004; Ricordi, Socci, et al., 1990; Van der Burg et al., 1998). Approximately 500 islets were removed from culture and spun down at 130*g. Islets were suspended in cold dextrose and spun down again. The washing was repeated one additional time. The islets were then resuspended in cold dextrose and incubated at 4 °C for 30 minutes. The islets were then spun down and resuspended in cold dextrose containing 26.2 μg/mL positive lys-sil sol. The islets were incubated at 4°C for 30 minutes and then washed three times with cold dextrose. Monolayer samples were then fixed for imaging. For LBL samples, the islets were then resuspended in cold dextrose containing 26.2 μg/mL negative lys-sil sol, incubated at 4°C for 15 minutes, and washed three times. This process was repeated two additional times for 15 minutes for each incubation step for a total of six alternating positive, negative lys-sil sol layers. To fix them for imaging, the islets were washed in PBS two times and then incubated in 4% paraformaldehyde in PBS for 15

minutes at 37°C. The islets were then washed with PBS and stained with 2.0 μM Hoechst 33342 nuclei stain in PBS for 15 minutes at room temperature. They were then washed, mounted onto slides and imaged with the Olympus Fluoview FV1000 LSCM.

5.3.10 Glucose Stimulated Insulin Secretion

Approximately 100 islets were removed from culture and coated with 26.2 μg/mL of positive lys-sil sol forming a monolayer coating following the above procedure or left uncoated (control). The islets were incubated for 30 minutes at 37 °C in a 2.8 mM glucose solution in KREBS buffer (25 mM HEPES, 115 mM NaCl, 24 mM $NaHCO_3$, 5 mM KCl, 1 mM $MgCl_2$, 0.1% BSA, 2.5 mM $CaCl_2$). They were then transferred to fresh wells containing 2.8 mM (low glucose) or 28 mM (high glucose) solution in KREBS buffer and incubated for 60 minutes. The solution was collected after each incubation period. A porcine insulin ELISA (Mercodia) was used to assay the insulin content of the samples in duplicate according to the manufacturers' instructions. Insulin concentration was normalized by total cellular protein to account for differences in cells number and islet size. Protein concentration was determined by the BCA™ Protein Assay Kit (Thermo Scientific, Waltham, MA) following the manufacturer's protocols.

5.4 Results and Discussion

5.4.1 Nanoparticle Characterization

To create stable, positively charged silica particles, surface modification was performed with N-trimethoxysilylpropyl-N,N,N-tri-methylammonium chloride (TMAPS)(Goodwin, Harbron, & Reynolds, 1990; Pham, Fullston, & Sagoe-Crentsil, 2007; A. Van Blaaderen & Vrij, 1993) as well as other functionalizing agents. The modification was assessed with zeta potential measurements as a function of the lys-sil sol pH (Figure 5.2). The unmodified silica

nanoparticles show slightly negative surface potential at low pH, and the zeta potential decreases to -90 mV when the pH is close to 9.0. The surface potential after surface modification by TMAPS becomes positive when the pH is 7.0 and further increases to around +40 mV when the pH is below 5. Alternative functionalizations and reaction conditions result in distinct behaviors (Figure 5.2) demonstrating that the surface potential of lys-sil sols can be finely tuned. The modified particles show similar monodispersity, colloidal stability, and evaporative assembly characteristics as those in the original lys-sil sols. By solvent evaporation, three-dimensional colloidal crystals with well-defined mesoporosity can be formed from the surface modified silica nanoparticles (Figure 5.3).

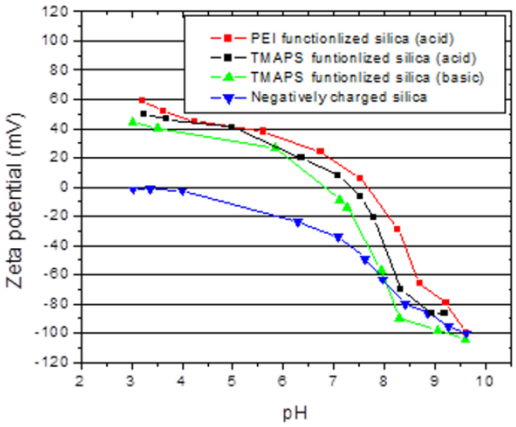

Figure 5.2: Zeta potential of surface unmodified and modified 20 nm lys-sil nanoparticle sols with different silanes. Red: Polyethyleneimine functionalized lys-sil sol under acid condition; Black: TMAPS functionalized lys-sil sol under acid condition; Green: TMAPS functionalized lys-sil sols under basic condition; Blue: Unmodified lys-sil sol. Data collected by Dr. Wei Fan.

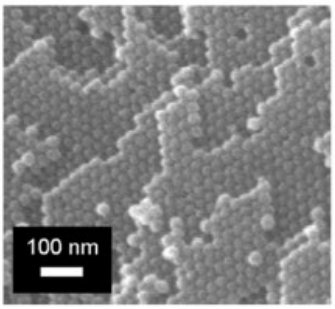

Figure 5.3: SEM image of colloidal crystals formed from 20 nm TMAPS modified lys-sil sols by solvent evaporation at pH=3.0.. Data collected by Dr. Wei Fan.

For optical observation, the silica nanoparticles were labeled with a fluorescent dye. Rhodamine 6G was incorporated by physical adsorption and subsequent capping with a silica outer shell (A. V. Blaaderen & Vrij, 1992). The UV-visible absorption spectra for the lys-sil sols with surface modified fluorescent nanoparticles show maximum absorption at approximately 526 nm, the same as the free dye, and intensity corresponding to 5 dye molecules per nanoparticle (Figure 5.4). Photographs of the sols before and after high speed centrifugation confirm that the dye is present in the nanoparticles (Figure 5.4 insets). The ability to precisely control fluorescent and non-fluorescent silica nanoparticle size and surface charge in an aqueous environment free of any stabilizing agent is unique to lys-sil sols and enables precise assembly through colloidal interactions. Zeta potential measurements indicate that positively charged fluorophore containing lys-sil sols have similar surface properties with the surface modified sols without dye (Figure 5.5).

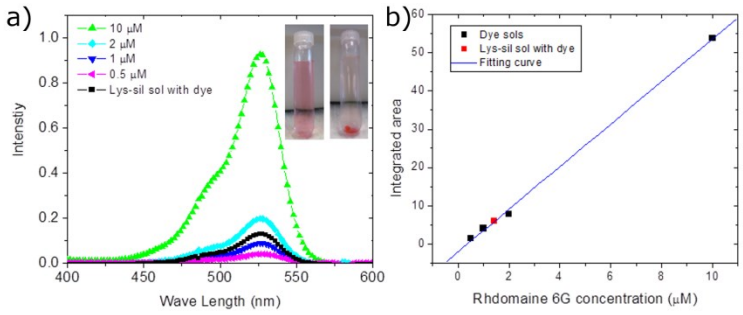

Figure 5.4: Determination of the number of Rhodamine 6G in silica nanoparticles.(A) UV-vis absorption spectra of Rhodamine 6G solution (10, 2, 1, 0.5 μM) and Rhodamine 6G containing lys-sil sol. The insets are images of a Rhodamine 6G containing silica sol before and after centrifugation. (B) Calibration curve of Rhodamine 6G solution and corresponding value of Rhodamine 6G containing lys-sil sol. By using the calibration curve, we found that the R6G concentration of the sols with dye was 1.42 μM, which corresponds to 5 R6G molecules per silica nanoparticle. Data collected by Dr. Wei Fan.

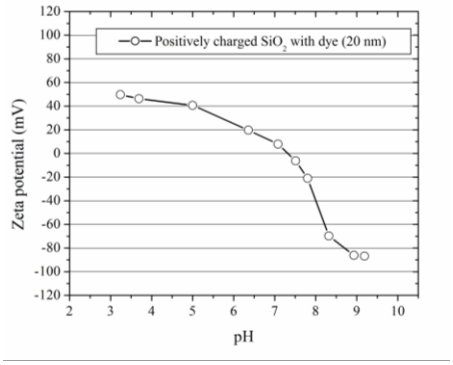

Figure 5.5: Zeta potential of surface modified 20 nm lys-sil sol with dye. Data collected by Dr. Wei Fan.

In addition to coatings on hard surfaces and self-assembly in solution, silica nanoparticles are also of interest for biological applications. More specifically, we are interested in creating silica membranes for cell encapsulation. The lys-sil sols are appropriate materials for encapsulation due to the fine pore size control imparted by ability to synthesize very small, monodispersed particles (T. M. Davis et al., 2006; Snyder et al., 2007) with controllable surface charge. Encapsulating cells within lys-sil sol films of controllable thickness (i.e., tens of nanometers,) in lieu of bulk encapsulation strategies could translate

to higher flux of chemical species. In addition, the porosity of such ordered nanoparticles films, imparted by the interstitial spacing between particles, can be tuned through particle size control and functionalization to dimensions commensurate with the passage of nutrients and immunological rejection.

In contrast to previous strategies that use EISA (Baca et al., 2006) or other deposition processes involving extensive silica polymerization (Carturan et al., 2004), we aim to form such coatings using layer by layer (LBL) assembly. In order to demonstrate deposition of these nanoparticles on living cell membranes, a rat insulinoma β cell line, INS-1 was used as a model system (Asfari et al., 1992). Cell membranes are primarily negative and therefore, for the first adsorption positively charged lys-sil sols were used. As the surface charge of modified silica nanoparticles is positive when the pH is below 7, dextrose solution (pH 4.8) was used as a coating solution in all experiments. The stability of silica nanoparticles in dextrose solution is demonstrated in Figure 5.6.

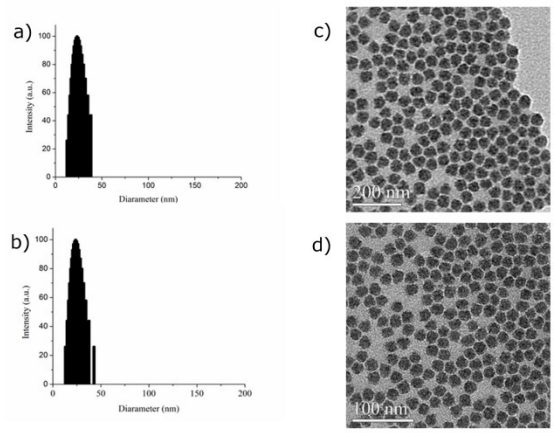

Figure 5.6: DLS and TEM images of surface modified silica nanoparticleswithout (A, B) and with (C, D) dye in dextrose solution after kept at room temperature for 1 day. The silica concentration in the lys-sil sol was 690 μg/mL. Data collected by Dr. Wei Fan.

5.4.2 Monolayer Encapsulation of INS-1 cells

The number of silica nanoparticles necessary to form a monolayer around each cell in the sample was determined, and concentrations of silica were added at 10 times (26.2 μg/mL) this monolayer concentration. Cytotoxicity of the nanoparticles towards INS-1 cells was assessed via trypan blue. It was found that exposure of INS-1 cells to lys-sil sols at 4°C or 37°C was not toxic (Figure 5.7). However, exposure at higher concentrations was toxic (Supporting information, Figure 5.26).

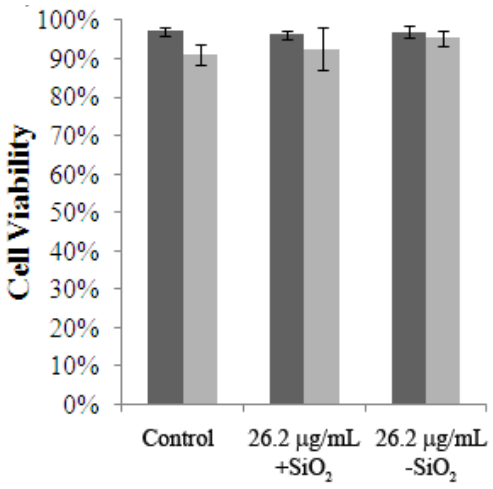

Figure 5.7: Cytotoxicity of lys-sil sols towards INS-1. Trypan blue assessment of cell viability after exposure to 26.2 μg/mL of positive or negative lys-sil sols for 30 minutes in dextrose at 4°C (dark bars, n=5) or 37°C (light bars, n=2).

Exposure of the INS-1 cells to 26.2 μg/mL of positive lys-sil sols in dextrose at 4°C resulted in assembly of the particles on the surface of the cell (Figure 5.8A, B). The confocal image demonstrates complete encapsulation of the INS-1 cells. The SEM image shows that the silica nanoparticles assemble densely on the surface of the cell and appear to form to the contours of the cells. However, when a higher concentration of silica was used (262 μg/mL) the cells were coated but closer inspection revealed that aggregates are present on the surface (5.8C, D).

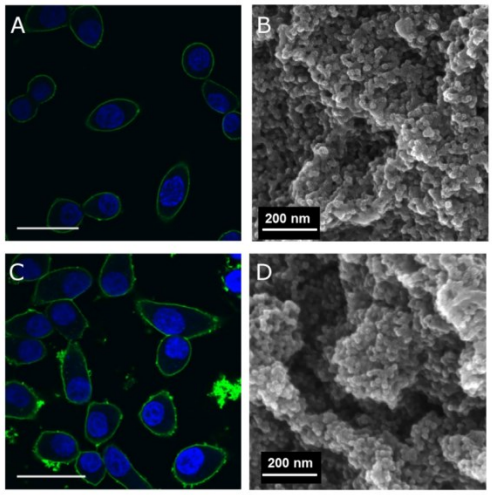

Figure 5.8: Monolayer assemblies of positive lys-sil sols on the surface of INS-1 cells. INS-1 cells were coated with 26.2 μg/mL (A, B) or 262 μg/mL (C, D) lys-sil sol in dextrose at 4°C. Confocal images (A, C) show the nucleus in blue and the lys-sil sol in green. Scale bars are 20 μM. SEM images (B, D) demonstrate the deposition of the particles on the surface of the INS-1 cells.

Monolayer coatings on INS-1 cells are stable for up to two hours in culture (37°C, complete medium) (Figure 5.9) but longer culture periods leads to internalization and possible desorption of the particles (Figure 5.10). Figure 5.9 displays a single confocal plane as well as the z projections along the lines on the image. The z projections demonstrate that the coatings cover the entire surface of the cell both immediately after coating and after two hours of culture. In Figure 5.10, immediately after formation the coatings are clearly around the periphery of the cell, but during the culture period some of the silica becomes internalized and gaps in the membrane coating become evident. Whether this is due to internalization, desorption, or membrane restructuring is unknown.

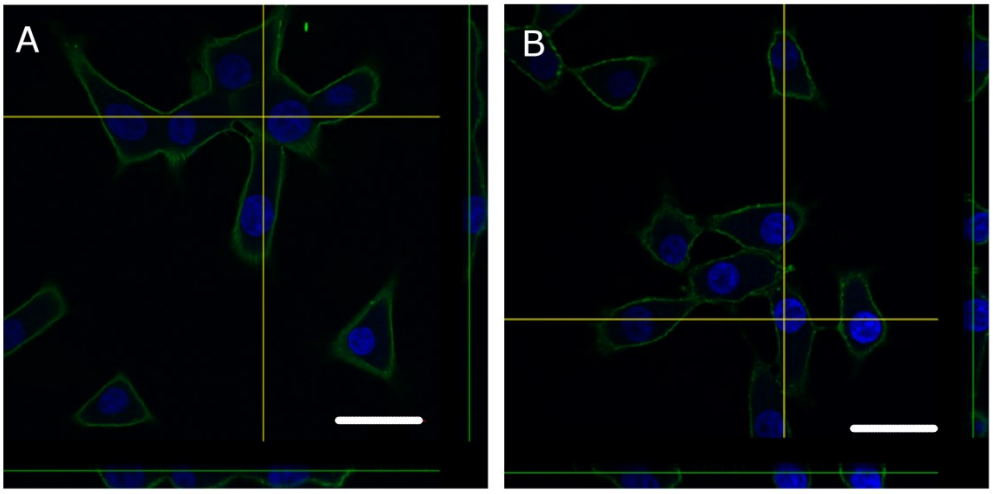

Figure 5.9: Monolayer coatings of positive lys-sil sols on INS-1 cells at 4°C in dextrose immediately after coating (A) and after two hours of regular culture (B). Z projections of the confocal image stack are shown for the lines and demonstrate the coating covers the entire surface of the cell. Lys-sil sols are green and nuclei are blue. Scale bars are 20 μm.

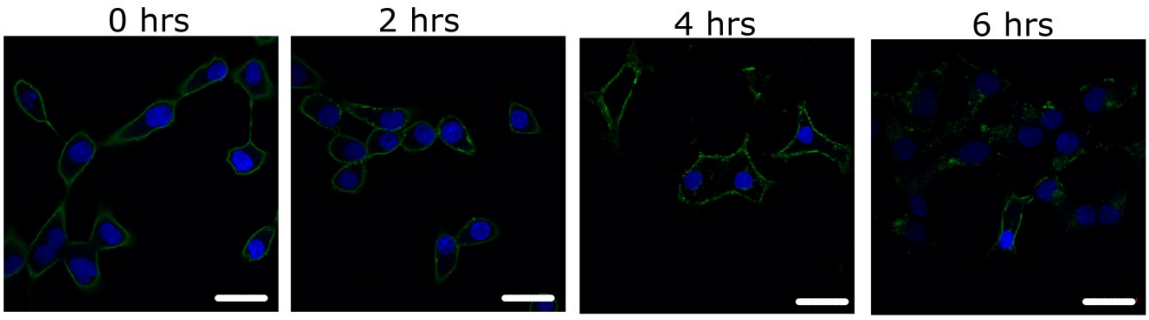

Figure 5.10: Time course stability of monolayer coatings of positive lys-sil sols on INS-1 cells at 4°C in dextrose followed by regular culture for 0, 2, 4, or 6 hours. Lys-sil sols are green and nuclei are blue. Scale bars are 20 μm.

5.4.3 Layer-by-Layer Encapsulation of INS-1 Cells

As mentioned previously, an advantage of encapsulation with lys-sil sols is the ability to control the membrane thickness by layer-by-layer (LBL) assembly of lys-sil particles with opposite charge. LBL assembly was accomplished by alternating positive and negative lys-sil sols for a total of six coating layers. Figure 5.11 demonstrates INS-1 cells coated at 4°C in

dextrose with a monolayer (A) and LBL (B). Figure 5.11 C and D give the relative fluorescent intensities along the red line in each image. The LBL assembly increases the fluorescence intensity associated with the lys-sil sols, demonstrating the increase in lys-sil absorption in the LBL assembly compared to the monolayer. SEM images comparing an uncoated cell to a cell coated by LBL assembly is shown in Figure 5.12. This figure demonstrates that despite the dynamics and complexity of the cell surface, densely packed coatings formed, contouring to the cell surface. INS-1 cells coated with varying amounts of lys-sil sols were also imaged by SEM and demonstrate the importance of lys-sil sol concentration during the coating protocol (Supporting information Figure 5.27).

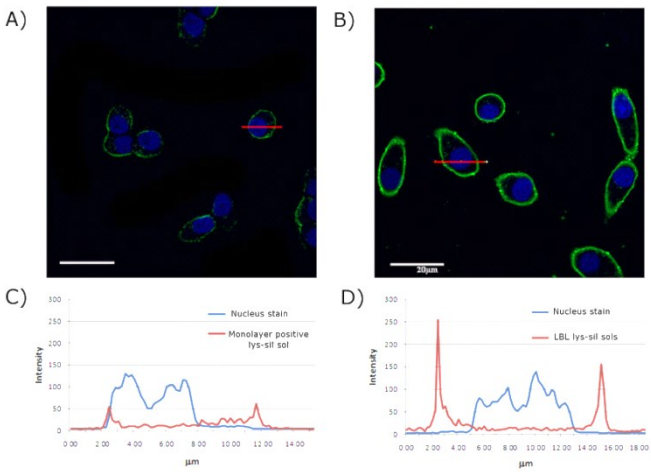

Figure 5.11: Monolayer (positive lys-sil sols) and LBL encapsulation of INS-1 cells at 4°C in dextrose. Confocal images of the monolayer (A) and LBL (B) samples demonstrate that both techniques form a complete layer but the LBL has stronger fluorescence intensity. Lys-sil sols are green and nuclei are blue. Scale bars are 20 µm. Graphs quantify the fluorescence intensity from each channel along the red line on the image for the monolayer sample (C) and LBL sample (D).

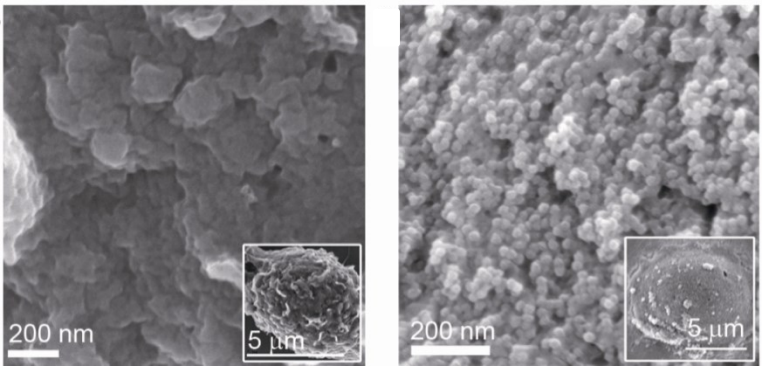

Figure 5.12: SEM images of coated INS-1 cells. Control INS-1 cells at 4°C (left) and INS-1 cells coated with lys-sil sols using the LBL protocol at 4°C (right). Insets show the entire cell.

INS-1 cells coated with LBL assembly at 4°C in dextrose can maintain their coatings for up to two hours in regular culture. Figure 5.13 demonstrates confocal images of INS-1 cells coated with six alternating layers of positively and negatively charged lys-sil sols immediately after coatings (0 hrs) and after two hours of culture at 37°C in regular culture conditions. The z projections along the lines on each image show that the coatings are covering the entire cell. The image of the sample immediately after coating shows green fluorescence on the slide away from the cell. This image slice is near the surface of the substrate and deposition of silica directly on the substrate was often seen in confocal samples.

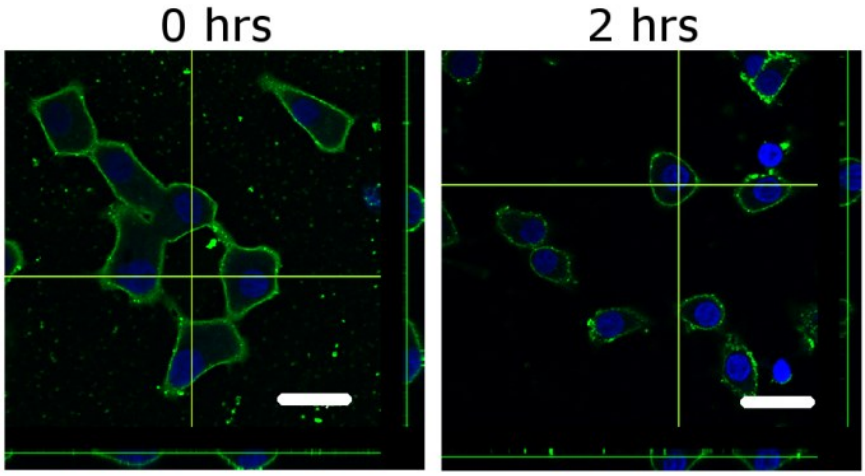

Figure 5.13: LBL coatings of INS-1 cells at 4°C in dextrose immediately after coating (0 hrs) and after two hours of regular culture (2 hrs). The z projections of the stacks along the lines are shown to the bottom and right of the images. Lys-sil sols are green and nuclei are blue. Scale bars are 20 μm.

However, similarly to the monolayer coatings, LBL coatings are not stable on the cell for long times in culture. Over the course of the culture period the lys-sil sol is partially internalized and gaps in the membrane coating occur. INS-1 cells are derived from an insulinoma and therefore are tumor cells that grow and divide. The coating could potentially be remodelling with the change in cell membrane size and composition. The images in Figure 5.14 show that even at 10 hours, some of the cells still display areas where the coating appears intact, however parts of the coating was internalized even at four hours.

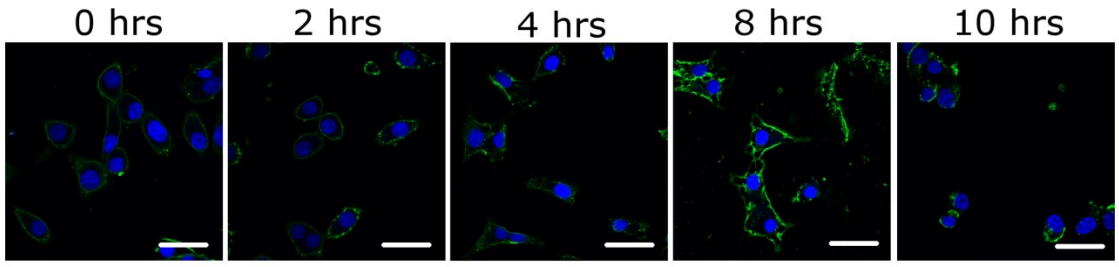

Figure 5.14: Stability of LBL coatings on INS-1 cells. Cells were coated with six alternating layers of positively and negatively charged lys-sil sols at 4°C in dextrose followed by regular culture for 0, 2, 4, 8, or 10 hours. Lys-sil sols are green and nuclei are blue. Scale bars are 20 μm.

The data above demonstrates that the lys-sil sols can be assembled on the surface of the cells. Both the monolayer and LBL methods resulted in good retention of the nanoparticle coatings on the cells up to approximately two hours of culture. However, for the intended application, longer stability of the coatings is required. For example, experiments testing the ability of encapsulation to protect again cytokine mediated toxicity demonstrated that at least 24 hours of cytokine incubation was necessary to increased caspase activation. The lack of stability of the coating for this duration prevented accurate determination of the lys-sil sol coatings' protective abilities (Supporting information Figure 5.28).

5.4.4 Encapsulation in the Presence of Trehalose

Motivated to increase the stability of the lys-sil coatings as well as allow for coatings to occur at 37°C, trehalose was added to the coating protocol. Trehalose is a disaccharide known to stabilize membranes by reducing lipid mobility and phase separation (Doxastakis, Sum, & de Pablo, 2005). We hypothesized that the reduction in membrane mobility would allow for the coatings to be performed at 37°C. Additionally, we thought supplementing trehalose to the culture medium might increase the stability of the coatings during culture. 180 mM of trehalose had been shown to decrease internalization of DNA-PEI complexes in a previous report (Tseng, Tang, Fang, & Su, 2007), presumably by decreasing endocytosis. However, the same report also noted that high concentrations of trehalose are toxic to cells.

To determine the toxicity of INS-1 cells to trehalose, cells were exposed to various concentrations of trehalose for one to 24 hours and their viability monitored via the WST-1 assay. Figure 5.15 shows that for short exposures, 50 or 150 mM trehalose do not exhibit marked toxicity to the cells. However higher concentrations decrease cell viability, especially with longer incubation times. When cells are exposed to trehalose containing

medium for four days of culture the effect on viability is more dramatic at all concentrations (Figure 5.16). This may be due to direct toxicity or a deleterious effect on cell proliferation.

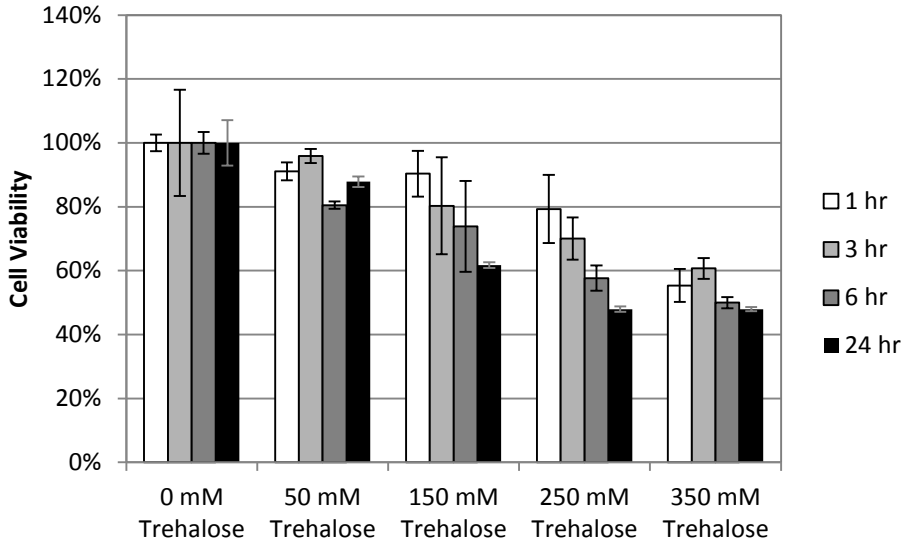

Figure 5.15: Trehalose toxicity towards INS-1 cells. INS-1 cells were exposed to culture medium supplemented with various concentrations of trehalose for 1, 3, 6, and 24 hours. Viability was measured by the WST-1 assay and normalized to the untreated controls (0 mM trehalose). Data represents the mean ± SD from n=1, 3 replicates per sample.

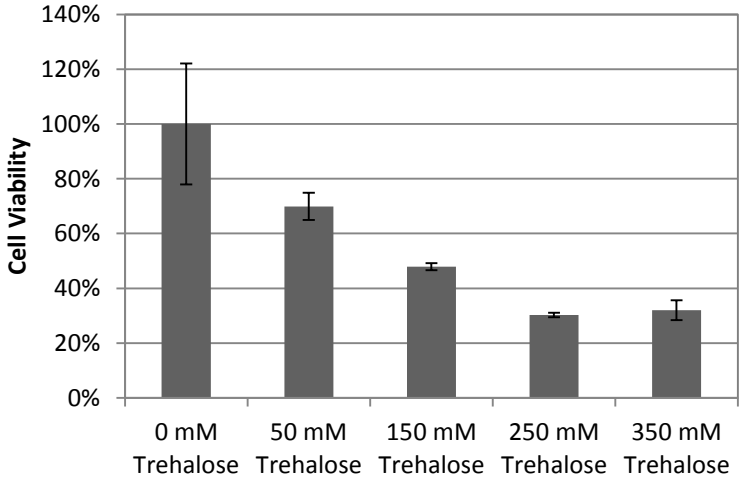

Figure 5.16: Four day exposure of INS-1 to trehalose supplemented culture medium. Viability was measured using the WST-1 assay and normalized to the untreated control (0 mM trehalose). Data represents the mean ± SD from n=1, 3 replicates per sample.

To investigate the ability of trehalose to inhibit endocytosis, INS-1 cells were incubated in complete medium supplemented with 0.1 mg/mL calcein and trehalose at various concentrations for 2.5 hours at 37°C. Calcein is a fluorescent probe that is taken up into cells via endocytosis. Figure 5.17 displays that endocytosis of calcein was lowered with the addition of trehalose at each concentration. Higher concentrations limited endocytosis to a greater extent but when coupled with the increased toxicity are not recommended for cell culture. Though the lower concentrations of trehalose had only a small effect on the endocytosis of calcein, the impact on membrane fluidity could still increase the stability of the lys-sil sol membranes. INS-1 cells were coated at 37°C in the presence of 50 or 150 mM trehalose in dextrose and cultured for 24 hours in culture medium supplemented with the same trehalose concentration. Confocal images in Figure 18 show that INS-1 cells were able to be coated at 37°C and were able to retain their membrane structure up to 24 hours of culture. Coating the cells at 37°C in the absence of trehalose resulted in particles penetrating the cell membrane (Figure 5.29, Supporting Information).

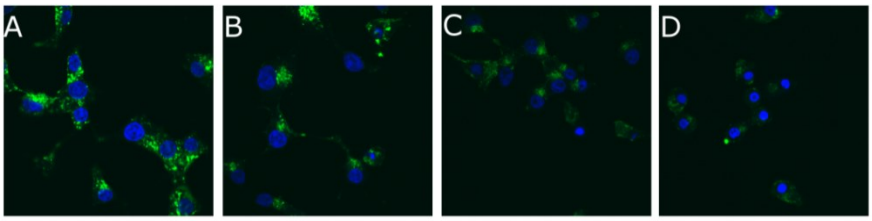

Figure 5.17: Effect of trehalose on calcein endocytosis. INS-1 cells were incubated in culture medium with 0.1 mg/mL calcein supplemented with no trehalose (A), 150 mM (B), 250 mM (C), or 350 mM (D) trehalose. Images show a single confocal plane with nuclei in blue and calcein in green.

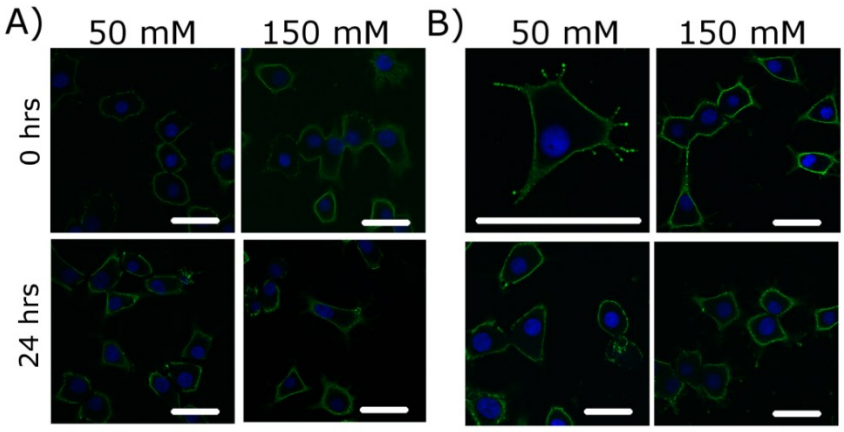

Figure 5.18: Confocal images of INS-1 cells coated at 37°C in the presence of 50 or 150 mM trehalose in dextrose. Cells were coated with a monolayer of positive lys-sil sol (A) or LBL (B). Images show the cells directly after coating (top row) or after 24 hours of culture in medium supplemented with the same concentration of trehalose (50 or 150 mM). Nuclei are blue and lys-sil sols are green. Scale bars are 20 μm.

5.4.5 Functional Activity of Encapsulated INS-1 Cells

We have demonstrated the encapsulation of INS-1 cells by fluorescently labeled lys-sil sols using either a monolayer or LBL method. The toxicity of the coating process was determined using the MTT assay. INS-1 cells were coated at 4°C in dextrose with a monolayer of positive lys-sil sols or LBL (six layers) and the viability measured directly after coating (0 hours) or after 60 hours of culture (60 hours). The data in Figure 5.19 show that either coating procedure does not affect the viability of cells compared to untreated controls. Based on previous results it is clear that at 60 hours the coatings no longer remain intact but the presence of the remaining silica either on or in the cells does not cause cell toxicity.

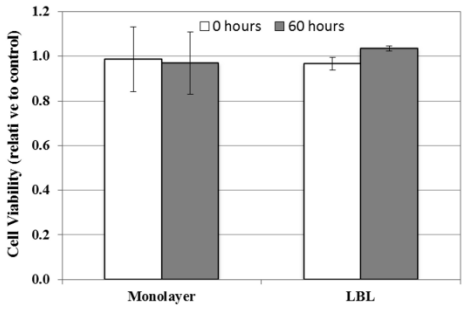

Figure 5.19: MTT assay of INS-1 cells coated with lys-sil sols in a monolayer or LBL. Cell viability was monitored directly after coating (white bars) or after 60 hours of regular culture (grey bars). Data is presented as the mean (normalized to untreated controls) ± SE of n=3 (0 hours) or n=2 (60 hours).

The hallmark test of INS-1 cell viability is glucose stimulation insulin secretion (GSIS). INS-1 cells are β cells that are capable of secreting insulin in response to an increase in glucose (Asfari et al., 1992). To test their ability to secrete insulin after encapsulation, INS-1 cells were encapsulated via the monolayer or LBL protocol at 4°C and immediately tested for glucose responsiveness at 37°C. Encapsulated INS-1 cells were incubated in 2.8 mM glucose in Krebs buffer for 30 minutes and then the buffer was replaced with fresh 2.8 mM glucose solution. The cells were incubated for one hour at 37°C. The medium was collected and 28 mM glucose in Krebs buffer was added to each well. The cells were incubated for an additional hour, the medium collected, and the cells lysed to determine total cell protein. The insulin secretion data is presented as the stimulation index, the insulin secretion at 28 mM glucose over the insulin secretion at 2.8 mM glucose.

$$Stimulation\ Index = \frac{Ins_{28\ mM}}{Ins_{2.8\ mM}}$$

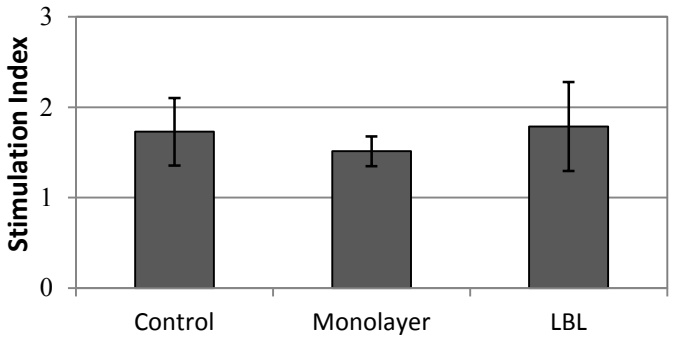

Figure 5.20: Glucose stimulated insulin secretion of INS-1 cells(Control) coated with a monolayer of positive lys-sil sol (Monolayer) or by six alternating layers of positively and negatively charged lys-sil sol (LBL). The mean stimulation index (insulin produced at 28 mM glucose/insulin produced at 2.8 mM glucose) ± SE of n=3 (3 repetitions per n) is displayed.

The data in Figure 5.20 indicate that the encapsulation protocol does not inhibit the secretion of insulin. However, closer examination of the process revealed that during the two hour GSIS protocol the silica was being internalized into the cell faster than during typical culture (data not shown). To attempt to analyze the ability of insulin to release with the coating still intact, the GSIS protocol was slightly adjusted. After the initial 2.8 mM glucose incubation, cells were exposed to 2.8 or 28 mM glucose solutions for one hour in parallel. After this GSIS protocol the monolayer coating has been mostly internalized (Figure 5.21 C) but the LBL coating remains primarily around the surface of the cells (Figure 5.21 D). The insulin response is also changed. INS-1 cells coated with a monolayer are capable of stimulated insulin secretion. However, cells encapsulated LBL have no stimulated insulin secretion, possibly due to the intact membrane around most of the cells. We hypothesized that insulin may not be able to be released from INS-1 cells with intact coatings for two reasons. First, the coatings may be negatively affecting the ability of glucose to enter the cell and/or affecting the cell's endocytosis/exocytosis functions. Secondly, insulin is stored in granules inside the cell. These granules consist of insulin monomers assembled into hexamers that form microcrystals (Dodson & Steiner, 1998). The

hexamer formation is driven by the presence of zinc ions in the cell. When the granule is released into the serum, the zinc concentration drops and the zinc ion forming the hexamer disappears, releasing the monomers (Dodson & Steiner, 1998). However when silica is present on the surface it is possible that the large microcrystals of insulin (50-500 μm, (Baker et al., 1988; Dodson & Steiner, 1998) cannot be released and therefore the monomers do not form. Encapsulated islets, on the other hand, may retain the ability to secrete insulin because only the cells on the perimeter of the islet will be interacting with the lys-sil sol. The other cells will be in contact with the interstitial space within the islet and therefore able to release the insulin crystals.

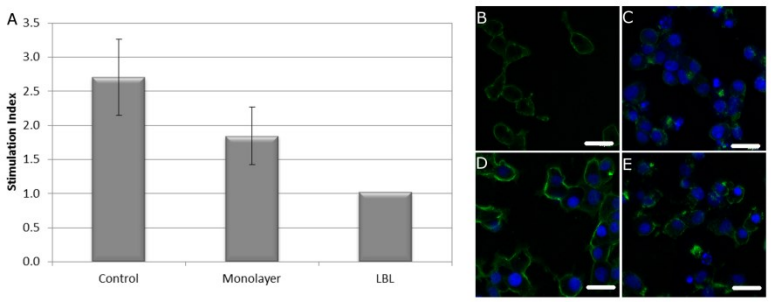

Figure 5.21: Glucose stimulated insulin secretion of INS-1 cells with modified protocol (A). The mean stimulation index (insulin produced at 28 mM glucose/insulin produced at 2.8 mM glucose) ± SE is displayed. Control and Monolayer, n=2; LBL, n=1 (3 repetitions per n). Confocal images of INS-1 cells immediately after encapsulation with a monolayer of positive lys-sil sols (B) or LBL (D) and after 28 mM glucose solution incubation (monolayer (C), LBL (E)). Confocal images show nuclei in blue and lys-sil sols in green. Scale bars are 20 μm. Nuclei stain is not present in B.

5.4.6 Encapsulation of Porcine Islets

Next we investigated lys-sil coatings on islets of Langerhans, large clusters of cells, including the insulin secreting β cells. Encapsulation of islets has been studied extensively (for a review, see ref.(Rabanel et al., 2009)) as a means of improving islet survival after *in vivo* transplantation. Figures 5.22A and B show porcine islets coated at 4°C with a single layer of

positively charged lys-sil sol and LBL assembly (six layers), respectively. Similar coatings can be obtained at 37°C in the presence of 100 mM trehalose (Figure 5.23). Additionally, response of monolayer coated islets to an increase in glucose concentration from 2.8 to 28 mM was not significantly different than uncoated islets, indicating no adverse effect of the coating on islet function (Figure 5.24). Confocal image of the islet after 28 mM glucose incubation indicates that the coating is still intact on the surface of the islet.

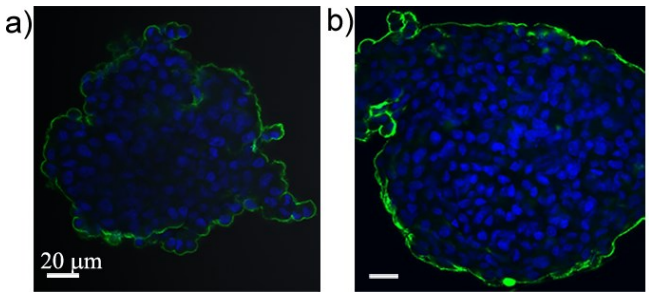

Figure 5.22: Encapsulation of porcine islets. Islets coated at 4°C with (A) positively charged lys-sil sol and (B) LBL assembly of six alternating layers from positively and negatively charged lys-sil sols. Confocal images show cell nucleus (blue) and the lys-sil particles (green). Scale bars are 20 µM.

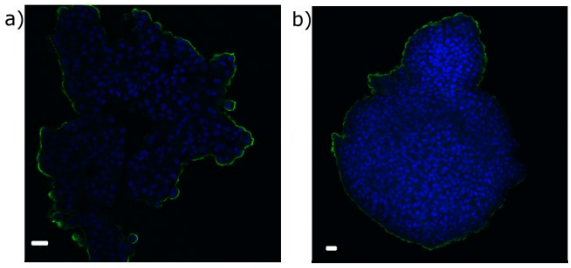

Figure 5.23: LBL encapsulation of porcine islets at 37°C in the presence of 100 µM trehalose. LBL assembly of six alternating layers from positively and negatively charged lys-sil sols immediately after coating (A) and after 2 hours of regular culture (B). Confocal images show cell nucleus (blue) and the lys-sil particles (green). Scale bar is 20 µm.

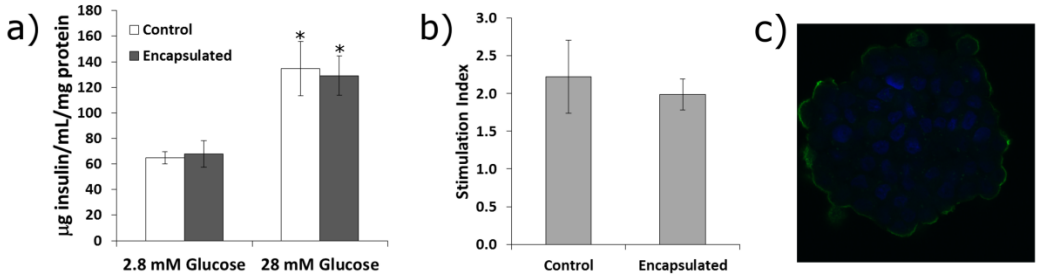

Figure 5.24: Glucose stimulated insulin release data for encapsulated islets. (A) Islets coated at 4°C with positive lys-sil sols (dark bars) respond to an increase in glucose concentration in a similar manner to uncoated cells (white bars). * indicates a significant increase over the 2.8 mM glucose value (n=5; *, p<0.05). (B) Stimulation index of control and encapsulated islets. No statistical difference between the samples (n=5, p=0.34). (C) Confocal image of encapsulated islet after incubation with 28 mM glucose solution and show cell nucleus (blue) and the lys-sil particles (green).

Although the coatings are stable on the surface of the islet after short periods of culture, longer incubation times lead to destruction of the coating. Figure 5.25 demonstrates porcine islets that were LBL coated at 4°C with 100 mM trehalose have continuous coatings immediately after encapsulated (Figure 5.25 A) but after 24 hours the coating is destroyed (Figure 5.25 B). Lys-sil sol resides inside cells at the periphery and near the core of the islet.

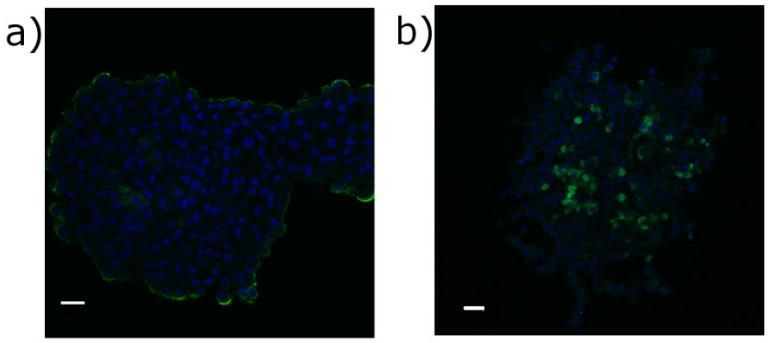

Figure 5.25: LBL encapsulation at 4°C in the presence of 100 mM trehalose in dextrose immediately after coating (a) and after 24 hours of regular culture (b). Confocal images show cell nucleus (blue) and the lys-sil particles (green). Scale bar is 20 μm.

Although stability of the encapsulation with lys-sil sols remains an issue, the simple formation, stability and demonstrated permeability of the lys-sil sol coatings indicate promise for immunoisolation applications. Future work with this system will focus on

improving stability by imparting further functionality onto the nanoparticles. Once stability is established, the permeability and immunoprotection properties will be probed.

5.5 Conclusions

In conclusion, size tuneable fluorescent and nonfluorescent silica nanoparticles with finely controllable surface charge were synthesized in benign conditions. These particles also offer advantages as a cell encapsulation material including pore size control, stability, and the ability to be visualized with confocal and electron microscopy. Living cells were encapsulated at 4°C and 37°C and encapsulated islets were shown to be able to be responsive to an increase in glucose concentration. Although here they have been deposited in the absence of polyelectrolytes or other LBL additives, they could also be used in conjunction with such components (Ai et al., 2002; Mansouri et al., 2009). Their potential applications for living cell imaging and encapsulation were also shown here while the ability to protect the cell from immunological attack and the long-term coating stability are issues under current investigation.

5.6 SUPPORTING INFORMATION

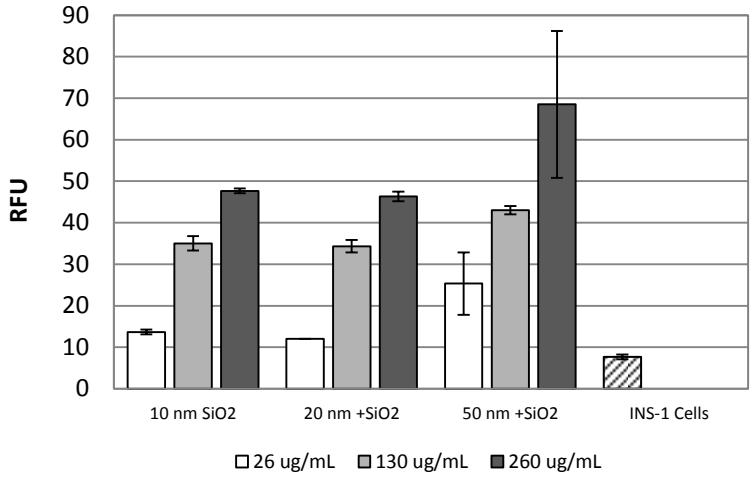

Figure 5.26: Sytox green fluorescence of INS-1 cells treated with varying concentrations of positive lys-sil sols (10, 20, and 50 nm in diameter).in media for 24 hours. Positive staining with sytox green represents increased necrotic cells. Data represents the mean RFU ± SD of n=1, 3 repetitions per sample. Data indicates that the increasing the concentrations of each size of nanoparticle results in increased cytotoxicity. Untreated cells are represented in the column filled with striped pattern.

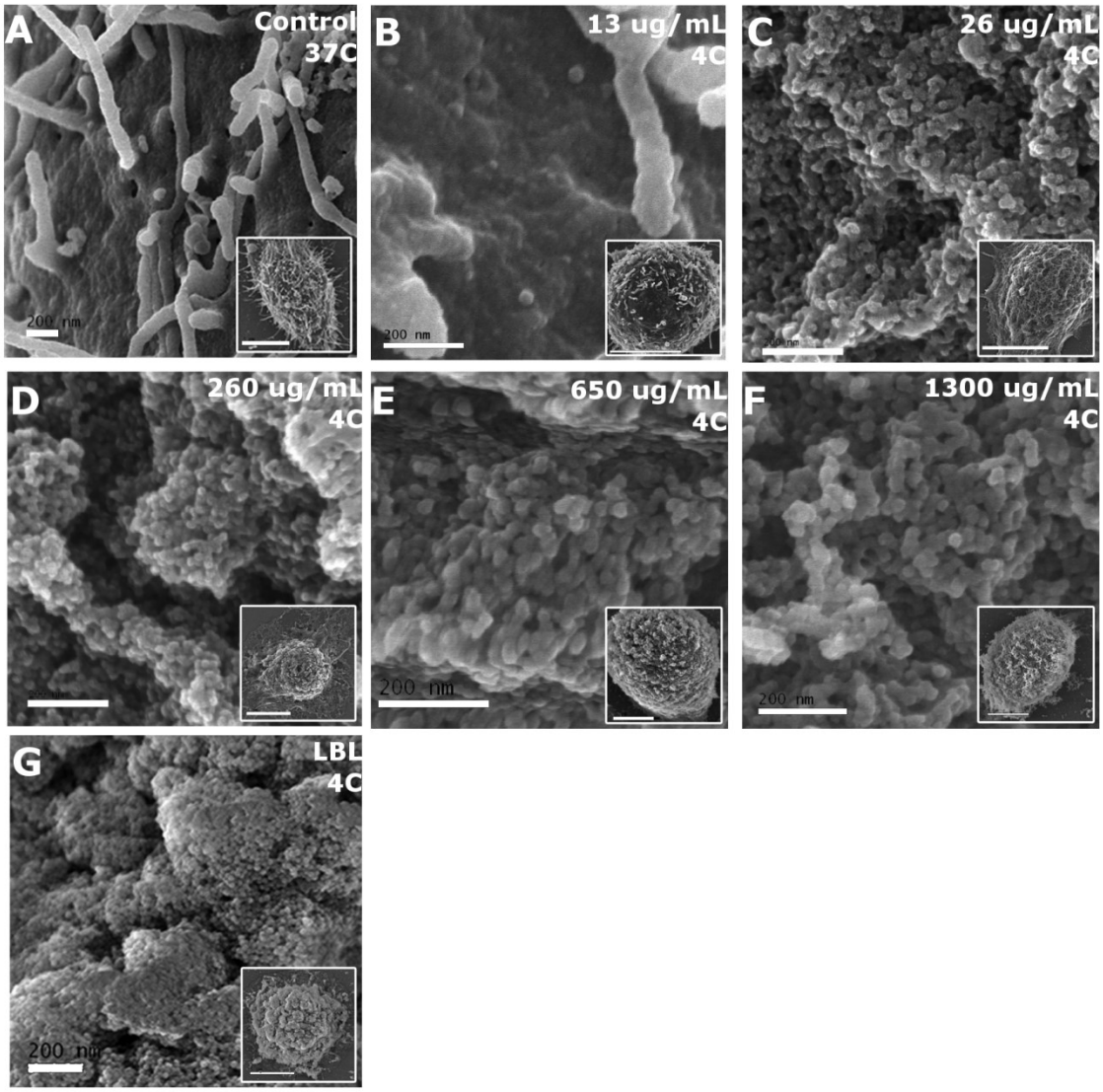

Figure 5.27: SEM images of INS-1 cells coated with varying concentrations of lys-sil sols. The insets are low magnification views of the cells in the larger image. A) Control cell at 37°C; B-F) INS-1 cells coated in dextrose for 30 minutes at 4°C with B) 13 μg/mL C) 26 μg/mL D) 260 μg/mL E) 650 μg/mL and F) 1300 μg/mL; G) INS-1 cells coated in dextrose at 4 °C by LBL with the first layer of lys-sil sol at 260 μg/mL and the remaining five layers at 26 μg/mL. Images demonstrate the importance of lys-sil sol concentration on the conformity of the coating. Scale bar for large images is 200 nm and for inset is 5 μm.

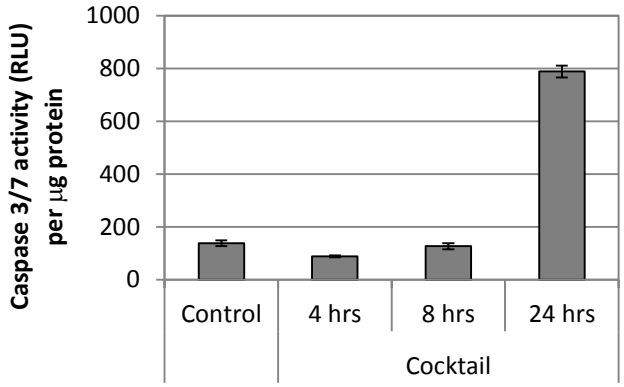

Figure 5.28: Caspase activity of INS-1 cells exposed to cytokine cocktail for 4, 8, or 24 hours. Cocktail consisted of 50 ng/mL TNF-α, 50 ng/mL IL-1β, and 100 ng/mL IFN-γ in cell culture medium. Data is presented at the mean ± SD. Control, n=2; Cocktail, n=1; 4 repetitions per n.

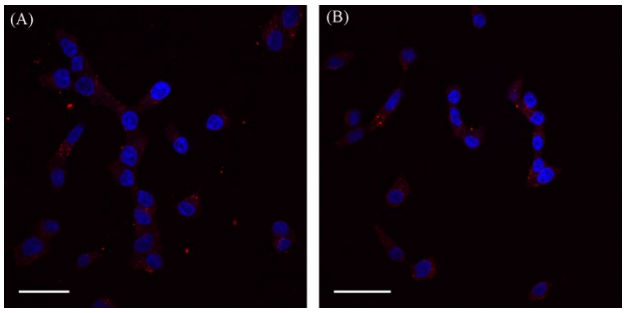

Figure 5.29: INS-1 cells coated at 37°C without trehalose.Confocal images of INS-1 cells obtained after contacting with positively charged (A) and negatively (B) charged lys-sil nanoparticle sols at 37 °C for 24 hours. The silica concentration in the lys-sil sols was 690 μg/mL. Red: silica nanoparticles; blue: cell nucleus. The scale bar is 20 μm.

CHAPTER 6

CONCLUDING REMARKS

Islet transplantation continues to provide both hope and challenges in the field of type 1 diabetes treatment. In these studies we have addressed two of the issues facing successful application of this treatment by looking at the interface of biology and materials design. We investigated the interactions of liposomes and silica nanoparticles with the surface of islets and β cells. By understanding their interactions, we were able to create favorable environments for the systems. Additionally, we looked at how the biomaterial interactions affected the functionality of the cells. We investigated both the effects on toxicity and endocrine functions of the treated cells. However, many of the stresses incurred by islets during the isolation and transplantation protocol lead to multiple problems downstream, making it difficult to gauge the success of a treatment *in vitro.* The hallmark assay for islet functionality remains *in vivo* testing which can provide the best estimate of the ability of a batch of islets to lower blood glucose levels in a diabetic patient.

The study of PR_b functionalized liposomes demonstrated the benefit imparted by adding targeting capability to the liposomes. Liposomes without PR_b showed little to no internalization into both porcine islet cells and rat β cells. We harnessed this result to deliver ATP to ischemic cells. Surprisingly, liposomal delivery of both ATP and lipids benefited the ischemic cells. We showed that even liposomes that do not bind or internalize were able to provide some protection by providing lipids to the ischemic cells. The most promising application of PR_b ATP liposomes may be in pancreas preservation. The

detrimental effects of ischemic periods may be partially ameliorated by addition of PR_b ATPL to the preservation solutions. However, PR_b targeted liposomes may also be useful for targeting the islets before, as well as after, transplantation. Injection of the liposomes into the portal vein may promote the interaction of the liposomes with the islets and could provide a mechanism to treat the cells post-transplant. While PR_b functionalized liposomes were used to deliver ATP in this work, the ability of PR_b to facilitate liposome internalization lends this system to other applications as well. Delivery of anti-apoptotic genes and antioxidants has shown promise and could benefit from a more effective delivery system.

We also investigated the ability of size-tunable silica nanoparticles to assemble on the surface of islets and β cells to create a permselective membrane. The particles assembled in both monolayers and layer-by-layer to create dense coatings on the cell surface. SEM images confirmed that the silica was completely covering the cell and conforming to the cell contours. The coating was formed at both 4°C and 37°C and was stable for two hours in culture. Islets coated with silica nanoparticles were capable of secreting insulin in response to a glucose challenge, indicating the retained functionality of the cells as well as the ability to transport glucose and insulin through the membrane. Attempts to characterize the immunoisolation properties of the membrane were limited by the instability of the coating during longer culture periods. After a few hours, the silica nanoparticles would be internalized into the cell or desorbed from the surface. Attempts to increase the stability by incorporation of trehalose into both the encapsulation and culture mediums were met with limited success. INS-1 cells had complete coatings at 24 hours of culture, but stable coatings on islets remained elusive. Ongoing work on this project includes incorporating crosslinking

functionality to the particles to create a network that will remain intact on the surface of cells. Additionally, utilizing the diverse sizes of silica particles could increase the stability of the coating. For example, perhaps increasing the size of the particles that are directly interacting with the membrane could reduce particle internalization during culture. Smaller particles could be assembled on top of the larger ones to provide the appropriate size selectivity. The flexibility of these particles is one of the biggest advantages to their use as an encapsulation material. Once a stable coating is created, porosity and immunoisolation properties will be investigated.

BIBLIOGRAPHY

Adil, M. M., Belur, L., Levine, R., Tisdale, A. W., McIvor, S., & Kokkoli, E. (n.d.). PR_b functionalized stealth liposomes for targeted delivery to metastatic colon cancer. *Biomaterial Science*.

Ah Kim, H., Lee, S., Park, J.-H., Lee, S., Lee, B.-W., Ihm, S. H., Kim, T., et al. (2009). Enhanced protection of Ins-1 beta cells from apoptosis under hypoxia by delivery of DNA encoding secretion signal peptide-linked exendin-4. *Journal of Drug Targeting*, *17*(3), 242–248. doi:10.1080/10611860902718664

Ai, H., Fang, M., Jones, S. a, & Lvov, Y. M. (2002). Electrostatic layer-by-layer nanoassembly on biological microtemplates: platelets. *Biomacromolecules*, *3*(3), 560–4.

Anderson, M. S., Venanzi, E. S., Klein, L., Chen, Z., Berzins, S. P., Turley, S. J., von Boehmer, H., et al. (2002). Projection of an immunological self shadow within the thymus by the aire protein. *Science*, *298*(5597), 1395–401. doi:10.1126/science.1075958

Aplin, a E., Stewart, S. a, Assoian, R. K., & Juliano, R. L. (2001). Integrin-mediated adhesion regulates ERK nuclear translocation and phosphorylation of Elk-1. *The Journal of Cell Biology*, *153*(2), 273–82.

Asfari, M., Janjic, D., Meda, P., Li, G., Halban, P. A., & Wollheim, C. B. (1992). Establishment of 2-mercaptoethanol-dependent differentiated insulin-secreting cell lines. *Endocrinology*, *130*(1), 167–178.

Atchison, N., Fan, W., Brewer, D. D., Arunagirinathan, M. a, Hering, B. J., Kumar, S., Papas, K. K., et al. (2011). Silica-nanoparticle coatings by adsorption from lysine-silica-nanoparticle Sols on inorganic and biological surfaces. *Angewandte Chemie International Edition*, *50*(7), 1617–21. doi:10.1002/anie.201006231

Atchison, N., Fan, W., Papas, K. K., Hering, B. J., Tsapatsis, M., & Kokkoli, E. (2010). Binding of the fibronectin-mimetic peptide, PR_b, to alpha5beta1 on pig islet cells increases fibronectin production and facilitates internalization of PR_b functionalized liposomes. *Langmuir*, *26*(17), 14081–14088. doi:10.1021/la101264h

Atkinson, M., & Eisenbarth, G. (2001). Type 1 diabetes: new perspectives on disease pathogenesis and treatment. *Lancet*, *358*(9277), 221–9. doi:10.1016/S0140-6736(01)05415-0

Avgoustiniatos, E. S., Hering, B. J., Rozak, P. R., Wilson, J. R., Tempelman, L. a, Balamurugan, a N., Welch, D. P., et al. (2008). Commercially available gas-permeable cell culture bags

may not prevent anoxia in cultured or shipped islets. *Transplantation Proceedings*, *40*(2), 395–400. doi:10.1016/j.transproceed.2008.01.059

Baca, H. K., Ashley, C., Carnes, E., Lopez, D., Flemming, J., Dunphy, D., Singh, S., et al. (2006). Cell-directed assembly of lipid-silica nanostructures providing extended cell viability. *Science*, *313*, 337–341. doi:10.1126/science.1126590

Baker, E. N., Blundell, T. L., Cutfield, J. F., Cutfield, S. M., Dodson, J., Dodson, G. U. Y. G., Hodgkin, D. M. C., et al. (1988). THE STRUCTURE OF 2Zn PIG INSULIN AT 1 . 5A RESOLUTION CRYSTALS. *Philosophical Transactions of the Royal Society of London*, *319*(1195), 369–456.

Ballian, N., & Brunicardi, F. C. (2007). Islet vasculature as a regulator of endocrine pancreas function. *World Journal of Surgery*, *31*(4), 705–714. doi:10.1007/s00268-006-0719-8

Beck, J., Angus, R., Madsen, B., Britt, D., Vernon, B., & Nguyen, K. T. (2007). Islet encapsulation: strategies to enhance islet cell functions. *Tissue engineering*, *13*(3), 589–599. doi:10.1089/ten.2006.0183

Belkin, V. M., Kozlova, N. I., Bychkova, V. V., & Shekhonin, B. V. (1996). Beta 1 integrin subunit dimerization via disulfide bonds. *Biochemistry and Molecular Biology International*, *40*(1), 53–60.

Benhamou, P. Y., Moriscot, C., Richard, M. J., Beatrix, O., Badet, L., Pattou, F., Kerr-Conte, J., et al. (1998). Adenovirus-mediated catalase gene transfer reduces oxidant stress in human, porcine and rat pancreatic islets. *Diabetologia*, *41*(9), 1093–100. doi:10.1007/s001250051035

Bennet, W., Sundbert, B., Lundgren, T., Tibell, A., Groth, C.-G., Richards, A., White, D. J., et al. (2000). Damage to porcine islets of langerhans after exposure to human blood in vitro, or after intraportal transplantation to cynomolgus monkeys. *Transplantation*, *69*(5), 711–719.

Berndt, P., Fields, G. B., & Tirrell, M. (1995). Synthetic lipidation of peptides and amino acids: monolayer structure and properties. *Journal of the American Chemical Society*, *117*(37), 9515–9522. doi:10.1021/ja00142a019

Berridge, M. V., Herst, P. M., & Tan, A. S. (2005). Tetrazolium dyes as tools in cell biology: New insights into their cellular reduction. (M. R. E.-G. B. T.-B. A. Review, Ed.)*Biotechnology Annual Review*, *Volume 11*, 127–152.

Blaaderen, A. V., & Vrij, A. (1992). Synthesis and Characterization of Colloidal Dispersions of Fluorescent , Monodisperse Silica Spheres. *Langmuir*, *81*(2), 2921–2931.

Bonner-Weir, S., & Orci, L. (1982). New perspectives on the microvasculature of the islets of Langerhans in the rat. *Diabetes*, *31*, 883–889.

Bottino, R., Balamurugan, a N., Tse, H., Thirunavukkarasu, C., Ge, X., Profozich, J., Milton, M., et al. (2004). Response of human islets to isolation stress and the effect of antioxidant treatment. *Diabetes*, *53*(10), 2559–68.

Bottino, R., Balamurugan, A. N., Smetanka, C., Bertera, S., He, J., Rood, P. P. M., Cooper, D. K. C., et al. (2007). Isolation outcome and functional characteristics of young and adult pig pancreatic islets for transplantation studies. *Xenotransplantation*, *14*(1), 74–82. doi:10.1111/j.1399-3089.2006.00374.x

Boyd, V., Cholewa, O. M., & Papas, K. K. (2010). Limitations in the use of Fluorescein Diacetate/Propidium Iodide (FDA/PI) and Cell Permeable Nucleic Acid Stains for Viability Measurements of Isolated Islets of Langerhans. *Current Trends in Biotechnology and Pharmacology*, *2*(2), 66–84.

Brandhorst, D, Brandhorst, H., Hering, B. J., Federlin, K., & Bretzel, R. G. (1999). Large variability of the intracellular ATP content of human islets isolated from different donors. *Journal of Molecular Medicine*, *77*(1), 93–95.

Brandhorst, Daniel, Iken, M., Bretzel, R. G., & Brandhorst, H. (2006). Pancreas storage in oxygenated perfluorodecalin does not restore post-transplant function of isolated pig islets pre-damaged by warm ischemia. *Xenotransplantation*, *13*(5), 465–70. doi:10.1111/j.1399-3089.2006.00340.x

Brandhorst, H., Brandhorst, D., Hering, B. J., & Bretzel, R. G. (1999). Significant progress in porcine islet mass isolation utilizing liberase HI for enzymatic low-temperature pancreas digestion. *Transplantation*, *68*(3), 355–61.

Brissova, M., Fowler, M. J., Nicholson, W. E., Chu, A., Hirshberg, B., Harlan, D. M., & Powers, A. C. (2005). Assessment of human pancreatic islet architecture and composition by laser scanning confocal microscopy. *The Journal of Histochemistry and Cytochemistry*, *53*(9), 1087–97. doi:10.1369/jhc.5C6684.2005

Burrows, L., Clark, K., Mould, A. P., & Humphries, M. J. (1999). Fine mapping of inhibitory anti-alpha5 monoclonal antibody epitopes that differentially affect integrin-ligand binding. *Biochemical Journal*, *344*, 527–533.

CDC. (2011). *Center for Disease Control and Prevention. National diabetes fact sheet: national estimates and general information on diabetes and prediabetes in the United States*. Atlanta, GA.

Cantley, J., Grey, T., Maxwell, P. H., & Withers, D. J. (2010). The hypoxia response pathway and beta-cell function. *Diabetes, Obesity and Metabolism*, *11*(Suppl 2), 159–167. doi:10.1111/j.1365-2036.2011.04905.x

Cardona, K., Korbutt, G. S., Milas, Z., Lyon, J., Cano, J., Jiang, W., Bello-Laborn, H., et al. (2006). Long-term survival of neonatal porcine islets in nonhuman primates by targeting costimulation pathways. *Nature Medicine*, *12*(3), 304–6. doi:10.1038/nm1375

Carlsson, P.-O., Liss, P., Andersson, a, & Jansson, L. (1998). Measurements of oxygen tension in native and transplanted rat pancreatic islets. *Diabetes*, *47*(7), 1027–32.

Carturan, G., Toso, D., Dal, R., & Monte, R. D. (2004). Encapsulation of functional cells by sol – gel silica : actual progress and perspectives for cell therapy. *Journal of Materials Chemistry*, *14*, 2087–2098.

Chaney, L. K., & Jacobson, B. S. (1983). Coating cells with colloidal silica for high yield isolation of plasma membrane sheets and identification of transmembrane proteins. *The Journal of Biological Chemistry*, *258*(16), 10062–72.

Chapat, S., Frey, V., Claperon, N., Bouchaud, C., Puisieux, F., Couvreur, P., Rossignol, P., et al. (1991). Efficiency of liposomal ATP in cerebral ischemia: bioavailability features. *Brain research bulletin*, *26*(3), 339–42.

Chen, C., Moreno, R., Samikannu, B., Bretzel, R. G., Schmitz, M. L., & Linn, T. (2011). Improved intraportal islet transplantation outcome by systemic IKK-beta inhibition: NF-κB activity in pancreatic islets depends on oxygen availability. *American Journal of Transplantation*, *11*(2), 215–24. doi:10.1111/j.1600-6143.2010.03390.x

Chen, P. S., Toribara, T. Y., & Warner, H. (1956). Microdetermination of phosphorus. *Analytical Chemistry*, *28*(11), 1756–1758. doi:10.1021/ac60119a033

Cheng, K., Ho, K., Stokes, R., Scott, C., Lau, S. M., Hawthorne, W. J., Connell, P. J. O., et al. (2010). Hypoxia-inducible factor-1α regulates β cell function in mouse and human islets. *The Journal of Clinical Investigation*, *120*(6), 2171–2183. doi:10.1172/JCI35846.Because

Chiang, B., Essick, E., Ehringer, W., Murphree, S., Hauck, M. A., Li, M., & Chien, S. (2007). Enhancing skin wound healing by direct delivery of intracellular adenosine triphosphate. *American Journal of Surgery*, *193*(2), 213–218. doi:10.1016/j.amjsurg.2006.08.069

Chien, S. (2010). Intracellular ATP Delivery Using Highly Fusogenic Liposomes. In V. Weissig (Ed.), *Liposomes, Methods in Molecular Biology* (Vol. 605, pp. 377–391). Totowa, NJ: Humana Press.

Cline, G. W., Pongratz, R. L., Zhao, X., & Papas, K. K. (2011). Rates of insulin secretion in INS-1 cells are enhanced by coupling to anaplerosis and Kreb's cycle flux independent of ATP synthesis. *Biochemical and Biophysical Research Communications*, *415*(1), 30–35. doi:10.1016/j.bbrc.2011.09.153

Colton, C. K., Papas, K. K., Pisania, A., Rappel, M. J., Powers, D. E., O'Neil, J. J., Omer, A., et al. (2007). Characterization of islet preparations. In C. Halberstadt & D. F. Emerich (Eds.), *Cell Transplantation from Laboratory to Clinic* (pp. 85–132). New York: Elsevier Inc.

Contreras, J. L., Bilbao, G., Smyth, C., Eckhoff, D. E., Xiang, X. L., Jenkins, S., Cartner, S., et al. (2001). Gene transfer of the Bcl-2 gene confers cytoprotection to isolated adult porcine pancreatic islets exposed to xenoreactive antibodies and complement. *Surgery*, *130*(2), 166–74. doi:10.1067/msy.2001.115828

Contreras, J. L., Eckstein, C., Smyth, C. a, Bilbao, G., Vilatoba, M., Ringland, S. E., Young, C., et al. (2004). Activated protein C preserves functional islet mass after intraportal transplantation: a novel link between endothelial cell activation, thrombosis, inflammation, and islet cell death. *Diabetes*, *53*(11), 2804–14.

Cozzi, E., & Bosio, E. (2008). Islet xenotransplantation: current status of preclinical studies in the pig-to-nonhuman primate model. *Current Opinion in Organ Transplantation*, *13*, 155–158.

Craig, J. A., Rexeisen, E. L., Mardilovich, A., Shroff, K., & Kokkoli, E. (2008). Effect of linker and spacer on the design of a fibronectin-mimetic peptide evaluated via cell studies and AFM adhesion forces. *Langmuir*, *24*(18), 10282–10292. doi:10.1021/la702434p

Crowther, N. J., Gotfredsen, C. F., Moody, A. J., & Green, I. C. (1989). Porcine islet isolation, cellular composition and secretory response. *Hormone and metabolic research*, *21*(11), 590–5. doi:10.1055/s-2007-1009296

Cruise, G. M., Hegre, O. D., Scharp, D. S., & Hubbell, J. a. (1998). A sensitivity study of the key parameters in the interfacial photopolymerization of poly(ethylene glycol) diacrylate upon porcine islets. *Biotechnology and bioengineering*, *57*(6), 655–65.

Cui, W., Barr, G., Faucher, K. M., Sun, X.-L., Safley, S. a, Weber, C. J., & Chaikof, E. L. (2004). A membrane-mimetic barrier for islet encapsulation. *Transplantation Proceedings*, *36*(4), 1206–8. doi:10.1016/j.transproceed.2004.04.059

Danen, E. H., & Yamada, K. M. (2001). Fibronectin, integrins, and growth control. *Journal of Cellular Physiology*, *189*(1), 1–13. doi:10.1002/jcp.1137

Davalli, A. M., Ogawa, Y., Scaglia, L., Wu, Y.-J., Hollister, J., Bonner-Weir, S., & Weir, G. C. (1995). Function, Mass, and Replication of Porcine and Rat Islets Transplanted Into Diabetic Nude Mice. *Diabetes*, *44*(1), 104–111.

Davalli, A. M., Scaglia, L., Zangen, D. H., Hollister, J., Bonner-Weir, S., & Weir, G. C. (1996). Vulnerability of Islets in the Immediate Posttransplantation Period: Dynamic Changes in Structure and Function . *Diabetes* , *45* (9), 1161–1167. doi:10.2337/diab.45.9.1161

Davis, M. M., & Bjorkman, P. J. (1988). T-cell antigen receptor genes and T-cell recognition. *Nature*, *334*, 395–402.

Davis, S. S. (1997). Biomedical applications of nanotechnology--implications for drug targeting and gene therapy. *Trends in biotechnology*, *15*(6), 217–24. doi:10.1016/S0167-7799(97)01036-6

Davis, T. M., Snyder, M. A., Krohn, J. E., & Tsapatsis, M. (2006). Nanoparticles in Lysine-Silica Sols. *Chemical Materials*, *9*(17), 5814–5816.

Deijnen, J. H. M. V., Hulstaert, C. E., Wolters, G. H. J., & Schilfgaarde, R. V. (1992). Significance of the peri-insular extracellular matrix for islet isolation from the pancreas of rat , dog , pig , and man. *Cell and Tissue Research*, 139–146.

Demirgöz, D., Garg, A., & Kokkoli, E. (2008). PR_b-targeted PEGylated liposomes for prostate cancer therapy. *Langmuir*, *24*(23), 13518–13524. doi:10.1021/la801961r

Demirgöz, D., Pangburn, T. O., Davis, K. P., Lee, S., Bates, F. S., & Kokkoli, E. (2009). PR_b-targeted delivery of tumor necrosis factor-α by polymersomes for the treatment of prostate cancer. *Soft Matter*, *5*(10), 2011–2019. doi:10.1039/b814217c

Derbinski, J., Schulte, a, Kyewski, B., & Klein, L. (2001). Promiscuous gene expression in medullary thymic epithelial cells mirrors the peripheral self. *Nature immunology*, *2*(11), 1032–9. doi:10.1038/ni723

Dionne, K. E., Colton, C. K., & Yarmush, M. L. (1993). Effect of Hypoxia on Insulin Secretion by Isolated Rat and Canine lslets of Langerhans. *Diabetes*, *42*(1), 12–21.

Dodson, G., & Steiner, D. (1998). The role of assembly in insulin's biosynthesis. *Current Opinion in Structural Biology*, *8*, 189–194.

Doxastakis, M., Sum, A. K., & de Pablo, J. J. (2005). Modulating membrane properties: the effect of trehalose and cholesterol on a phospholipid bilayer. *The Journal of Physical Chemistry B*, *109*(50), 24173–81. doi:10.1021/jp054843u

Dufrane, D., & Gianello, P. (2008). Pig islet xenotransplantation into non-human primate model. *Transplantation*, *86*(6), 753–60. doi:10.1097/TP.0b013e3181840f55

Dufrane, D., Goebbels, R. M., Fdilat, I., Guiot, Y., & Gianello, P. (2005). Impact of Porcine Islet Size on Cellular Structure and Engraftment After Transplantation: Adult Versus Young Pigs. *Pancreas*, *30*(2), 138–147.

Dvoriantchikova, G., Barakat, D. J., Hernandez, E., Shestopalov, V. I., & Ivanov, D. (2010). Liposome-delivered ATP effectively protects the retina against ischemia-reperfusion injury. *Molecular Vision*, *16*(December), 2882–2890.

Elayat, A. A., El-Naggar, M. M., & Tahir, M. (1995). An immunocytochemical and morphometric study of the rat pancreatic islets. *Journal of Anatomy*, *186*, 629–637.

Emamaullee, J. A., Liston, P., Korneluk, R. G., Shapiro, A. M. J., & Elliott, J. F. (2005). XIAP overexpression in islet beta-cells enhances engraftment and minimizes hypoxia-reperfusion injury. *American Journal of Transplantation*, *5*(6), 1297–1305. doi:10.1111/j.1600-6143.2005.00891.x

Emamaullee, J. A., Rajotte, R. V., Liston, P., Korneluk, R. G., Lakey, J. R. T., Shapiro, A. M. J., & Elliott, J. F. (2005). XIAP overexpression in human islets prevents early posttransplant apoptosis and reduces the islet mass needed to treat diabetes. *Diabetes*, *54*(9), 2541–8.

Emamaullee, J. A., & Shapiro, A. M. J. (2006). Interventional strategies to prevent beta-cell apoptosis in islet transplantation. *Diabetes*, *55*(7), 1907–1914. doi:10.2337/db05-1254

Fan, W., Snyder, M. A., Kumar, S., Lee, P.-S., Yoo, W. C., McCormick, A. V., Lee Penn, R., et al. (2008). Hierarchical nanofabrication of microporous crystals with ordered mesoporosity. *Nature Materials*, *7*(12), 984–91. doi:10.1038/nmat2302

Fenske, D., Maurer, N., & Cullis, P. (2003). Encapsulation of weakly-basic drugs, antisense oligonucleotides, and plasmid DNA within large unilamellar vesicles for drug delivery applications. In V.P. Torchilin & V. Weissig (Eds.), *Liposomes: A Practical Approach* (2nd ed., pp. 167–191). Oxford: Oxford University Press.

Fiske, C. H., & Subbarow, Y. (1925). The colorimetric determination of phosphorus. *Journal of Biological Chemistry*, *66*, 375–400.

Fretz, M. M., Koning, G. A., Mastrobattista, E., Jiskoot, W., & Storm, G. (2004). OVCAR-3 cells internalize TAT-peptide modified liposomes by endocytosis. *Biochimica et Biophysica Acta*, *1665*(1-2), 48–56. doi:10.1016/j.bbamem.2004.06.022

Frisch, S. M., & Screaton, R. a. (2001). Anoikis mechanisms. *Current opinion in cell biology*, *13*(5), 555–62.

Froud, T., Ricordi, C., Baidal, D. a, Hafiz, M. M., Ponte, G., Cure, P., Pileggi, A., et al. (2005). Islet transplantation in type 1 diabetes mellitus using cultured islets and steroid-free immunosuppression: Miami experience. *American Journal of Transplantation*, *5*(8), 2037–46. doi:10.1111/j.1600-6143.2005.00957.x

Fuller, J. E., Zugates, G. T., Ferreira, L. S., Ow, H. S., Nguyen, N. N., Wiesner, U. B., & Langer, R. S. (2008). Intracellular delivery of core-shell fluorescent silica nanoparticles. *Biomaterials*, *29*(10), 1526–32. doi:10.1016/j.biomaterials.2007.11.025

García, A. J., Schwarzbauer, J. E., & Boettiger, D. (2002). Distinct activation states of alpha5beta1 integrin show differential binding to RGD and synergy domains of fibronectin. *Biochemistry*, *41*(29), 9063–9069.

Garg, A., & Kokkoli, E. (2011). pH-Sensitive PEGylated Liposomes Functionalized With a Fibronectin-Mimetic Peptide Show Enhanced Intracellular Delivery to Colon Cancer Cells. *Current Pharmaceutical Biotechnology*, *12*(8), 1135–1143. doi:10.2174/138920111796117328

Garg, A., Tisdale, A. W., Haidari, E., & Kokkoli, E. (2009). Targeting colon cancer cells using PEGylated liposomes modified with a fibronectin-mimetic peptide. *International Journal of Pharmaceutics*, *366*(1-2), 201–210. doi:10.1016/j.ijpharm.2008.09.016

Gazda, L. S., Vinerean, H. V., Laramore, M. a, Diehl, C. H., Hall, R. D., Rubin, A. L., & Smith, B. H. (2007). Encapsulation of porcine islets permits extended culture time and insulin independence in spontaneously diabetic BB rats. *Cell Transplantation*, *16*(6), 609–20.

Geenen, V. (2012). Thymus and type 1 diabetes: An update. *Diabetes research and clinical practice*, 1–7. doi:10.1016/j.diabres.2012.05.023

Giancotti, F. G. (1999). Integrin Signaling. *Science*, *285*(5430), 1028–1033. doi:10.1126/science.285.5430.1028

Giuliani, M., Moritz, W., Bodmer, E., Dindo, D., Kugelmeier, P., Lehmann, R., Gassmann, M., et al. (2005). Central necrosis in isolated hypoxic human pancreatic islets: evidence for postisolation ischemia. *Cell Transplantation*, *14*, 67–76.

Gkretsi, V., Zhang, Y., Tu, Y., Chen, K., Stolz, D. B., Yang, Y., Watkins, S. C., et al. (2005). Physical and functional association of migfilin with cell-cell adhesions. *Journal of Cell Science*, *118*(Pt 4), 697–710. doi:10.1242/jcs.01638

Godfrey, K. J., Mathew, B., Bulman, J. C., Shah, O., Clement, S., & Gallicano, G. I. (2012). Stem cell-based treatments for Type 1 diabetes mellitus: bone marrow, embryonic, hepatic, pancreatic and induced pluripotent stem cells. *Diabetic Medicine*, *29*(1), 14–23. doi:10.1111/j.1464-5491.2011.03433.x

Goodwin, J. W., Harbron, R. S., & Reynolds, P. A. (1990). Functionalization of colloidal silica and silica surfaces via silylation reactions. *Colloid & Polymer Science*, *268*, 766–777.

Gray, D. W. (2001). An overview of the immune system with specific reference to membrane encapsulation and islet transplantation. *Annals of the New York Academy of Sciences*, *944*, 226–39.

Grey, S. T., Arvelo, M. B., Hasenkamp, W., Bach, F. H., & Ferran, C. (1999). A20 inhibits cytokine-induced apoptosis and nuclear factor kB-dependent gene activation in islets. *Journal of Experimental Medicine*, *190*(8), 1135–1145.

Grey, S. T., Longo, C., Shukri, T., Patel, V. I., Csizmadia, E., Daniel, S., Arvelo, M. B., et al. (2003). Genetic engineering of a suboptimal islet graft with A20 preserves beta cell mass and function. *Journal of Immunology*, *170*(12), 6250–6256.

Groot, M. D., Sc, M., Schuurs, T. A., Ph, D., Leuvenink, H. G. . D., Schilfgaarde, R. V., de Groot, M., et al. (2003). Macrophage overgrowth affects neighboring nonovergrown encapsulated islets. *Journal of Surgical Research*, *115*(2), 235–241. doi:10.1016/j.jss.2003.07.008

Hartlen, K. D., Athanasopoulos, A. P. T., & Kitaev, V. (2008). Facile preparation of highly monodisperse small silica spheres (15 to >200 nm) suitable for colloidal templating and formation of ordered arrays. *Langmuir*, *24*(5), 1714–20. doi:10.1021/la7025285

Hartner, W. C., Verma, D. D., Levchenko, T. S., Bernstein, E. A., & Torchilin, V. P. (2009). ATP-loaded liposomes for treatment of myocardial ischemia. *WIREs Nanomedicine and Nanobiotechnology*, *1*, 530–539. doi:10.1002/wnan.046

Hayashi, K., Ochiai, T., Ishinoda, Y., Okamoto, T., Maruyama, T., Tsuda, K., & Tsubouchi, H. (1997). Relationship between cellular ATP content and cellular functions of primary cultured rat hepatocytes in hypoxia. *Journal of Gastroenterology and Hepatology*, *12*(3), 249–256.

Hering, B. J., Kandaswamy, R., Ansite, J. D., Eckman, P. M., Nakano, M., Sawada, T., Matsumoto, I., et al. (2005). Single-donor, marginal-dose islet transplantation in patients with type 1 diabetes. *The Journal of the American Medical Association*, *293*(7), 830–835. doi:10.1001/jama.293.7.830

Hering, B. J., Kandaswamy, R., Harmon, J. V., Ansite, J. D., Clemmings, S. M., Sakai, T., Paraskevas, S., et al. (2004). Transplantation of Cultured Islets from Two-Layer Preserved Pancreases in Type 1 Diabetes with Anti-CD3 Antibody. *American Journal of Transplantation*, *4*(3), 390–401. doi:10.1046/j.1600-6143.2003.00351.x

Hering, B. J., Matsumoto, I., Sawada, T., Nakano, M., Sakai, T., Kandaswamy, R., & Sutherland, D. E. R. (2002). Impact of two-layer pancreas preservation on islet isolation and transplantation. *Transplantation*, *74*(12), 1813–1816. doi:10.1097/01.TP.0000038292.24519.C3

Hering, B. J., & Walawalkar, N. (2009). Pig-to-nonhuman primate islet xenotransplantation. *Transplant Immunology*, *21*(2), 81–6. doi:10.1016/j.trim.2009.05.001

Hering, B. J., Wijkstrom, M., Graham, M. L., Hårdstedt, M., Aasheim, T. C., Jie, T., Ansite, J. D., et al. (2006). Prolonged diabetes reversal after intraportal xenotransplantation of wild-type porcine islets in immunosuppressed nonhuman primates. *Nature Medicine*, *12*(3), 301–3. doi:10.1038/nm1369

Hogan, A., Pileggi, A., & Ricordi, C. (2008). Transplantation: current developments and future directions; The future of clinical islet transplantation as a cure for diabetes. *Frontiers in Bioscience*, *13*, 1192–1205.

Homo-Delarche, F., & Boitard, C. (1996). Autoimmune diabetes : the role of the islets of Langerhans. *Immunology Today*, *17*(10), 456–460.

Hudrisier, D., Feau, S., Bonnet, V., Romagnoli, P., & Van Meerwijk, J. P. M. (2003). In vivo maintenance of T-lymphocyte unresponsiveness induced by thymic medullary epithelium requires antigen presentation by radioresistant cells. *Immunology*, *108*(1), 24–31.

Hwang, N., Varghese, S., Zhang, Z., & Elisseeff, J. (2006). Chondrogenic differentiation of human embryonic germ cell derived cells in hydrogels. *Tissue Engineering*, *12*(9), 2695–2706. doi:10.1109/IEMBS.2006.259710

Ilieva, A., Yuan, S., Wang, R., Agapitos, D., Hill, D. J., & Rosenberg, L. (1999). Pancreatic islet cell survival following islet isolation: the role of cellular interactions in the pancreas. *The Journal of Endocrinology*, *161*(3), 357–64.

Inui, O., Teramura, Y., & Iwata, H. (2010). Retention dynamics of amphiphilic polymers PEG-lipids and PVA-Alkyl on the cell surface. *ACS applied materials & interfaces*, *2*(5), 1514–20. doi:10.1021/am100134v

Jansson, L., & Carlsson, P.-O. (2002). Graft vascular function after transplantation of pancreatic islets. *Diabetologia*, *45*(6), 749–763. doi:10.1007/s00125-002-0827-4

Jay, T. R., Heald, K. a, Carless, N. J., Topham, D. E., & Downing, R. (1999). The distribution of porcine pancreatic beta-cells at ages 5, 12 and 24 weeks. *Xenotransplantation*, *6*(2), 131–40.

Jin, Y., Kannan, S., Wu, M., & Zhao, J. X. (2007). Toxicity of luminescent silica nanoparticles to living cells. *Chemical research in toxicology*, *20*(8), 1126–33. doi:10.1021/tx7001959

Kenyon, N. S., Ranuncoli, A., Masetti, M., Chatzipetrou, M., & Ricordi, C. (1998). Islet transplantation: present and future perspectives. *Diabetes/metabolism reviews*, *14*(4), 303–13.

Khalil, I. A., Kogure, K., Akita, H., & Harashima, H. (2006). Uptake Pathways and Subsequent Intracellular Trafficking in Nonviral Gene Delivery. *Science And Technology*, *58*(1), 32–45. doi:10.1124/pr.58.1.8.32

Khaw, B.-A., Torchilin, V. P., Vural, I., & Narula, J. (1995). Plug and seal: Prevention of hypoxic cardiocyte death by sealing membrane lesions with antimyosin-liposomes. *Nature Medicine*, *1*(11), 1195–1198.

Kim, H. A., Lee, B.-W., Kang, D., Kim, J. H., Ihm, S. H., & Lee, M. (2009). Delivery of hypoxia-inducible VEGF gene to rat islets using polyethylenimine. *Journal of drug targeting*, *17*(1), 1–9. doi:10.1080/10611860802392982

Kim, S., Bell, K., Mousa, S. A., & Varner, J. A. (2000). Regulation of angiogenesis in vivo by ligation of integrin alpha5beta1 with the central cell-binding domain of fibronectin. *The American Journal of Pathology*, *156*(4), 1345–62.

Kim, W. H., Lee, J. W., Gao, B., & Jung, M. H. (2005). Synergistic activation of JNK/SAPK induced by TNF-α and IFN-γ: Apoptosis of pancreatic β-cells via the p53 and ROS pathway. *Cellular Signalling*, *17*(12), 1516–1532.

Kin, T., Korbutt, G. S., Kobayashi, T., Dufour, J. M., & Rajotte, R. V. (2005). Reversal of diabetes in pancreatectomized pigs after transplantation of neonatal porcine islets. *Diabetes*, *54*(4), 1032–9.

Kirchhof, N., Shibata, S., Wijkstrom, M., Kulick, D. M., Salerno, C. T., Clemmings, S. M., Heremans, Y., et al. (2004). Reversal of diabetes in non-immunosuppressed rhesus macaques by intraportal porcine islet xenografts precedes acute cellular rejection. *Xenotransplantation*, *11*(5), 396–407. doi:10.1111/j.1399-3089.2004.00157.x

Kisiday, J., Jin, M., Kurz, B., Hung, H., Semino, C., Zhang, S., & Grodzinsky, a J. (2002). Self-assembling peptide hydrogel fosters chondrocyte extracellular matrix production and cell division: implications for cartilage tissue repair. *Proceedings of the National Academy of Sciences of the United States of America*, *99*(15), 9996–10001. doi:10.1073/pnas.142309999

Klibanov, A. L., Maruyama, K., Torchilin, V. P., & Huang, L. (1990). Amphipathic polyethyleneglycols effectively prolong the circulation time of liposomes. *FEBS letters*, *268*(1), 235–7.

Kobayashi, T., Aomatsu, Y., Iwata, H., Kin, T., Kanehiro, H., Hisanaga, M., Ko, S., et al. (2003). Indefinite islet protection from autoimmune destruction in nonobese diabetic mice by agarose microencapsulation without immunosuppression. *Transplantation*, *75*(5), 619–25. doi:10.1097/01.TP.0000053749.36365.7E

Kokkoli, E., Mardilovich, A., Wedekind, A., Rexeisen, E. L., Garg, A., & Craig, J. A. (2006). Self-assembly and applications of biomimetic and bioactive peptide-amphiphiles. *Soft Matter*, *2*(12), 1015–1024. doi:10.1039/b608929a

Kokkoli, E., Ochsenhirt, S. E., & Tirrell, M. (2004). Collective and single-molecule interactions of alpha5beta1 integrins. *Langmuir*, *20*(6), 2397–404.

Korb, V., Tep, K., Escriou, V., Richard, C., Scherman, D., Cynober, L., Chaumeil, J., et al. (2008). Current data on ATP-containing liposomes and potential prospects to enhance cellular energy status for hepatic applications. *Critical Reviews in Therapeutic Drug Carrier Systems*, *25*(4), 305–345.

Krishnamurthy, M., Li, J., Al-Masri, M., & Wang, R. (2008). Expression and function of alphabeta1 integrins in pancretic beta (INS-1) cells. *Journal of Cell Communication and Signaling*, *2*(3-4), 67–79. doi:10.1007/s12079-008-0030-6

Kuroda, Y, Kawamura, T., Suzuki, Y., Fujiwara, H., Yamamoto, K., & Saitoh, Y. (1988). A new, simple method for cold storage of the pancreas using perfluorochemical. *Transplantation*, *46*(3), 457–460.

Kuroda, Yoshikazu, Fujino, Y., Morita, A., Tanioka, Y., Ku, Y., & Saitoh, Y. (1992). Oxygenation of the human pancreas during preservation by a two-layer (University of Wisconsin solution/perfluorochemical) cold-storage method. *Transplantation*, *54*(3), 561–562.

Lakey, J. R., Rajotte, R. V., Warnock, G. L., & Kneteman, N. M. (1995). Human pancreas preservation prior to islet isolation. Cold ischemic tolerance. *Transplantation*, *59*(5), 689–694.

Lakey, J. R. T., Burridge, P. W., & Shapiro, A. M. J. (2003). Technical aspects of islet preparation and transplantation. *Transplant international : official journal of the European Society for Organ Transplantation*, *16*(9), 613–32. doi:10.1007/s00147-003-0651-x

Lakey, J. R. T., Tsujimura, T., Shapiro, A. M. J., & Kuroda, Y. (2002). Preservation of the human pancreas before islet isolation using a two-layer (UW solution-perfluorochemical) cold storage method. *Transplantation*, *74*(12), 1809–1811. doi:10.1097/01.TP.0000038314.77538.55

Lanza, R. P., Kuhtreiber, W. M., Ecker, D., Staruk, J. E., & Chick, W. L. (1995). Lanza-1995-Alginate encapsulation or porcine islets.PDF. *Transplantation*, *59*(10), 1377–1384.

Larson, D. R., Ow, H., Vishwasrao, H. D., Heikal, A. a., Wiesner, U., & Webb, W. W. (2008). Silica Nanoparticle Architecture Determines Radiative Properties of Encapsulated Fluorophores. *Chemistry of Materials*, *20*(8), 2677–2684. doi:10.1021/cm7026866

Law, W., Yong, K., Roy, I., Xu, G., Ding, H., Bergey, E. J., Zeng, H., et al. (2008). Optically and Magnetically Doped Organically Modified Silica Nanoparticles as Efficient Magnetically Guided Biomarkers for Two-Photon Imaging of Live Cancer Cells †. *The Journal of Physical Chemistry*, *112*, 7972–7977.

Lazard, D., Vardi, P., & Bloch, K. (2012). Induction of beta-cell resistance to hypoxia and technologies for oxygen delivery to transplanted pancreatic islets. *Diabetes/Metabolism Research and Reviews*, *28*(6), 475–484. doi:10.1002/dmrr.2294

Leahy, D. J., Aukhil, I., & Erickson, H. P. (1996). 2.0 A crystal structure of a four-domain segment of human fibronectin encompassing the RGD loop and synergy region. *Cell*, *84*(1), 155–64.

Lee, H. J., Lee, J.-S., Chansakul, T., Yu, C., Elisseeff, J. H., & Yu, S. M. (2006). Collagen mimetic peptide-conjugated photopolymerizable PEG hydrogel. *Biomaterials*, *27*(30), 5268–76. doi:10.1016/j.biomaterials.2006.06.001

Lee, J. W., & Juliano, R. L. (2000). alpha5beta1 integrin protects intestinal epithelial cells from apoptosis through a phosphatidylinositol 3-kinase and protein kinase B-dependent pathway. *Molecular Biology of the Cell*, *11*(6), 1973–87.

Lee, R. J., & Huang, L. (1996). Folate-targeted, anionic liposome-entrapped polylysine-condensed DNA for tumor cell-specific gene transfer *. *Biochemistry*, *271*(14), 8481–8487.

Lenzen, S., Drinkgern, J., & Tiedge, M. (1996). Low antioxidant enzyme gene expression in pancreatic islets compared with various other mouse tissues. *Free radical biology & medicine*, *20*(3), 463–6.

Lepore, D. a, Shinkel, T. a, Fisicaro, N., Mysore, T. B., Johnson, L. E. a, d' Apice, A. J. F., & Cowan, P. J. (2004). Enhanced expression of glutathione peroxidase protects islet beta cells from hypoxia-reoxygenation. *Xenotransplantation*, *11*(1), 53–9. doi:10.1111/j.1399-3089.2004.00082.x

Levchenko, T. S., Hartner, W. C., Verma, D. D., Bernstein, E. A., & Torchilin, V. P. (2010). ATP loaded liposomes for targeted treatment in models of myocardial ischemia. In V. Weissig (Ed.), *Liposomes, Methods in Molecular Biology* (Vol. 605, pp. 361–375). Totowa, NJ: Humana Press. doi:10.1007/978-1-60327-360-2

Levine, R. M., Scott, C. M., & Kokkoli, E. (2012). Peptide functionalized nanoparticles for nonviral gene delivery. *Soft Matter*, *in press*.

Li, C., & Jackson, R. M. (2002). Reactive species mechanisms of cellular hypoxia-reoxygenation injury. *American Journal of Physiology - Cell physiology*, *282*(2), C227–C241. doi:10.1152/ajpcell.00112.2001

Li, X., Chen, H., & Epstein, P. N. (2004). Metallothionein protects islets from hypoxia and extends islet graft survival by scavenging most kinds of reactive oxygen species. *The Journal of Biological Chemistry*, *279*(1), 765–71. doi:10.1074/jbc.M307907200

Liang, W, Levchenko, T. S., & Torchilin, V. P. (2004). Encapsulation of ATP into liposomes by different methods: optimization of the procedure. *Journal of Microencapsulation*, *21*(3), 251–61. doi:10.1080/02652040410001673900

Liang, Wei, Levchenko, T. S., Khaw, B.-A., & Torchilin, V. P. (2004). ATP-containing immunoliposomes specific for cardiac myosin. *Current drug delivery*, *1*(1), 1–7.

Lim, F., & Sun, A. M. (1980). Microencapsulated Islets as Bioartificial Endocrine Pancreas. *Science*, *210*, 908–910.

Lin, Y., Tsai, C., Huang, H., Kuo, C.-T., Hung, Y., Huang, D.-M., Chen, Y.-C., et al. (2005). Well-Ordered Mesoporous Silica Nanoparticles as Cell Markers. *Chemistry of Materials*, (17), 4570–4573.

Linn, T., Schmitz, J., Hauck-Schmalenberger, I., Lai, Y., Bretzel, R. G., Brandhorst, H., & Brandhorst, D. (2006). Ischaemia is linked to inflammation and induction of angiogenesis in pancreatic islets. *Clinical and Experimental Immunology*, *144*(2), 179–187. doi:10.1111/j.1365-2249.2006.03066.x

Liston, A., Gray, D. H. D., Lesage, S., Fletcher, A. L., Wilson, J., Webster, K. E., Scott, H. S., et al. (2004). Gene dosage--limiting role of Aire in thymic expression, clonal deletion, and organ-specific autoimmunity. *The Journal of experimental medicine*, *200*(8), 1015–26. doi:10.1084/jem.20040581

Loo, C., Lowery, A., Halas, N., West, J., & Drezek, R. (2005). Immunotargeted nanoshells for integrated cancer imaging and therapy. *Nano letters*, *5*(4), 709–11. doi:10.1021/nl050127s

Lopez-Ramirez, M., Fischer, R., Torres-Badillo, C., Davies, H., Logan, K., Pfizenmaier, K., Sharrack, B., et al. (2012). Role of caspases in cytokine-induced barrier breakdown in human brain endothelial cells. *Journal of Immunology*, *189*(6), 3130–3139. doi:10.2144/000113917

Luo, D., Han, E., Belcheva, N., & Saltzman, W. M. (2004). A self-assembled, modular DNA delivery system mediated by silica nanoparticles. *Journal of Controlled Release*, *95*(2), 333–41. doi:10.1016/j.jconrel.2003.11.019

Maeda, H., Wu, J., Sawa, T., Matsumura, Y., & Hori, K. (2000). Tumor vascular permeability and the EPR effect in macromolecular therapeutics: a review. *Journal of Controlled Release*, *65*(1-2), 271–84.

Mansouri, S., Fatisson, J., Miao, Z., Merhi, Y., Winnik, F. M., & Tabrizian, M. (2009). Silencing red blood cell recognition toward Anti-A antibody by means of polyelectrolyte layer-by-layer assembly in a two-dimensional model system. *Langmuir*, *25*(24), 14071–8. doi:10.1021/la9016799

Mardilovich, A., Craig, J. A., McCammon, M. Q., Garg, A., & Kokkoli, E. (2006). Design of a novel fibronectin-mimetic peptide-amphiphile for functionalized biomaterials. *Langmuir*, *22*(7), 3259–32564. doi:10.1021/la052756n

Mardilovich, A., & Kokkoli, E. (2004). Biomimetic peptide-amphiphiles for functional biomaterials: the role of GRGDSP and PHSRN. *Biomacromolecules*, *5*(3), 950–957. doi:10.1021/bm0344351

Mardilovich, A., & Kokkoli, E. (2005). Patterned Biomimetic Membranes: Effect of Concentration and pH. *Langmuir*, *21*(16), 7468–7475. doi:10.1021/la0468085

Matsuda, T., Suzuki, Y., Tanioka, Y., Toyama, H., Kakinoki, K., Hiraoka, K., Fujino, Y., et al. (2003). Pancreas preservation by the 2-layer cold storage method before islet isolation

protects isolated islets against apoptosis through the mitochondrial pathway. *Surgery*, *134*(3), 437–445. doi:10.1067/S0039-6060(03)00165-X

Matsumoto, S., Qualley, S. a, Goel, S., Hagman, D. K., Sweet, I. R., Poitout, V., Strong, D. M., et al. (2002). Effect of the two-layer (University of Wisconsin solution-perfluorochemical plus O2) method of pancreas preservation on human islet isolation, as assessed by the Edmonton Isolation Protocol. *Transplantation*, *74*(10), 1414–9. doi:10.1097/01.TP.0000034206.66890.B0

McCall, M., & Shapiro, A. M. J. (2012). Update on islet transplantation. *Cold Spring Harbor Perspectives in Medicine*, *2*(7), 1–16. doi:10.1101/cshperspect.a007823

Menger, M. D., Yamauchi, J., & Vollmar, B. (2001). Revascularization and microcirculation of freely grafted islets of Langerhans. *World Journal of Surgery*, *25*(4), 509–515. doi:10.1007/s002680020345

Menger, M., Jaeger, S., Walter, P., Feifel, G., Hammersen, F., & Messmer, K. (1989). Angiogenesis and hemodynamics of microvasculature of transplanted islets of Langerhans. *Diabetes*, *38*(Suppl 1), 199–201. doi:10.2144/000113897

Meredith, J. E., & Schwartz, M. A. (1997). Integrins, adhesion and apoptosis. *Trends in Cell Biology*, *7*(4), 146–50. doi:10.1016/S0962-8924(97)01002-7

Michiels, C. (2004). Physiological and pathological responses to hypoxia. *The American Journal of Pathology*, *164*(6), 1875–1882. doi:10.1016/S0002-9440(10)63747-9

Miura, S., Teramura, Y., & Iwata, H. (2006). Encapsulation of islets with ultra-thin polyion complex membrane through poly(ethylene glycol)-phospholipids anchored to cell membrane. *Biomaterials*, *27*(34), 5828–35. doi:10.1016/j.biomaterials.2006.07.039

Moritz, W., Meier, F., Stroka, D., Giuliani, M., Kugelmeier, P., Lehmann, R., Candinas, D., et al. (2002). Apoptosis in hypoxic human pancreatic islets correlates with HIF-1α expression. *The FASEB Journal*, *16*(7), 745–747.

Mould, A. P., Askari, J. A., & Humphries, M. J. (2000). Molecular basis of ligand recognition by integrin alpha5beta1. *The Journal of Biological Chemistry*, *275*(27), 20324–36. doi:10.1074/jbc.M000572200

Mustapa, M. F. M., Bell, P. C., Hurley, C. a, Nicol, A., Guénin, E., Sarkar, S., Writer, M. J., et al. (2007). Biophysical characterization of an integrin-targeted lipopolyplex gene delivery vector. *Biochemistry*, *46*(45), 12930–44. doi:10.1021/bi701014y

Nachas, N., & Pinson, A. (1992). Anoxic injury accelerates phosphatidylcholine degradation cardiac myocytes by phospholipase C. *FEBS Letters*, *298*(2), 301–305.

Nadithe, V., Mishra, D., & Bae, Y. H. (2012). Poly(ethylene glycol) cross-linked hemoglobin with antioxidant enzymes protects pancreatic islets from hypoxic and free radical stress and extends islet functionality. *Biotechnology and Bioengineering*, *109*(9), 2392–2401. doi:10.1002/bit.24501

Nagata, N., Asuka, I., Inoue, K., & Tabata, Y. (2002). Co-culture of extracellular matrix suppresses the cell death of rat pancreatic islets. *Journal of Biomaterials Science Polymer Edition*, *13*(5), 579–590.

Narang, A. S., Cheng, K., Henry, J., Zhang, C., Sabek, O., Fraga, D., Kotb, M., et al. (2004). Vascular endothelial growth factor gene delivery for revascularization in transplanted human islets. *Pharmaceutical research*, *21*(1), 15–25.

Narang, A. S., & Mahato, R. I. (2006). Biological and Biomaterial Approaches for Improved Islet Transplantation. *Pharmacological Reviews*, *58*(2), 194–243. doi:10.1124/pr.58.2.6.194

Neff, N. T., Lowrey, C., Decker, C., Tovar, A., Damsky, C., Buck, C., & Horwitz, A. F. (1982). A monoclonal antibody detaches embryonic skeletal muscle from extracellular matrices. *The Journal of Cell Biology*, *95*(2 Pt 1), 654–66.

Neveux, N., De Bandt, J. P., Chaumeil, J. C., & Cynober, L. (2002). Hepatic preservation, liposomally entrapped adenosine triphosphate and nitric oxide production: a study of energy state and protein metabolism in the cold-stored rat liver. *Scandinavian Journal of Gastroenterology*, *37*(9), 1057–1063.

Neveux, N., De Bandt, J. P., Fattal, E., Hannoun, L., Poupon, R., Chaumeil, J. C., Delattre, J., et al. (2000). Cold preservation injury in rat liver: effect of liposomally-entrapped adenosine triphosphate. *Journal of hepatology*, *33*(1), 68–75.

Oku, N., Kendall, D. a., & MacDonald, R. C. (1982). A simple procedure for the determination of the trapped volume of liposomes. *Biochimica et Biophysica Acta*, *691*(2), 332–340. doi:10.1016/0005-2736(82)90422-9

Oz, G., Wildey, G. M., Kendir, S., & Papas, K. K. (2007). Vitamin E homologs improve bioenergetics of porcine islets and INS-1 cells under anoxia. *Diabetologia*, *50*(Suppl 1), S184–S185.

O'Brien, V., Frisch, S. M., & Juliano, R. L. (1996). Expression of the integrin alpha5 subunit in HT29 colon carcinoma cells suppresses apoptosis triggered by serum deprivation. *Experimental Cell Research*, *224*(1), 208–13. doi:10.1006/excr.1996.0130

Pangburn, T. O., Bates, F. S., & Kokkoli, E. (2012). Polymersomes functionalized via "click" chemistry with the fibronectin mimetic peptides PR_b and GRGDSP for targeted delivery to cells with different levels of α5β1 expression. *Soft Matter*, *8*(16), 4449–4461. doi:10.1039/c2sm06922a

Pangburn, T. O., Georgiou, K., Bates, F. S., & Kokkoli, E. (2012). Targeted Polymersome Delivery of siRNA Induces Cell Death of Breast Cancer Cells Dependent upon Orai3 Protein Expression. *Langmuir*, *28*(35), 12816–12830. doi:10.1021/la300874z

Pangburn, T. O., Petersen, M. A., Waybrant, B., Adil, M. M., & Kokkoli, E. (2009). Peptide- and aptamer-functionalized nanovectors for targeted delivery of therapeutics. *Journal of Biomechanical Engineering*, *131*(7), 074005. doi:10.1115/1.3160763

Papas, K. K., Bauer, A. C., Avgoustiniatos, E. S., Papas, G. A., & Hering, B. J. (2005). Vitamin E homologs protect cultured islets from anoxia-induced death: Implications in islet processing and engraftment.

Papas, K. K., Colton, C. K., Nelson, R. A., Rozak, P. R., Avgoustiniatos, E. S., Scott, W. E., Wildey, G. M., et al. (2007). Human islet oxygen consumption rate and DNA measurements predict diabetes reversal in nude mice. *American Journal of Transplantation*, *7*(3), 707–13. doi:10.1111/j.1600-6143.2006.01655.x

Papas, K. K., Hering, B. J., Guenther, L., Gunther, L., Rappel, M. J., Colton, C. K., & Avgoustiniatos, E. S. (2005). Pancreas oxygenation is limited during preservation with the two-layer method. *Transplantation Proceedings*, *37*(8), 3501–4. doi:10.1016/j.transproceed.2005.09.085

Papas, K. K., Long Jr., R. C., Constantinidis, I., & Sambanis, A. (1996). Effects of oxygen on metabolic and secretory activities of bTC3. *Biochimica et Biophysica Acta*, *1291*, 163–166.

Papas, K. K., Pisania, A., Wu, H., Weir, G. C., & Colton, C. K. (2007). A stirred microchamber for oxygen consumption rate measurements with pancreatic islets. *Biotechnology and Bioengineering*, *98*(5), 1071–1082. doi:10.1002/bit

Papas, K. K., Suszynski, T. M., & Colton, C. K. (2009). Islet Assessment for Transplantation. *Current Opinion in Organ Transplantation*, *14*(6), 674–682. doi:10.1097/MOT.0b013e328332a489.Islet

Paraskevas, S., Maysinger, D., Wang, R., Duguid, T. P., & Rosenberg, L. (2000). Cell loss in isolated human islets occurs by apoptosis. *Pancreas*, *20*(3), 270–6.

Park, J.-H., Gu, L., von Maltzahn, G., Ruoslahti, E., Bhatia, S. N., & Sailor, M. J. (2009). Biodegradable luminescent porous silicon nanoparticles for in vivo applications. *Nature Materials*, *8*(4), 331–6. doi:10.1038/nmat2398

Paños, G., Moreno, A., Jiménez-Marín, A., Garrido, J. J., de la Mulas, J. M., Ordás, J., & Llanes, D. (2004). Through monoclonal antibodies developed using two immunization strategies. *Hybridoma and Hybridomics*, *23*(5), 271–278.

Pearce, T. R., Shroff, K., & Kokkoli, E. (2012). Peptide Targeted Lipid Nanoparticles for Anticancer Drug Delivery. *Advanced Materials*, *24*, 3803–3822. doi:10.1002/adma.201200832

Pelisek, J., Gaedtke, L., DeRouchey, J., Walker, G. F., Nikol, S., & Wagner, E. (2006). Optimized lipopolyplex formulations for gene transfer to human colon carcinoma cells under in vitro conditions. *The journal of gene medicine*, *8*(2), 186–197. doi:10.1002/jgm.836

Pham, K. N., Fullston, D., & Sagoe-Crentsil, K. (2007). Surface Charge Modification of Nano-Sized Silica Colloid. *Australian Journal of Chemistry*, *60*, 662–666. doi:10.1071/CH07138

Pierschbacher, M. D., & Ruoslahti, E. (1984). Cell attachment activity of fibronectin can be duplicated by small synthetic fragments of the molecule. *Nature*, *309*, 30–33.

Pileggi, A., Cobianchi, L., Inverardi, L., & Ricordi, C. (2006). Overcoming the challenges now limiting islet transplantation: a sequential, integrated approach. *Annals of the New York Academy of Sciences*, *1079*, 383–98. doi:10.1196/annals.1375.059

Pinkse, G. G. M., Bouwman, W. P., Jiawan-Lalai, R., Terpstra, O. T., Bruijn, J. A., & de Heer, E. (2006). Integrin signaling via RGD peptides and anti-beta1 antibodies confers resistance to apoptosis islets of Langerhans. *Diabetes*, *55*, 312–317. doi:10.4103/0972-124X.85675

Pope, E. J. A., Braun, K., & Peterson, C. M. (1997). Bioartificial Organs I : Silica Gel Encapsulated Pancreatic Islets for the Treatment of Diabetes Mellitus. *Journal of Sol-Gel Science and Technology*, *8*, 635–639.

Posselt, A. M., Bellin, M. D., Tavakol, M., Szot, G. L., Frassetto, L. A., Masharani, U., Kerlan, R. K., et al. (2010). Islet transplantation in type 1 diabetics using an immunosuppressive protocol based on the anti-LFA-1 antibody efalizumab. *American Journal of Transplantation*, *10*(8), 1870–80. doi:10.1111/j.1600-6143.2010.03073.x

Posselt, A. M., Szot, G. L., Frassetto, L. a, Masharani, U., Tavakol, M., Amin, R., McElroy, J., et al. (2010). Islet transplantation in type 1 diabetic patients using calcineurin inhibitor-free immunosuppressive protocols based on T-cell adhesion or costimulation blockade. *Transplantation*, *90*(12), 1595–1601. doi:10.1097/TP.0b013e3181fe1377

Pugliese, A. (1998). Insulin expression in the thymus, tolerance, and type 1 diabetes. *Diabetes/Metabolism Reviews*, *14*(4), 325–7.

Pugliese, A., Zeller, M., Fernandez Jr., A., Zalcberg, L. J., Bartlett, R. J., Ricordi, C., Pietropaolo, M., et al. (1997). The insulin gene is transcribed in the human thymus and transcription levels correlate with allelic variation at the INS VNTR-IDDM2 susceptibility locus for type 1 diabetes. *Nature Genetics*, *15*, 293–297.

Puri, A., Jang, H., Yavlovich, A., Masood, M. A., Veenstra, T. D., Luna, C., Aranda-Espinoza, H., et al. (2011). Material properties of matrix lipids determine the conformation and intermolecular reactivity of diacetylenic phosphatidylcholine in the lipid bilayer. *Langmuir*, *27*(24), 15120–15128. doi:10.1021/la203453x

Rabanel, J., Banquy, X., Zouaoui, H., Mokhtar, M., & Hildgen, P. (2009). Progress Technology in Microencapsulation Methods for Cell Therapy. *Biotechnology Progress*, *25*(4), 946–963. doi:10.1021/bp.226

Rabinovitch, A. (1998). An update on cytokines in the pathogenesis of insulin-dependent diabetes mellitus. *Diabetes/metabolism reviews*, *14*(2), 129–51.

Rabinovitch, A., & Suarez-Pinzon, W. L. (2007). Roles of cytokines in the pathogenesis and therapy of type 1 diabetes. *Cell Biochemistry and Biophysics*, *48*(2-3), 159–163. doi:10.1007/s12013-007-0029-2

Rabinovitch, A., Suarez-Pinzon, W., Strynadka, K., Ju, Q., Edelstein, D., Brownlee, M., Korbutt, G. S., et al. (1999). Transfection of human pancreatic islets with an anti-apoptotic gene (bcl-2) protects beta-cells from cytokine-induced destruction. *Diabetes*, *48*(6), 1223–9.

Ramakers, B. E. I., van den Heuvel, M., Tsichlis I Spithas, N., Brinkhuis, R. P., van Hest, J. C. M., & Löwik, D. W. P. M. (2012). Polymerization-Induced Color Changes of Polydiacetylene-Containing Liposomes and Peptide Amphiphile Fibers. *Langmuir*, *28*(4), 2049–2055. doi:10.1021/la203836y

Redick, S. D., Settles, D. L., Briscoe, G., & Erickson, H. P. (2000). Defining Fibronectin ' s Cell Adhesion Synergy Site by Site-directed Mutagenesis. *Cell*, *149*(2), 521–527.

Rexeisen, E. L., Fan, W., Pangburn, T. O., Taribagil, R. R., Bates, F. S., Lodge, T. P., Tsapatsis, M., et al. (2010). Self-assembly of fibronectin mimetic peptide-amphiphile nanofibers. *Langmuir*, *26*(3), 1953–1959. doi:10.1021/la902571q

Richard, C., Thibaudeau, K., Charreau, B., Loirat, M., Naulet, J., Blanchard, D., Soulillou, J., et al. (1998). Characterization of murine monoclonal antibody specific for swine beta 1 integrin. *Xenotransplantation*, *5*, 75–83.

Ricordi, C., & Edlund, H. (2008). Toward a renewable source of pancreatic beta-cells. *Nature Biotechnology*, *26*(4), 397–8. doi:10.1038/nbt0408-397

Ricordi, C., Gray, D. W., Hering, B. J., Kaufman, D. B., Warnock, G. L., Kneteman, N. M., Lake, S. P., et al. (1990). Islet isolation assessment in man and large animals. *Acta diabetologica latina*, *27*(3), 185–95.

Ricordi, C., Socci, C., Davalli, A. M., Staudacher, C., Baro, P., Vertova, A., Sassi, I., et al. (1990). Isolation of the elusive pig islet. *Surgery*, *107*(6), 688–694.

Ricordi, C., & Strom, T. B. (2004). Clinical islet transplantation: advances and immunological challenges. *Nature reviews. Immunology*, *4*(4), 259–68. doi:10.1038/nri1332

Ris, F., Hammar, E., Bosco, D., Pilloud, C., Maedler, K., Donath, M. Y., Oberholzer, J., et al. (2002). Impact of integrin-matrix matching and inhibition of apoptosis on the survival of purified human beta-cells in vitro. *Diabetologia*, *45*(6), 841–50. doi:10.1007/s00125-002-0840-7

Robertson, R P. (1999). Prevention of recurrent hypoglycemia in type 1 diabetes by pancreas transplantation. *Acta diabetologica*, *36*(1-2), 3–9.

Robertson, R Paul. (2010). Islet transplantation a decade later and strategies for filling a half-full glass. *Diabetes*, *59*(6), 1285–1291. doi:10.2337/db09-1846

Rood, P. P. M., Buhler, L. H., Bottino, R., Trucco, M., & Cooper, D. K. C. (2006). Pig-to-nonhuman primate islet xenotransplantation: a review of current problems. *Cell Transplantation*, *15*(2), 89–104.

Rosenberg, L., Wang, R., Paraskevas, S., & Maysinger, D. (1999). Structural and functional changes resulting from islet isolation lead to islet cell death. *Surgery*, *126*(2), 393–8.

Rother, K. I., & Harlan, D. M. (2004). Challenges facing islet transplantation for the treatment of type 1 diabetes mellitus. *Journal of Clinical Investigation*, *114*(7), 877–883. doi:10.1172/JCI200423235.The

Ruoslahti, E. (1996). RGD and other recognition sequences for integrins. *Annual Review of Cell and Developmental Biology*, *12*, 697–715. doi:10.1146/annurev.cellbio.12.1.697

Ryan, E. A., Lakey, J. R. T., Paty, B. W., Imes, S., Korbutt, G. S., Kneteman, N. M., Bigam, D., et al. (2002). Successful islet transplantation: continued insulin reserve provides long-term glycemic control. *Diabetes*, *51*(7), 2148–57.

Ryan, E. A., Paty, B. W., Senior, P. A., Bigam, D., Alfadhli, E., Kneteman, N. M., Lakey, J. R. T., et al. (2005). Five-year follow-up after clinical islet transplantation. *Diabetes*, *54*(7), 2060–2069.

Ryan, E. A., Paty, B. W., Senior, P. a, & Shapiro, A. M. J. (2004). Risks and side effects of islet transplantation. *Current diabetes reports*, *4*(4), 304–9.

Ryu, G. R., Lee, M.-K., Lee, E., Ko, S.-H., Ahn, Y.-B., Kim, J.-W., Yoon, K.-H., et al. (2009). Activation of AMP-activated protein kinase mediates acute and severe hypoxic injury to pancreatic beta cells. *Biochemical and Biophysical Research Communications*, *386*(2), 356–362. doi:10.1016/j.bbrc.2009.06.039

Safley, S. a, Kapp, J. a, & Weber, C. J. (2002). Proliferative and cytokine responses in CTLA4-Ig-treated diabetic NOD mice transplanted with microencapsulated neonatal porcine ICCs. *Cell Transplantation*, *11*(7), 695–705.

Sandra, A., & Pagano, R. E. (1979). Liposome-cell interactions. Studies of lipid transfer using isotopically asymmetric vesicles. *Journal of Biological Chemistry* , *254* (7), 2244–2249.

Santra, S., Zhang, P., Wang, K., Tapec, R., & Tan, W. (2001). Conjugation of biomolecules with luminophore-doped silica nanoparticles for photostable biomarkers. *Analytical chemistry*, *73*(20), 4988–93.

Sawhney, A. S., Pathak, C. P., & Hubbell, J. A. (1994). Modification of islet of Langerhans surfaces with immunoprotective poly(ethylene glycol) coatings via interfacial photopolymerization. *Biotechnology and Bioengineering*, *43*, 383–386. doi:10.1002/bit.260431124

Schernthaner, G. (1993). Immunogenicity and allergenic potential of animals and human insulins. *Diabetes Care*, *16*, 155–165.

Schindler, H. (1979). Exchange and interactions between lipid layers at the surface of a liposome solution. *Biochimica et Biophysica Acta*, *555*, 316–336.

Schwartz, M. A., & Ingber, D. E. (1994). Integrating with Integrins. *Molecular Biology of the Cell*, *5*(April), 389–393.

Scott III, W E, Weegman, B. P., Ferrer-Fabrega, J., Stein, S. A., Anazawa, T., Kirchner, V. A., Rizzari, M. D., et al. (2011). Pancreas oxygen persufflation increases ATP levels as shown by nuclear magnetic resonance. *Transplantation Proceedings*, *42*(6), 2011–2015. doi:10.1016/j.transproceed.2010.05.091

Scott III, William E, O'Brien, T. D., Ferrer-Fabrega, J., Avgoustiniatos, E. S., Weegman, B. P., Anazawa, T., Matsumoto, S., et al. (2010). Persufflation improves pancreas preservation when compared with the two-layer method. *Transplantation Proceedings*, *42*(6), 2016–2019. doi:10.1016/j.transproceed.2010.05.092

Shapiro, A. M. J., Lakey, J. R. T., Paty, B. W., Senior, P. A., Bigam, D. L., & Ryan, E. a. (2005). Strategic Opportunities in Clinical Islet Transplantation. *Transplantation*, *79*(10), 1304–1307. doi:10.1097/01.TP.0000157300.53976.2A

Shapiro, A. M. J., Lakey, J. R. T., Ryan, E. A., Korbutt, G. S., Toth, E., Warnock, G. L., Kneteman, N. M., et al. (2000). Islet transplantation in seven patients with type 1 diabetes mellitus using a glucocorticoid-free immunosuppressive regimen. *The New England Journal of Medicine*, *343*(4), 230–238.

Shapiro, A. M. J., & Ricordi, C. (2004). Unraveling the secrets of single donor success in islet transplantation. *American Journal of Transplantation*, *4*(3), 295–298. doi:10.1046/j.1600-6143.2003.00375.x

Shapiro, A. M. J., Ricordi, C., Hering, B. J., Auchincloss, H., Lindblad, R., Robertson, R. P., Secchi, A., et al. (2006). International trial of the Edmonton protocol for islet transplantation. *The New England Journal of Medicineournal of medicine*, *355*(13), 1318–30. doi:10.1056/NEJMoa061267

Shroff, K., & Kokkoli, E. (2012). PEGylated liposomal doxorubicin targeted to α5β1-expressing MDA-MB-231 breast cancer cells. *Langmuir*, *28*(10), 4729–4736. doi:10.1021/la204466g

Shroff, K., Pearce, T. R., & Kokkoli, E. (2012). Enhanced integrin mediated signaling and cell cycle progression on fibronectin mimetic peptide amphiphile monolayers. *Langmuir*, *28*(3), 1858–1865. doi:10.1021/la203322t

Shroff, K., Rexeisen, E. L., Arunagirinathan, M. A., & Kokkoli, E. (2010). Fibronectin-mimetic peptide-amphiphile nanofiber gels support increased cell adhesion and promote ECM production. *Soft Matter*, *6*(20), 5064–5072. doi:10.1039/c0sm00321b

Snyder, M. A., Demirgöz, D., Kokkoli, E., & Tsapatsis, M. (2009). Benign, 3D encapsulation of sensitive mammalian cells in porous silica gels formed by Lys–Sil nanoparticle assembly. *Microporous and Mesoporous Materials*, *118*(1-3), 387–395. doi:10.1016/j.micromeso.2008.09.013

Snyder, M. A., Lee, J. A., Davis, T. M., Scriven, L. E., & Tsapatsis, M. (2007). Silica nanoparticle crystals and ordered coatings using lys-sil and a novel coating device. *Langmuir*, *23*(20), 9924–8. doi:10.1021/la701063v

Steiner, D. J., Kim, A., Miller, K., & Hara, M. (2010). Pancreatic islet plasticity: Interspecies comparison of islet architecture and composition. *Islets*, *2*(3), 135–145.

Stolz, D. B., & Jacobson, B. S. (1992). Examination of transcellular membrane protein polarity of bovine aortic endothelial cells in vitro using the cationic colloidal silica microbead membrane-isolation procedure. *Journal of Cell Science*, *103 (Pt 1*, 39–51.

Stöber, W., Fink, A., & Bohn, E. (1968). Controlled Growth of Monodisperse Silica Spheres in the Micron Size Range. *Journal of Colloid and Interface Science*, *26*, 62–69.

Suszynski, T M, Avgoustiniatos, E. S., Stein, S. A., Falde, E. J., Hammer, B. E., & Papas, K. K. (2011). Assessment of tissue-engineered islet graft viability by fluorine magnetic resonance spectroscopy. *Transplantation Proceedings*, *43*(9), 3221–3225. doi:10.1016/j.transproceed.2011.09.009

Suszynski, Thomas M, Papas, K. K., & Avgoustiniatos, E. S. (n.d.). Oxygenation of the intraportally transplanted islet.

Suszynski, Thomas M, Rizzari, M. D., Scott III, W. E., Tempelman, L. A., Taylor, M. J., & Papas, K. K. (2012). Persufflation (or gaseous oxygen perfusion) as a method of organ preservation. *Cryobiology*, *64*(3), 125–143. doi:10.1016/j.cryobiol.2012.01.007

Sutherland, D. E. R., Steffes, M. W., Bauer, E. G., McManus, D., Noe, B. D., & Najarian, J. S. (1974). Isolation of human and islet and porcine islets of Langerhans in pigs transplantation. *Journal of Surgical Research*, *16*, 102–111.

Takagi, J. (2004). Structural basis for ligand recognition by RGD (Arg-Gly-Asp)-dependent integrins. *Biochemical Society Transactions*, *32*(3), 403–406.

Takahashi, S., Abe, T., Gotoh, J., & Fukuuchi, Y. (2002). Substrate-dependence of reduction of MTT: a tetrazolium dye differs in cultured astroglia and neurons. *Neurochemistry International*, *40*(5), 441–8.

Tanioka, Y., Sutherland, D. E., Kuroda, Y., Gilmore, T. R., Asaheim, T. C., Kronson, J. W., & Leone, J. P. (1997). Excellence of the two-layer method (University of Wisconsin solution/perfluorochemical) in pancreas preservation before islet isolation. *Surgery*, *122*(2), 435–441.

Tep, K., Korb, V., Richard, C., Escriou, V., Largeau, C., Vincourt, V., Bessodes, M., et al. (2009). Formulation and evaluation of ATP-containing liposomes including lactosylated ASGPr ligand. *Journal of Liposome Research*, *19*(4), 287–300. doi:10.3109/08982100902838682

Teramura, Y., & Iwata, H. (2009a). Islet encapsulation with living cells for improvement of biocompatibility. *Biomaterials*, *30*(12), 2270–5. doi:10.1016/j.biomaterials.2009.01.036

Teramura, Y., & Iwata, H. (2009b). Surface modification of islets with PEG-lipid for improvement of graft survival in intraportal transplantation. *Transplantation*, *88*(5), 624–30. doi:10.1097/TP.0b013e3181b230ac

Teramura, Y., & Iwata, H. (2010a). Cell surface modification with polymers for biomedical studies. *Soft Matter*, *6*(6), 1081. doi:10.1039/b913621e

Teramura, Y., & Iwata, H. (2010b). Bioartificial pancreas microencapsulation and conformal coating of islet of Langerhans. *Advanced Drug Delivery Reviews*, *62*(7-8), 827–40. doi:10.1016/j.addr.2010.01.005

Teramura, Y., Kaneda, Y., & Iwata, H. (2007). Islet-encapsulation in ultra-thin layer-by-layer membranes of poly(vinyl alcohol) anchored to poly(ethylene glycol)-lipids in the cell membrane. *Biomaterials*, *28*(32), 4818–25. doi:10.1016/j.biomaterials.2007.07.050

Teramura, Y., Minh, L. N., Kawamoto, T., & Iwata, H. (2010). Microencapsulation of islets with living cells using polyDNA-PEG-lipid conjugate. *Bioconjugate chemistry*, *21*(4), 792–6. doi:10.1021/bc900494x

Thomas, C. E., Ehrhardt, A., & Kay, M. a. (2003). Progress and problems with the use of viral vectors for gene therapy. *Nature reviews. Genetics*, *4*(5), 346–58. doi:10.1038/nrg1066

Thomas, F. T., Contreras, J. L., Bilbao, G., Ricordi, C., Curiel, D. T., & Thomas, J. M. (1999). Anoikis, extracellular matrix, and apoptosis factors in isolated cell transplantation. *Surgery*, *126*(2), 299–304.

Tiedge, M., Lortz, S., Munday, R., & Lenzen, S. (1998). Complementary action of antioxidant enzymes in the protection of bioengineered insulin-producing RINm5F cells against the toxicity of reactive oxygen species. *Diabetes*, *47*(10), 1578–85.

Tiedge, M., Lortz, S., Munday, R., & Lenzen, S. (1999). Protection against the co-operative toxicity of nitric oxide and oxygen free radicals by overexpression of antioxidant enzymes in bioengineered insulin-producing RINm5F cells. *Diabetologia*, *42*(7), 849–55. doi:10.1007/s001250051237

Tiwari, J. L., Schneider, B., Barton, F., & Anderson, S. a. (2012). Islet Cell Transplantation in Type 1 Diabetes: An Analysis of Efficacy Outcomes and Considerations for Trial Designs. *American Journal of Transplantation*, no–no. doi:10.1111/j.1600-6143.2012.04038.x

Torchilin, Vladimir P. (2005). Recent advances with liposomes as pharmaceutical carriers. *Nature reviews. Drug discovery*, *4*(2), 145–60. doi:10.1038/nrd1632

Torney, F., Trewyn, B. G., Lin, V. S.-Y., & Wang, K. (2007). Mesoporous silica nanoparticles deliver DNA and chemicals into plants. *Nature nanotechnology*, *2*(5), 295–300. doi:10.1038/nnano.2007.108

Tseng, W.-C., Tang, C.-H., Fang, T.-Y., & Su, L.-Y. (2007). Trehalose enhances transgene expression mediated by DNA-PEI complexes. *Biotechnology progress*, *23*(6), 1297–304. doi:10.1021/bp070224m

Vafiadis, P., Bennett, S. T., Todd, J. A., Nadeau, J., Grabs, R., Goodyer, C. G., Wickramasinghe, S., et al. (1997). Insulin express in human thymus is modulated by INS VNTR alleles at the IDDM2 locus. *Nature Genetics*, *15*, 289–1992.

Van Belle, T., & von Herrath, M. (2008). Immunosuppression in islet transplantation. *The Journal of clinical investigation*, *118*(5), 1625–1628. doi:10.1172/JCI35639.Autoimmunity

Van Blaaderen, A., & Vrij, A. (1993). Synthesis and Characterization of Monodisperse Spheres Colloidal. *Journal of Colloid and Interface Science*, *156*, 1–18.

Van der Burg, M. P., Basir, I., & Bouwman, E. (1998). No porcine islet loss during density gradient purification in a novel iodixanol in University of Wisconsin solution. *Transplantation Proceedings*, *30*(2), 362–3.

Van der Windt, D. J., Bottino, R., Casu, A., Campanile, N., & Cooper, D. K. C. (2007). Rapid loss of intraportally transplanted islets: an overview of pathophysiology and preventive strategies. *Xenotransplantation*, *14*(4), 288–97. doi:10.1111/j.1399-3089.2007.00419.x

Verma, D. D., Hartner, W. C., Levchenko, T. S., Bernstein, E. A., & Torchilin, V. P. (2005). ATP-loaded liposomes effectively protect the myocardium in rabbits with an acute experimental myocardial infarction. *Pharmaceutical Research*, *22*(12), 2115–2120. doi:10.1007/s11095-005-8354-x

Verma, D. D., Levchenko, T. S., Bernstein, E. A., & Torchilin, V. P. (2005). ATP-loaded liposomes effectively protect mechanical functions of the myocardium from global ischemia in an isolated rat heart model. *Journal of Controlled Release*, *108*(2-3), 460–471. doi:10.1016/j.jconrel.2005.08.029

Vistica, D. T., Skehan, P., Scudiero, D., Monks, A., Pittman, A., & Boyd, M. R. (1991). Tetrazolium-based Assays for Cellular Viability : A Critical Examination of Selected Parameters Affecting Formazan Production Tetrazolium-based Assays for Cellular Viability : A Critical Examination of Selected Parameters Affecting Formazan Production, 2515–2520.

Wang, J., Wan, R., Mo, Y., Li, M., Zhang, Q., & Chien, S. (2010). Intracellular delivery of adenosine triphosphate enhanced healing process in full-thickness skin wounds in diabetic rabbits. *American Journal of Surgery*, *199*(6), 823–832. doi:10.1016/j.amjsurg.2009.05.040

Wang, R., Li, J., Lyte, K., Yashpal, N. K., Fellows, F., & Goodyer, C. G. (2005). Subunits in development of the human fetal pancreas. *Diabetes*, *54*, 2080–2089.

Wang, R., Paraskevas, S., & Rosenberg, L. (1999). Characterization of integrin expression in islets isolated from hamster, canine, porcine, and human pancreas. *The Journal of Histochemistry and Cytochemistry*, *47*(4), 499–506.

Wang, R., & Rosenberg, L. (1999). Maintenance of beta-cell function and survival following islet isolation requires re-establishment of the islet-matrix relationship. *The Journal of Endocrinology*, *163*(2), 181–90.

Wang, T., Adcock, J., Kühtreiber, W., Qiang, D., Salleng, K. J., Trenary, I., & Williams, P. (2008). Successful allotransplantation of encapsulated islets in pancreatectomized canines for diabetic management without the use of immunosuppression. *Transplantation*, *85*(3), 331–7. doi:10.1097/TP.0b013e3181629c25

Wattendorf, U. T. A., & Merkle, H. P. (2008). PEGylation as a Tool for the Biomedical Engineering of Surface Modified Microparticles. *Journal of Pharmaceutical Sciences*, *97*(11), 4655–4669. doi:10.1002/jps

Weber, L. M., & Anseth, K. S. (2008). Hydrogel encapsulation environments functionalized with extracellular matrix interactions increase islet insulin secretion. *Matrix Biology*, *27*(8), 667–73. doi:10.1016/j.matbio.2008.08.001

Weber, L. M., Hayda, K. N., Haskins, K., & Anseth, K. S. (2007). The effects of cell-matrix interactions on encapsulated beta-cell function within hydrogels functionalized with matrix-derived adhesive peptides. *Biomaterials*, *28*(19), 3004–11. doi:10.1016/j.biomaterials.2007.03.005

White, S. a, Shaw, J. a, & Sutherland, D. E. R. (2009). Pancreas transplantation. *Lancet*, *373*(9677), 1808–17. doi:10.1016/S0140-6736(09)60609-7

Wicker, L. S., Miller, B. J., Coker, L. Z., McNally, S. E., Scott, S., Mullen, Y., & Appel, M. C. (1987). Genetic control of diabetes and insulitis in the nonobese diabetic (NOD) mouse. *The Journal of experimental medicine*, *165*(6), 1639–54.

Wileman, T., Harding, C., & Stahl, P. (1985). Receptor-mediated endocytosis. *The Biochemical Journal*, *232*(1), 1–14.

Willcox, a, Richardson, S. J., Bone, a J., Foulis, a K., & Morgan, N. G. (2009). Analysis of islet inflammation in human type 1 diabetes. *Clinical and experimental immunology*, *155*(2), 173–81. doi:10.1111/j.1365-2249.2008.03860.x

Wilson, J. T., Cui, W., & Chaikof, E. L. (2008). Layer-by-layer assembly of a conformal nanothin PEG coating for intraportal islet transplantation. *Nano letters*, *8*(7), 1940–8. doi:10.1021/nl080694q

Wilson, J. T., Cui, W., Kozlovskaya, V., Kharlampieva, E., Pan, D., Qu, Z., Krishnamurthy, V. R., et al. (2011). Cell surface engineering with polyelectrolyte multilayer thin films. *Journal of the American Chemical Society*, *133*(18), 7054–64. doi:10.1021/ja110926s

Witkowski, P., Liu, Z., Guo, Q., Poumian-Ruiz, E., Cernea, S., Herold, K., & Hardy, M. A. (2005). Two-layer method in short-term pancreas preservation for successful islet isolation. *Transplantation Proceedings*, *37*(8), 3398–3401. doi:10.1016/j.transproceed.2005.09.050

Wucherpfennig, K. W., & Eisenbarth, G. S. (2001). Type 1 diabetes. *Nature Immunology2*, *2*(9), 767–768.

Xie, D., Smyth, C. a, Eckstein, C., Bilbao, G., Mays, J., Eckhoff, D. E., & Contreras, J. L. (2005). Cytoprotection of PEG-modified adult porcine pancreatic islets for improved

xenotransplantation. *Biomaterials*, *26*(4), 403–12. doi:10.1016/j.biomaterials.2004.02.048

Yavlovich, A., Singh, A., Blumenthal, R., & Puri, A. (2011). A novel class of photo-triggerable liposomes containing DPPC:DC(8,9)PC as vehicles for delivery of doxorubcin to cells. *Biochimica et Biophysica Acta*, *1808*(1), 117–126. doi:10.1016/j.bbamem.2010.07.030

Yavlovich, A., Singh, A., Tarasov, S., Capala, J., Blumenthal, R., & Puri, A. (2009). Design of Liposomes Containing Photopolymerizable Phospholipids for Triggered Release of Contents. *Journal of Thermal Analysis and Calorimetry*, *98*(1), 97–104. doi:10.1007/s10973-009-0228-8

Yokoi, T., Sakamoto, Y., Terasaki, O., Kubota, Y., Okubo, T., & Tatsumi, T. (2006). Periodic arrangement of silica nanospheres assisted by amino acids. *Journal of the American Chemical Society*, *128*(42), 13664–5. doi:10.1021/ja065071y

Yoon, K. B. (2007). Organization of zeolite microcrystals for production of functional materials. *Accounts of Chemical Research*, *40*(1), 29–40. doi:10.1021/ar000119c

Yu, K. O., Grabinski, C. M., Schrand, A. M., Murdock, R. C., Wang, W., Gu, B., Schlager, J. J., et al. (2008). Toxicity of amorphous silica nanoparticles in mouse keratinocytes. *Journal of Nanoparticle Research*, *11*(1), 15–24. doi:10.1007/s11051-008-9417-9

Yu, L., Suh, H., Koh, J. J., & Kim, S. W. (2001). Systemic administration of TerplexDNA system: pharmacokinetics and gene expression. *Pharmaceutical research*, *18*(9), 1277–83.

Zhang, Z. J., Davidson, L., Eisenbarth, G., & Weiner, H. L. (1991). Suppression of diabetes in nonobese diabetic mice by oral administration of porcine insulin. *Proceedings of the National Academy of Sciences of the United States of America*, *88*(22), 10252–6.

Zhang, Z., Vuori, K., Reed, J. C., & Ruoslahti, E. (1995). The alpha5beta1 integrin supports survival of cells on fibronectin and up-regulates Bcl-2 expression. *Science*, *92*(June), 6161–6165.

Appendix 1

Characterization and Functional Assays

To understand the interactions between biomaterials and cells, full characterization of the materials is necessary. Throughout this work different characterization techniques are utilized to understand the materials. The application of some of these techniques, as well as technical notes, is described below.

A1.1 Liposome Preparation and Characterization

The following sections detail the preparation and characterization techniques used to prepare liposomes. Many of these techniques were developed by previous members of the Kokkoli group and adjusted to suit the applications found in this work.

A1.1.1 Liposome Purification

Liposomes are formed by drying a solution of lipids (DPPC, CHOL, PR_b, PEG2000, and RHOD) in a round bottom flask to create a thin film. The film is hydrated with a solution containing the desired encapsulate (i.e. ATP, calcein, buffer), freeze-thawed to increase encapsulation volume (Oku, Kendall, & MacDonald, 1982), and extruded through membranes to size the liposomes appropriately. Following extrusion, unencapsulated material is separated from the liposomes using gel chromatography. Using FPLC, the liposomes are filtered over a Sepharose CL-4B gel filtration column at 0.87 mL/min and fractions containing liposomes collected for further use. Liposomes prepared for this work

were all prepared in HBSE buffer (10 mM HEPES, 150 mM NaCl, 0.1 mM EDTA, pH 7.4) which was also used as the mobile phase for separation. The FPLC traces shown in Figure A1.1 demonstrate the separation achieved. Fractions from the first peak contain liposomes and are collected and pooled for further use.

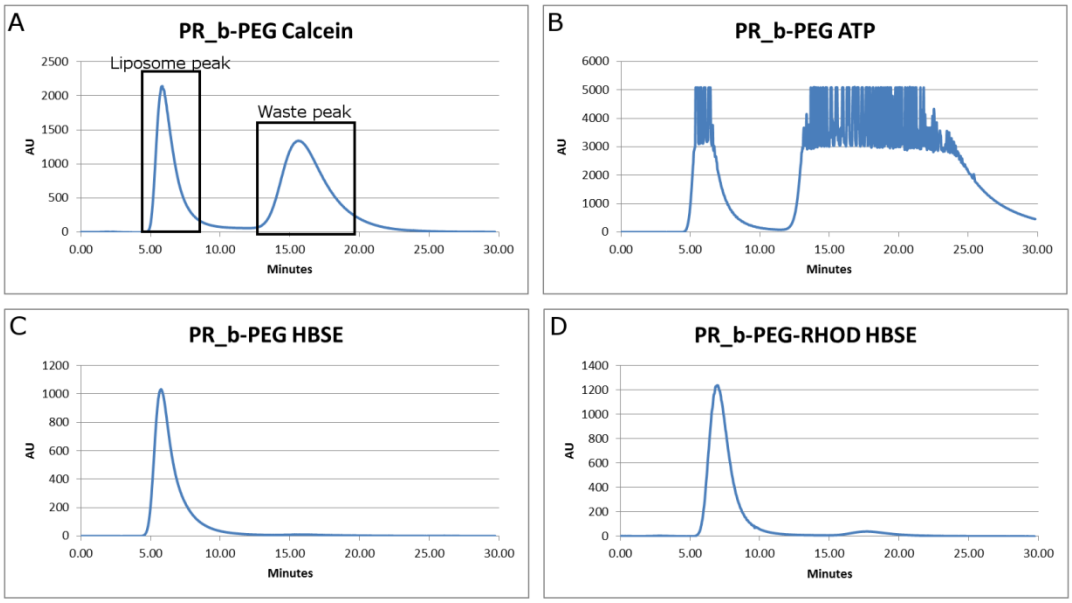

Figure A1.1: FPLC traces of PR_b-PEG liposomes encapsulating A) 2 mM calcein, B) ATP, and C) HBSE only. D) PR_b-PEG liposomes with 1 mol% rhodamine B labeled DPPE encapsulating HBSE. The traces indicate the absorbance at 254 nm in arbitrary units. Liposomes are contained in the first peak and the unencapsulated material is in the second peak (as indicated in A).

A1.1.2 Phosphorus Determination

To determine the total amount of phospholipids in the liposome samples, a phosphorus assay was employed. This assay is adapted from literature reports on colorimetric phosphorus determination (P. S. Chen et al., 1956; Fiske & Subbarow, 1925). Small amounts of the samples are digested in sulfuric acid (8.9N) at 200-215°C, followed by ashing with hydrogen peroxide at the same temperature. Once the samples are cooled to ambient temperature, the phosphorus content is determined through the reaction between phosphate and ammonium molybdate. This reaction produces phosphomolydate acid which

is then reduced to form a blue complex by ascorbic acid. The reaction between the digested sample, ammonium molybdate(IV) tetrahydrate (0.25% w/v), and ascorbic acid (0.1% w/v) is heated at 100°C for 7 minutes and cooled to room temperature before reading the absorbance at 820 nm. A standard curve is generated with known amounts of phosphorus to determine the relationship between absorption and phosphorus concentration. Phosphorus concentration of the samples is determined using the standard curve. Total lipid content is estimated by the stoichiometric ratio of the initial formulation. Typically phospholipids accounted for 65 mol% of the formulation.

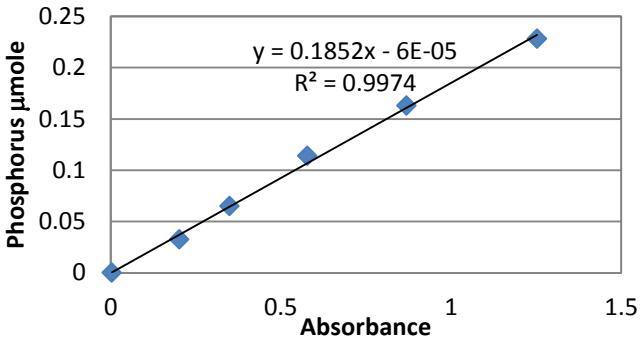

Figure A1.2: Phosphorus determination standard curve. Absorbance was measured at 820 nm.

Liposomes containing ATP have additional phosphorus from the encapsulated ATP. Phosphorus resulting from the ATP (determined by HPLC) is subtracted from total phosphorus. Remaining phosphorus results from the phospholipids. Phospholipid determination in this manner results in lipid concentrations in the normal range of liposome formulations.

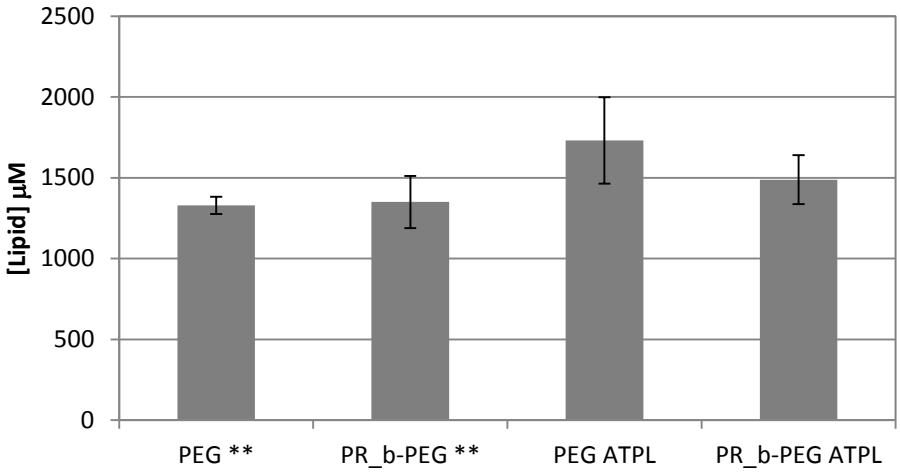

Figure A1.3: Average lipid concentrations for liposome formulations. PEG and PR_b-PEG** are average lipid concentrations for liposome formulations encapsulating buffer or calcein. Data is presented as mean ± SE. PEG** n=20, PR_b-PEG** n=26, PEG ATPL n=4, PR_b-PEG ATPL n=11.**

A1.1.3 PR_B DETERMINATION

Liposomes are prepared with a known amount of PR_b peptide-amphiphile however the final PR_b concentration must be determined after purification to account for losses. PR_b concentration is found using the Pierce® BCA Protein Assay Kit (Thermo Scientific, Rockford, IL). This kit utilizes the reduction of Cu^{+2} to Cu^{+1} by protein in an alkaline medium and the colorimetric detection of the Cu^{+1} cation with a reagent containing bicinchoninic acid. A PR_b standard diluted from a 1 mg/mL stock solution is run alongside the unknown samples to determine the PR_b concentration in the unknowns (Figure A1.4). The liposomes are lysed with sodium dodecyl sulfate (SDS) to determine the total amount of PR_b peptide-amphiphile incorporated into the liposomes. When 5 mol% PR_b was incorporated into the liposome formulations, the final content was typically around 2 mol%.

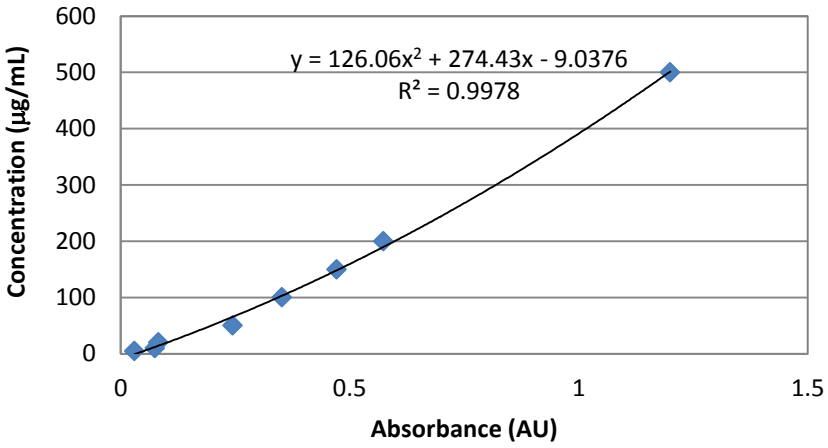

Figure A1.4: BCA PR_b standard curve. PR_b standards were diluted from a 1 mg/mL stock solution of PR_b peptide amphiphile. Absorbance was read at 562 nm on a plate reader.

A1.1.4 ATP Encapsulation Analysis

Encapsulated ATP concentration was determined using reversed phase HPLC. Protocol was adopted from Liang et al. (2004). Liposomes were lysed with 0.4% (v/v) sodium dodecyl sulfate (SDS) in distilled water. The chromatography was performed on an Xterra Prep MS C_{18} 150*10 mm stainless steel column (Waters Corp., Milford, MA) packed with 5 μm beads. The isocratic elution was run at room temperature with the 96/4 (v/v) mixture of 0.1 M KH_2PO_4 buffer, pH 6.0, and methanol at a flow rate of 1 mL/min. The UV absorbance was detected at 254 nm on an Agilent 1100 series HPLC (Santa Clara, CA). 20 μL of standards or lysed liposome sample was injected per run with the peak eluting at approximately 11 minutes. The standard curve was generated by injecting known amounts of ATP and calculating the area under the curve. ATP standards were prepared and run each time liposome formulations were evaluated. A typical standard curve is shown in Figure A1.5. Figure A1.6 demonstrates that the apparent concentration of ATP changes with increasing incubation time in SDS until it plateaus around two hours. Therefore, liposomes were

incubated with SDS for approximately two hours before analysis to ensure ATP was completely released.

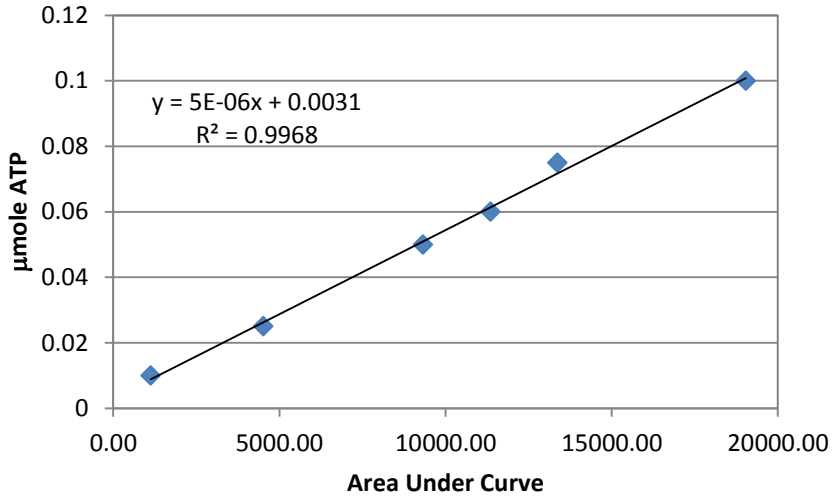

Figure A1.5: Standard curve for determination of encapsulated ATP via HPLC. **Curves were generated by UV detection at 254 nm on an Agilent 1100 series HPLC.**

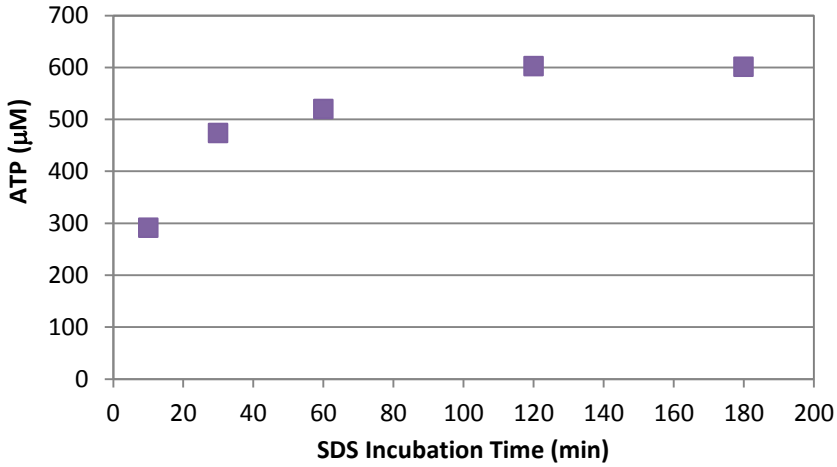

Figure A1.6: Effect of ATP liposome incubation time with 0.4% SDS on apparent ATP concentration.

A1.2 Functional Assays

Throughout the presented work functional assays are used to measure cells' responses to biomaterials under various conditions. The assays were generally performed according to the manufacturer's protocol but some aspects required special attention to control the assay's reproducibility.

A1.2.1 WST-1 Assay

Tetrazolium salts including 3-(4,5-dimethylthiazol-2-yl)-2,5-diphenyltetrazolium bromide (MTT), 2,3-bis-(2-methoxy-4-nitro-5-sulfophenyl)-2H-tetrazolium-5-carboxanilide (XTT), 3-(4,5-dimethylthiazol-2-yl)-5-(3-carboxymethoxyphenyl)-2-(4-sulfophenyl)-2H-tetrazolium (MTS), and 2-(4-Iodophenyl)-3-(4-nitrophenyl)-5-(2,4-disulfophenyl)-2H-tetrazolium (WST-1) are used to assay cell proliferation and viability. These salts are converted to a formazan dye by mitochondrial dehydrogenase. Most of the tetrazolium salts are reduced to a formazan dye that is insoluble in water and must be solubilized with organic solvents before reading. However, WST-1 produces a water soluble formazan dye, therefore simplifying the protocol and removing the requirement for media removal prior to reading the assay in a multiwall plate. WST-1 is reduced outside the cell by trans-plasma membrane electron transport via the 1-methoxyPMS electron carrier. The NADH that is responsible for the reduction of WST-1 is derived mainly from the mitochondrial TCA cycle (Berridge, Herst, & Tan, 2005). Therefore this assay is a useful tool for measuring the metabolic activity of cells.

In this work the WST-1 assay was used to determine the metabolic activity of INS-1 cells exposed to various treatments and conditions. The premixed WST-1 reagent was added to the cell cultures at a 1:10 dilution in all cases followed by three hour incubation at 37°C, 5%

CO_2. The WST-1 manufacturer's protocol recommends incubation with the reagent for 0.5-4 hours, dependent on cell type, density, and other factors. The incubation time was determined by visual inspection of color change and reading absorbance at multiple time points. Three hours provided adequate signal/noise ratio and was used for all WST-1 assays using INS-1 cells.

Experiments comparing the metabolic activity of INS-1 exposed to ischemia and normal conditions exposed a few technical issues. First, only interior wells were used for all experiments performed in a 96-well plate to prevent issues stemming from evaporation of the media, which occurs preferentially in the outermost wells (direct observation, unpublished data). The outside wells were instead filled with buffer. Secondly, the ischemia portion of the incubation protocol was performed in glucose depleted minimal medium. However, the extent of WST-1 reduction is dependent on the concentration of glucose in the medium (Takahashi et al., 2002; Vistica et al., 1991). Therefore the media was replaced with complete medium before the assay was completed. To limit the number of cells lost during the media change the 96-well plate was inverted over a collection dish to drain the wells and gently placed on a paper towel to wick the remaining media away. 100 μL of complete media was then added drop wise using a multichannel pipette, followed by 10 μL of WST-1 reagent. Data was normalized to INS-1 cells cultured in parallel under normal conditions for each experiment.

A1.2.2 Glucose Stimulated Insulin Secretion

Glucose stimulated insulin secretion (GSIS) was used to probe the functional activity of both INS-1 β cells and porcine islets. The specific glucose challenge protocol is documented in the experimental section of the appropriate chapters. Following the glucose challenge the

secreted insulin was determined by ELISA. Porcine islet insulin secretion samples were diluted either 10x or 20x with the Calibrator 0 (0 μg/mL insulin) contained in the kit before being analyzed by ELISA. However, for the protocols involving INS-1 cells, 3-8x dilutions were more appropriate. The extent of dilution was dependent on the level of glucose stimulation. Higher dilutions lowered the insulin concentration below the range of the ELISA. Standards were run to determine insulin concentration of the unknown samples. The standard curve was generated using a cubic spline (Figure A1.7). The ELISA plate was incubated for two hours on a rotary shaker at 300 rpm and room temperature. Following six washes with the wash buffer provided, the ELISA wells were developed with TMB substrate for 15 minutes and stopped with the Stop buffer provided in the kit. Absorbance was measured at 450 nm on a Synergy H1 plate reader (Biotek, Winooski, VT).

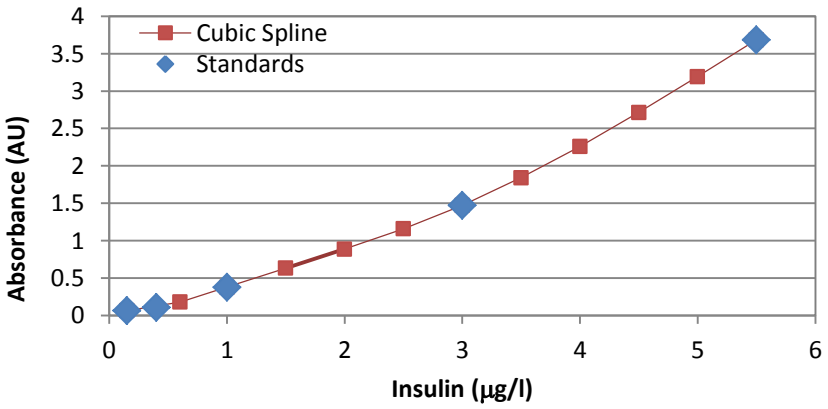

Figure A1.7: Insulin ELISA standard curve. Absorbance was read at 450 nm.

APPENDIX 2

TREATMENT OF ISCHEMIC ISLETS WITH TARGETED ATP LIPOSOMES

Islets are exposed to damaging ischemic conditions during many stages of the islet isolation and transplantation protocol (Emamaullee, Liston, et al., 2005; Lazard et al., 2012; Linn et al., 2006; Moritz et al., 2002; Nadithe et al., 2012). Chapter 4 discusses the application of targeted liposomes encapsulating ATP to protect INS-1 β cells from ischemic conditions. However, the primary aim of targeted ATP liposomes is the application to whole islet cell clusters. The study in Chapter 3 demonstrated the ability of PR_b functionalized liposomes to increase internalization of liposomes into islet cells. This study was extended to investigate the ability of PR_b functionalized ATP liposomes to protect islet cells from ischemia. The following information outlines the methods and results from this study. Also included is a discussion on the issues that prompted a switch from studying whole islets to single β cells.

A2.1 PORCINE ISLETS UNDER ISCHEMIA

Islets are highly vascularized structures (M. D. Menger et al., 2001) which suffer under conditions of limited oxygen (Avgoustiniatos et al., 2008). We hypothesized that delivery of ATP through PR_b targeted liposomes would promote better cell viability after ischemic conditions. To test this hypothesis, islets cultured in an anoxic environment were exposed to liposome formulations containing ATP and changes in morphology and live/dead staining were monitored. Previous data from the Papas group indicated that islets

dissociated when they were cultured in an anoxic environment (95% N_2, 5% CO_2, 37°C) (Papas, Bauer, Avgoustiniatos, Papas, & Hering, 2005). We theorized that treatment with PR_b functionalized ATP liposomes (PR_b ATPL) would prevent this dissociation.

A2.1.1 Time Lapse Imaging of Islets Under Anoxia

In order to monitor changes in islet morphology over long periods in a controlled environment, the LiveCell system (Pathology Devices, Inc., Westiminster, MD) was used (Figure A2.1). This system combines temperature, humidity, and environmental (i.e. CO_2 or N_2 level) controls in a microscope stage mounted chamber. The chamber was designed to fit on inverted microscope stages and allow for monitoring of live cells over long periods. The Nikon Eclipse TE 300 inverted light microscope (Nikon Inc., Tokyo, Japan) equipped with a Nikon high pressure mercury arc lamp was used to image the islets. Images were captured using a SPOT RT CCD camera (Diagnostic Instruments, Sterling Heights, MI) and Metamorph imaging software (Molecular Devices Corp., Sunnyvale, CA).The automated stage allowed for time lapse images of multiple points to be acquired automatically.

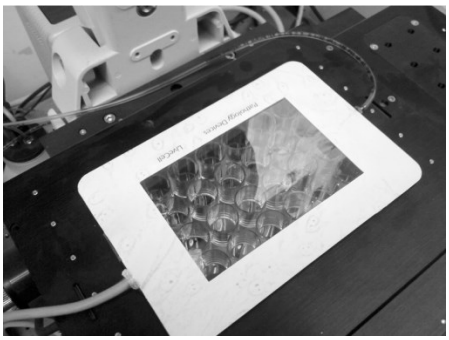

Figure A2.1: LiveCell chamber used for time lapse image collection. Chamber allows for temperature, humidity, and environmental control.

To ensure that islets could remain viable in the LiveCell chamber for extended periods, islets were seeded into wells in complete medium and cultured for 40 hours in the LiveCell

chamber under normal conditions (100% air, 37°C, 80% relative humidity). Following the normal culture period, the chamber environment was switched to 100% N_2, 37°C, 80% relative humidity and cultured for 72 additional hours. Figure A2.2 shows that the islets remained intact during the 40 hours of normal culture but started to dissociate after being cultured in 100% N_2. The dissociation is evident by a flattening out and spreading of the islets over time. Large islets had more apparent dissociation at earlier time points compared to small islets. This could be due to the presence of an hypoxic core prior to the change to an anoxic environment (Giuliani et al., 2005).

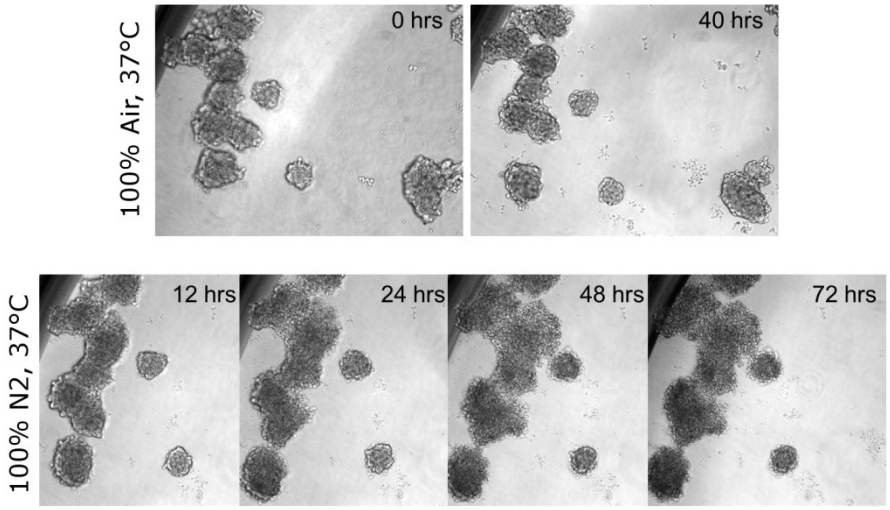

Figure A2.2: Porcine islet exposed to 40 hours of a normal environment (100% air, 37°C, top row) followed by 72 hours of an anoxic environment (100% N_2, 37°C, bottom row) in the LiveCell chamber. 20X magnification.

We hypothesized that delivery of ATP to islets would prevent the dissociation of the islets and based on previous results (Atchison et al., 2010) that delivery would be enhanced via PR_b functionalized liposomes. Characterization of the liposomes used in the following studies is shown in Table A2.1. To test this hypothesis, islets were incubated with liposomes for three hours under normal conditions and then washed and placed under anoxia for 24

hours. Following the 24 hours of anoxia the environment was switched to 100% air and the islets were monitored for an additional 16 hours. Images were acquired every hour. The final 16 hours of normal culture were included to determine if reoxygenation increased the dissociation of the islets. Reoxygenation occurring after a hypoxic or anoxic period has been shown to decrease cell survival in islets, as well as other cell models (Lepore et al., 2004; C. Li & Jackson, 2002).

Table A2.1: Characterization of liposomes used in islet anoxia studies. Liposomes are composed of DPPC, cholesterol, and PR_b (where indicated). Data is presented as mean ± standard deviation of n= 3-12 formulations.

	ATPL	PR_b ATPL	PR_b HBSE
ATP μM	396 ±147	623 ±221	-
Diameter	108 ± 16	103 ± 17	125 ± 15
Zeta potential	-4.1 ± 5.7	-0.7 ± 6.0	-8.3 ± 5.4
PR_b (mol%)	-	0.8 ± 1.2	0.4 ± 0.2

Figure A2.3 shows images for islets treated with buffer only (control), PR_b ATPL and free ATP at 150 μM, and PR_b HBSE at 250 μM lipids. Images at zero hours (first column) represent the islets directly after treatment incubation and washing. The second column images are the same islets after 24 hours of anoxia and the third column are the islets after the final 16 hours of normal environment. The control sample (top row) again demonstrates that larger islets dissociate more noticeably than smaller islets at the same time point. If islets of similar size are compared, the samples receiving treatment seem to have less dissociation at both the 24 and 40 hour time point compared to the control. However, there is not a discernible difference between the different treatments. Within all treatment groups islet dissociation is still occurring, however it lags behind the dissociation seen in the control sample. Then degree of spreading can be qualitatively assessed but due to the complex 3D structure of the islets, a quantitative assessment would be difficult.

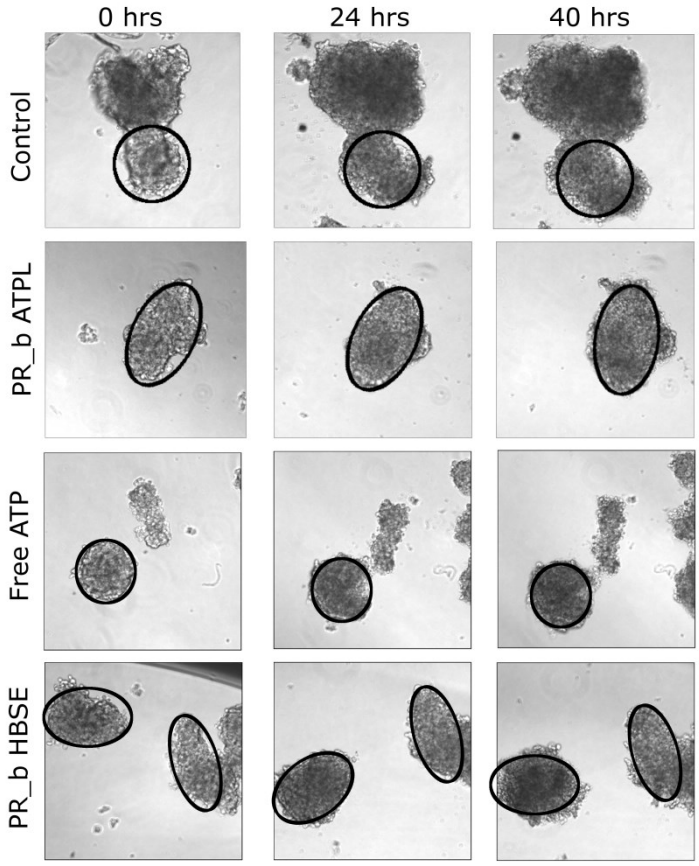

Figure A2.3: Porcine islets exposed 24 hours of anoxia followed by 16 hours of normal culture. Islets were treated with buffer only (Control), PR_b ATPL and Free ATP at 150 μM ATP, or PR_b HBSE liposomes at 250 μM lipid. Treatments were incubated with islets for three hours prior to anoxia initiation. Samples were washed and resuspended in culture medium prior to anoxia initiation. Boundaries created around islet at time zero are overlaid on the 24 and 40 hour images. 20X magnification.

A2.1.2 Live/Dead Staining of Anoxic Islets

To attempt to discern the status of the islets after the period of anoxia, islets were stained with FDA/PI (live/dead). Islets were treated with liposomes or free ATP, same as above, but were stained and imaged immediately after 16 hours of anoxia. A sample lysed with ethanol was included to demonstrate complete dead staining. For morphological and live/dead analyses, islets were cultured in complete medium in tissue culture plates in the LiveCell chamber for up to 112 hours. Environments consisted of 100% humidified air or N_2 at 37°C.

Images were collected approximately once an hour for the duration of the experiment. Samples treated with liposomes were given the liposomes at the onset of the experiment and cultured without washing. Islets were stained after the final time point with 110 nM FDA for 45 minutes and 75 nM PI during the last 10 minutes for live/dead imaging analysis. Islets treated with liposomes or free ATP were incubated with liposomes either before or during the anoxic period. Islets treated before were incubated with treatments for three hours in 100% air at 37°C, washed with PBS, and added to 96 well plates in culture medium. Liposomes and ATP were added at 150 μM ATP. For live/dead images a FITC filter (excitation BP465-495, emission BP515-555; Nikon 96107M B-2E/C C12353) was used to collect fluorescein diacetate (FDA) fluorescence and a rhodamine filter (excitation BP528-553, emission 590LP; Nikon DM575 G-2A) was used to collect propidium iodide (PI) fluorescence.

Samples treated with ATPL (nontargeted ATP liposomes), PR_b ATPL, free ATP, and PR_b HBSE all demonstrated live/dead staining similar to normoxic controls. Islets in the anoxic control sample were small and had only minimal FDA staining. Staining by PI, which is a marker of necrotic cells, was not increased in any of the anoxic samples, contrary to expected results. Staining with FDA/PI has been shown to have limited utility in terms of accurately inferring islet viability (Boyd et al., 2010). However, comparing the ATPL, PR_b ATPL, and PR_b HBSE samples, there is no obvious difference between the three treatments. Each appears similar to the normoxic control in terms of FDA staining intensity. The lack of quantitative assessment and inherent differences in individual islets make this type of experiment difficult to interpret.

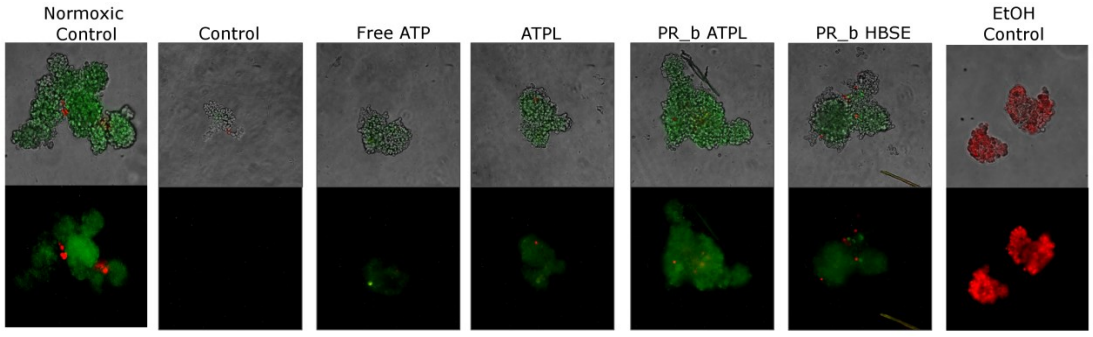

Figure A2.4: Live/dead images of porcine islets incubated under anoxic conditions for 16 hours. Islets were stained with FDA (live, green) and PI (red, dead) and imaged with fluorescence microscopy. The top row is the fluorescence overlaid onto the brightfield image. 20X magnification.

A.2.1.3 Caspase 3/7 Activity of Anoxic Islets

The previous experiments gave a qualitative assessment of the function of the various treatments, however an accurate picture of the effect on viability was difficult to discern. Based on previous work by the Papas group (Papas, Bauer, et al., 2005) caspase 3/7, a marker of cell apoptosis, increased in porcine islets after exposure to six hours of anoxia. They demonstrated a three-fold increase in caspase 3/7 activity when comparing normoxic islets to islets after six hours of anoxia. We hypothesized that liposomal delivery of ATP could decrease the caspase 3/7 activity and provide a quantitative assessment of function. Porcine islets were treated with liposomes or free ATP for five hours under normal conditions, washed, resuspended in culture medium, and placed in a water jacketed chamber flushed with 100% N_2 for six hours. Caspase 3/7 activity was measured using the Caspase-Glo® 3/7 Assay (Promega, Madison, WI) according to manufacturer's directions. Caspase 3/7 activity was normalized to total DNA content using the Quant-it™ PicoGreen® dsDNA Reagent Kit (Invitrogen, Carlsbad, CA).

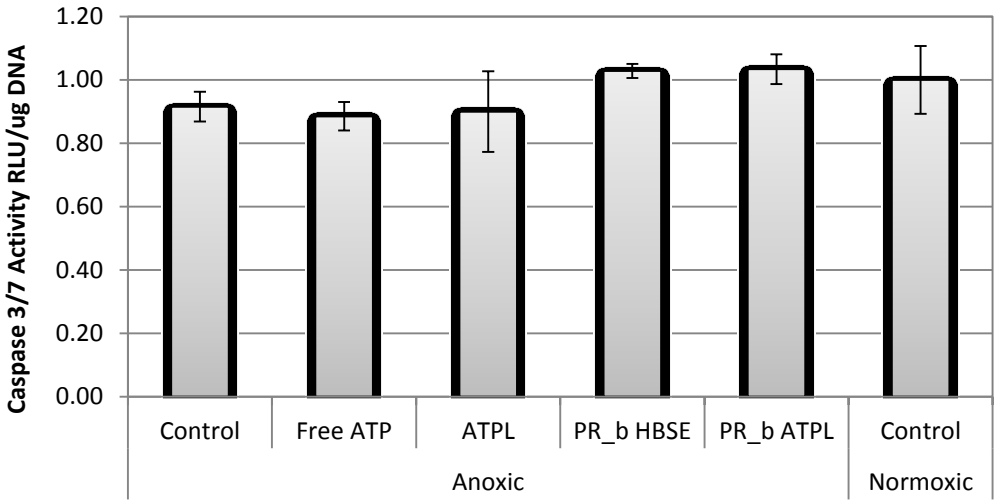

Figure A2.5: Caspase 3/7 activity of porcine islets after six hours of anoxia. Islets were treated with buffer, free ATP or ATPL at 150 μM ATP, or HBSE liposomes at 250 μM lipids for five hours prior to anoxia initiation. Data is presented as mean ± SE of n=2 experiments with three repetitions per n and is normalized to the normoxic control.

Figure A2.5 demonstrates that caspase 3/7 activity of islets under six hours of anoxia is unchanged relative to the normoxic control. In fact, there is no significant difference between any of the samples and the normoxic control. This result was unexpected and possibly explained by the addition of a c-Jun N-terminal kinase (JNK) inhibitor (W. H. Kim, Lee, Gao, & Jung, 2005; Lopez-Ramirez et al., 2012) to the porcine isolation protocol (K.K. Papas, personal communication, April 2011). It is also possible that the window of caspase activation occurs prior to or after the point examined in this experiment.

To investigate the time frame of caspase 3/7 activation, the Magic Red™ Caspase 3 & 7 Assay Kit (ImmunoChemistry Technologies LLC, Eagan, MN) was employed. This assay allows for the real time detection of caspase activation in living cells by microscopy. The active form of caspases 3 & 7 hydrolyze the Magic Red DEVD target sequences, converting them to a fluorescent form (ex/em 590/630nm). Islets were incubated with 5 μM Magic Red substrate in the same medium used in the experiment. Time lapse fluorescent images were

acquired starting immediately after Magic Red addition. The Magic Red substrate can hydrolyze over time in aqueous environments, so medium controls were included to account for background fluorescence.

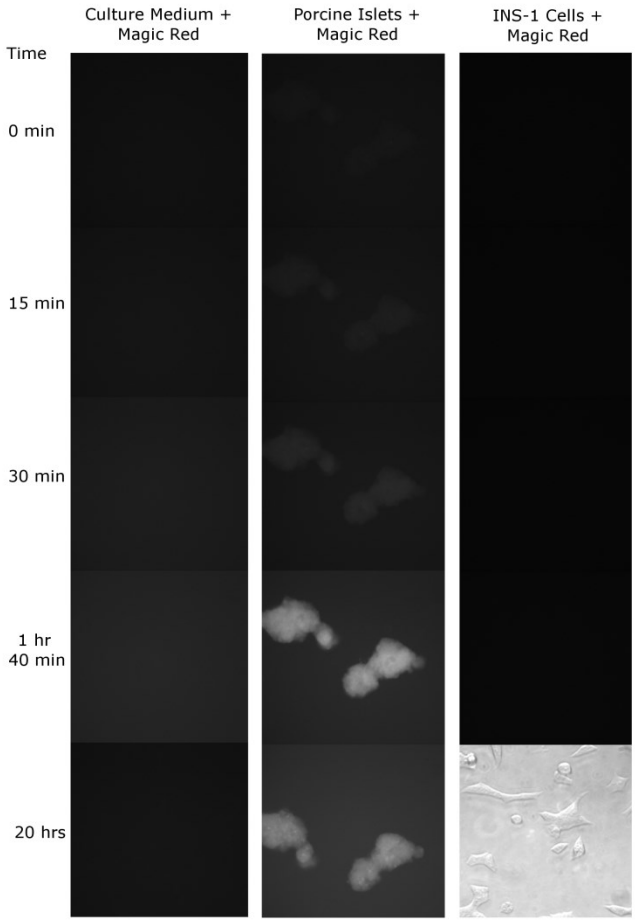

Figure A2.6: Caspase detection by Magic Red in porcine islets under normoxic conditions. Islets were incubated with 5 μM Magic Red and imaged over time. Culture medium with Magic Red was analyzed to account for background. INS-1 cells were imaged up to 1 hr 40 minutes. The bottom image is a brightfield image. Images were captured using the rhodamine filter. Islets and medium, 20X magnification; INS-1 cells, 40X magnification.

Normoxic porcine islets had increasing fluorescence over the first few hours, which was maintained over at least 20 hours. The high level of caspase 3/7 activation in the normoxic islets could partially explain why no difference could be discerned between anoxic and

normoxic islets. Unstained islets exhibited no background fluorescence at the settings employed in these images (data not shown). To ensure that the Magic Red substrate was not nonspecifically cleaving in an endocrine cell environment, INS-1 beta cells were incubated with the Magic Red substrate and imaged under similar conditions. The INS-1 cells did not exhibit measureable fluorescence during 5 hours of normoxia, indicating that the caspase substrate was working correctly.

A2.2 Discussion

The data above demonstrate the complexity involved in measuring a change in islet viability, especially if the change is small and transient. In the analysis of the efficacy of liposomal delivery of ATP, the lack of difference between the individual liposome treatments (ATPL, PR_b ATPL, and PR_b HBSE) was difficult to explain. PR_b functionalized liposomes have been shown to have greater binding and internalization into porcine islet cells (Chapter 3, (Atchison et al., 2010)). Therefore, it was expected that they would outperform nontargeted formulation (ATPL) in terms of ATP delivery. However, both ATPL and PR_b ATPL performed similarly in the qualitative analysis of morphology and live/dead staining. More noticeably however, was the function of the PR_b HBSE treatment. This treatment also slightly improved the qualitative assessment of islet dissociation and live/dead staining compared to controls. Since the improvements were small and qualitative only, no conclusions could effectively be drawn from these experiments.

To better understand how the ATP liposomes were interacting with the islet cells, INS-1 β cells were employed for remaining studies. INS-1 cells are grown in culture and allow for easier processing in multiwall plate assays. By removing the variable of inconsistent cell viability at the onset of an experiment, the effect of the liposomes could more accurately be

compared between samples and between experiments. Additionally, the liposomes would have the same opportunity to interact with every cell, removing the complicating factor of a 3D cell aggregate. Work involving INS-1 cells and ATPL is discussed in Chapter 4. While the study with INS-1 cells reveals interesting mechanisms of liposome/cell interactions, the ultimate utility of this system with islets will need to be reevaluated.